

Title	ペプチド創薬を目的とした新規環化反応の発見とその特性評価
Author(s)	田村, 崇
Citation	
Issue Date	2022-03
Type	Thesis or Dissertation
Text version	ETD
URL	http://hdl.handle.net/10119/17779
Rights	
Description	Supervisor:芳坂 貴弘, 先端科学技術研究科, 博士

Doctoral Dissertation

**Development of novel peptide cyclization
for peptide drug discovery and evaluation
of their properties**

TAKASHI TAMURA

Supervisor : Takahiro Hohsaka

Graduated School of Materials Science and Technology

Japan Advanced Institute of Science and Technology

Material Science

March 2022

Table of Contents

Chapter 1	
Background and Overview	1
Chapter 2	
Reaction Characteristics and Versatility of Thiazoline Ring-Bridged Peptide Cyclization	25
Chapter 3	
Membrane Permeability of Thiazoline Ring-Bridged Cyclic Peptides	45
Chapter 4	
Expression of Thiazoline Ring-Bridged Cyclic Peptides in Cell-Free Translation	57
Chapter 5	
Conclusion	74
List of Publications	75
Acknowledgments	76

Chapter 1

Background and Overview

1. 1 Introduction

Recently, drug discovery research on intracellular protein-protein interactions (PPIs) has been expected to be one of the next generation of breakthrough drugs. In this thesis, I report on the development of a technology to search for drug-like peptides for the development of drugs targeting intracellular PPIs. Small molecular drugs, which have been the mainstream until now, can reach into cells, but the protein interface that forms PPIs has a wide and shallow structure and cannot exert sufficient binding force. In addition, biologics have binding power to PPIs due to their large molecular weight, but they cannot cross the cell membrane. In contrast, cyclic peptides are expected to have both cell membrane permeability and affinity for therapeutic target protein surfaces. However, cyclic peptides have been shown to be permeable to cell membranes in only a few cases, such as cyclosporin A (CSA). So far, there is no universal method for peptides to be permeable to cell membranes. In addition, there is a need for a potent peptide library with high cell membrane permeability that are useful for intracellular PPIs as drug discovery target.

In recent years, cyclic peptides with a ring structure in the main chain has been reported as a new method for improvement of the peptide permeability to cell membrane due to intramolecular hydrogen bonds offsetting the polarity of amide bonds. Originally, cyclic peptides were known to be characterized by metabolic stability and high target binding, and have been shown to be a modality with high potential for pharmaceuticals. Cyclic peptides have been shown to have metabolic stability and high affinity for drug discovery targets, and are becoming a modality with high pharmaceutical potential.

Therefore, I set a goal to search for new peptide cyclization reactions that generate a ring structure in the main chain of cyclic peptides, and to develop technologies that can construct cell membrane-permeable peptide libraries. I expect that the solution of this research problem will contribute to the proposal of universal peptide molecular design with cell membrane permeability and the development of peptide libraries targeting intracellular PPIs.

The new cyclization reaction, which is the key to this project, must proceed in water due to be applied to peptide display methods such as mRNA display. Therefore, it is desirable that the process proceeds spontaneously without catalyst, without amino acid sequence dependence, and in high yield.

In this thesis, I found that the new peptide cyclization reaction with thiazoline ring in the peptide main chain, which was inspired by Luciferin biosynthesis, proceeded spontaneously in water. In addition, to demonstrate the usefulness of peptides as peptide drugs, I examined the model cell membrane permeability of cyclic peptides having a thiazoline ring. Furthermore, I report the utilization of the peptide cyclization reaction with thiazoline ring in cell-free translation for future application to mRNA/cDNA display, a method for obtaining peptides that can bind to drug targets.

1. 2 Status of peptide drugs

Until now, drug discovery has focused on two modalities: small molecules (molecular weight ~500) and biologics such as antibody drugs (molecular weight > 5000) (Fig. 1-1). Small molecules could act on intracellular disease-causing targets due to their high cell membrane permeability, and they could be administered orally, which has advantages in terms of dosing convenience, but they have low selectivity for binding to targets, and their dosing may be limited due to side effects.

Biologics have the advantage of a large molecular structure that allows them to develop specific binding properties and therefore have low side effects. They also have high affinity to extracellular targets and are expected to have long-lasting drug effects.

However, the usage of biologics would be restricted due to their inability to bind to intracellular targets. More than 50 peptide drugs, a type of biologics, have been approved so far, including Copaxone, Victosa, Sandstatin, Cubicin, and Lupron. Peptide drugs, including insulin and the analogues, have annual sales of about \$50 billion in 2015 and account for about 5 % of total pharmaceutical sales¹). Conventional peptide drugs are mostly of the type that act on extracellular targets, and have modified structures of some of the endogenous peptides.

Peptide drugs are considered to be a modality that could be possessed both the membrane permeability of small molecules and with target-specific affinity of biologics because their molecular weight is in the middle range between small molecules and biologics. In addition, unlike biologics, it is relatively easy to modify peptides with functional molecules to improve their pharmacological activity or adjust their stability in blood. Furthermore, it could be synthesized at a lower cost than biologics. Based on these backgrounds, peptide drugs have recently been the focus of much research as a next-generation pharmaceutical modality. However, a number of peptides have problems such as low cell membrane permeability and linear peptides are easily degraded by metabolic enzymes.

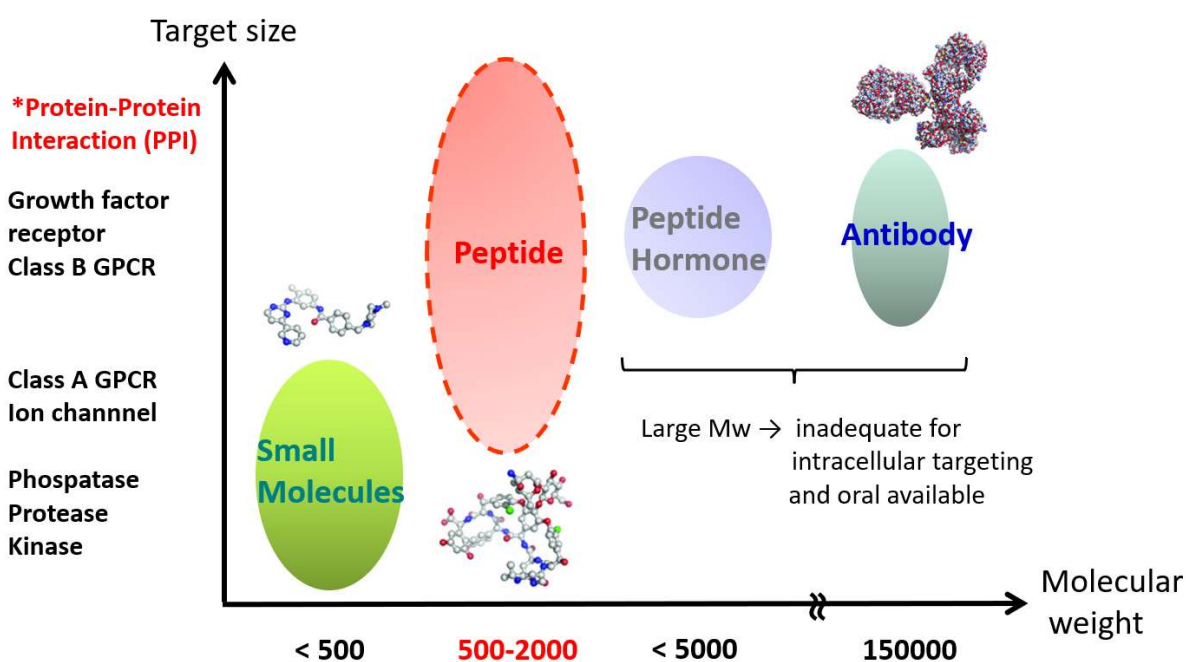


Fig. 1-1 Status of peptide drugs.

1.3 Peptide drug discovery targeting PPIs

Protein-protein interaction (PPI) plays an extremely important role in biological activities such as enzyme activity, signal transduction, and protein homeostasis, and is involved in the origin and progression of diseases. Based on the results of the human genome analysis completed in 2003, the total number of PPIs present in the body is estimated to be more than 300,000 patterns²⁾. The relationship between the proteins involved in PPI and the disease is summarized in Table 1-1³⁻²⁹⁾.

The contact surface area between proteins involved in PPI is large, ranging from 1500 to 3000 Å², and the shape of the PPI contact interface is generally flat or looped. On the other hand, proteins that can be involved in small molecules are grooved or pocketed with a contact surface area of 300-1000 Å². In addition, most PPIs are found in the cytoplasm and nucleus of cells, which cannot be reached by biologics due to large molecular structures.

Since peptides are considered to be a modality that can combine intracellular migration and target-specific affinity, they are expected to be a promising drug discovery modality for intracellular PPI targets³⁰⁾, and peptide drug discovery is underway for anticancer agents, angiogenesis inhibitors, and infectious diseases³¹⁾. If peptide drug discovery technology that regulates intracellular PPI can be established, it is expected to provide an excellent treatment for many diseases for which there has been no effective treatment or current treatments are not effective.

Table 1-1 Types of PPIs and corresponding diseases.

Proteins involved in PPI	Related disease	Ref.	Shape of PPI ³⁾	
MDM-2/p53	AML, CML, sarcoma and Solid tumors	3	Helix with a discontinuous epitope binding into a groove	
Bcl-xL/BAD(BAK)	Bcl-ABL leukemia	4		
ZipA/FtsZ	Bacterial infection	5		
S100B/p53	malignant melanoma	6		
β-catenin/TCF3 (TCF4)	Colon cancer	7		
Mcl-1/BH3	AML, Multiple myeloma	8		
SUR2/ESX	HER2-overexpressing cancers	9		
XIAP/SMAC	AML, lymphoma and solid tumors	3		Continuous epitope on β -sheet or β -strand and loops binding into surface with pockets
HIV integrase/LEDGF	HIV	10		
Integrins	IBD, ulcerative colitis and Crohn's disease	11		
RAD51/BRCA2	Ovarian, Brest cancer	12		
PDZ domains	ischemic brain damage	13		
NRP1/VEGFA	Skin cancer, endothelial cell migration	14		
Menin/MLL	Hepatocellular carcinoma	15		
YAP/TEAD	mesothelioma	16		
KEAP1/NRF2	Neurodegenerative Diseases	17	Binding into pocket in α β -propeller	
WDR5/MLL	AML	18		
Bromodomains	lung inflammation and asthma	19	Peptide with an anchor residue owing to post-translational modification binding into a pocket	
PDEδ/KRAS	pancreatic cancer	20		
SH2 domains	X-linked lymphoproliferative disease Breast cancer	21		
PLK1 PBD/peptide	AML, urothelial cancer	22		
VHL/HIF1α	Colon cancer	23		
IL-2/IL-2R	Renal cancer, Cancer immunotherapy	24	Two proteins both presenting discontinuous epitopes	
TNF/TNFR	Rheumatoid arthritis, IBD (inflammatory bowel disease)	25		
E2/E1	Viral infection	26		
MYC/MAX	tumor	27	A pair of helices with an elongated binding interaction	
NEMO/IKK	Rheumatoid arthritis, IBD (inflammatory bowel disease)	28		
Annexin II/P11 (S100A10)	Multiple myeloma, cancer metathesis	29		

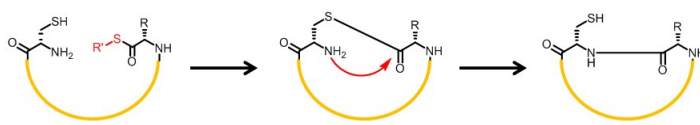

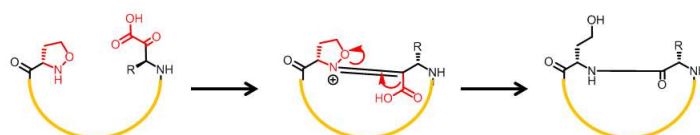
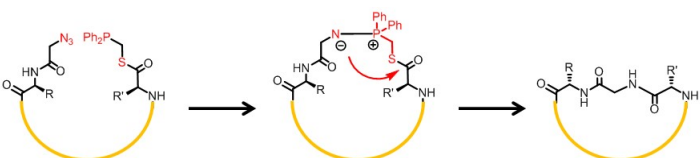
*Bold indicates intracellular PPI.

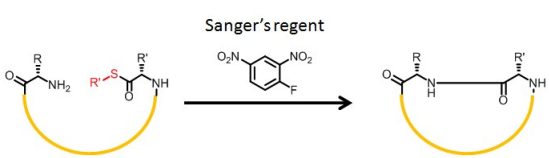
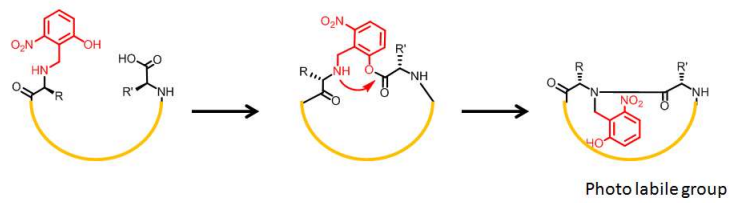
1. 4 Reactions for peptide cyclization

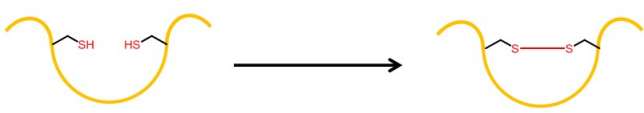
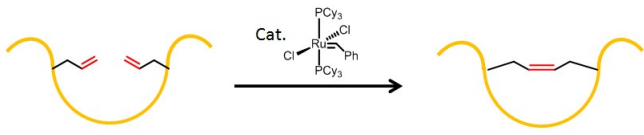
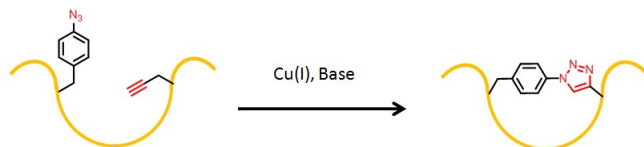
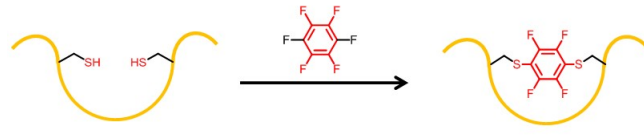
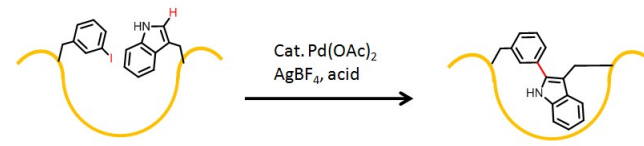
Many peptides have poor metabolic stability and bioavailability, making them unsuitable for pharmaceutical use. On the other hand, among peptides, cyclic peptides are highly resistant to exo- and endo-peptidases³²), and most of the approved peptide drugs are cyclic peptides³³). In addition, cyclic peptides are thought to have less entropy loss when binding to disease-causing targets because these molecules are constrained, and thus their target-binding ability is enhanced more readily than that of linear peptides³⁴). In addition, dissociation after the peptide binds to a target is slowed down, and the drug effect may be sustained for a long time³⁵). These characteristics are very useful for pharmaceuticals, and the drug discovery of cyclic peptides is expected to remain highly promising.

Many reviews have been reported on peptide cyclization methods³⁶). There are two types of cyclic peptides: head-to-tail cyclic peptides in which the N-terminal amino group is linked to the C-terminal carboxyl group by an amide bond, and side chain to side chain cyclic peptides in which the functional groups of the amino acid side chains are used to link the peptides by their characteristic chemical reactions. Table 1-2 shows the different types of cyclization reactions³⁷⁻⁴⁷).

Table 1-2 Example of cyclization reaction.

Type	Reaction	Ref
Head to tail (amide formation)	Native chemical ligation 	37
	Aminolysis of peptide thioester 	38
	KAHA ligation 	39
	Staudinger ligation (Traceless ligation) 	40

Head to tail (amide formation)	Sanger's Reagent 	41
	2-hydroxy-6-nitrobenzyl (HnB) 	42

Type	Reaction	Ref
Side chain to side chain	Disulfide 	43
	Ring closing metathesis 	44
	Huisgen reaction 	45
	Perfluoroaryl-Cysteine S_NAr reaction 	46
	C-H activation 	47

1. 5 Membrane permeability of cyclic peptides

Cyclic peptides are attracting attention as a drug discovery tool targeting intracellular PPIs. However, as predicted by Lipinski's 'Rule of 5'⁴⁸⁾, a well-known drug discovery index for low molecular weight compounds, the concern is that cell membrane permeability worsens as the molecular weight increases.

Molecular design to control the membrane permeability of cyclic peptides has been developed using Cyclosporin A (Fig. 1-2), a membrane permeable cyclic peptide consisting of 11 residues and a product of microbial metabolism. A number of studies on flexibility of the peptide molecular structure to adapt to the external environment⁴⁹⁾ (Fig. 1-3), N-methylation⁵⁰⁾, and shielding of the solvated surface by side chain design⁵¹⁾ (Fig. 1-4) have contributed to improve membrane permeability.

These improved cell membrane permeability effects are thought to be due to the increased passive diffusion of peptides into the low-polarity cell membrane when the polarity of the amide bonds can be offset by the intramolecular hydrogen bonds and the molecular structure surrounding the amide bonds. The improvement of cell membrane permeability by these molecular designs is expected to improve intestinal mesenteric absorption as well. Cellular evaluation showed that the cyclic peptides obtained by closed-ring metathesis, which is a side chain to side chain type cyclization method, can bind to intracellular MDM2/MDMX⁵²⁾. These results indicate that ring-closing metathesis-type cyclic peptides are an effective method for increasing cell membrane permeability. Based on these findings, ALRN-6924, a closed-ring metathesis cyclic peptide, has been applied to clinical development (Phase IIa) as an anti-tumor agent.

Furthermore, it has been reported that the incorporation of a ring structure into the main chain of cyclic peptides promotes the formation of intramolecular hydrogen bonds and enhances the cell membrane permeability of cyclic peptides. For example, Sanguinamide A (Fig. 1-5), a naturally occurring cyclic peptide of Mw 721 with a thiazole ring in its main chain, has a higher bioavailability (typically less than 2 %) than other peptides of similar molecular weight. This is thought to be due to that the hydrophobic ring structure forms two intramolecular hydrogen bonds, and shields the polarity of the amide group to suppress the polarity of the peptide molecule surface⁵³⁾. Shuto et al. introduced a rigid cyclopropane ring into the peptide main chain and investigated the correlation between the control of peptide molecular structure and cell membrane permeability. Solution structure analysis using NMR revealed that the cyclopropane ring-incorporated peptide molecules are anchored in a conformation favorable for passive diffusion and exhibit high cell membrane permeability⁵⁴⁾.

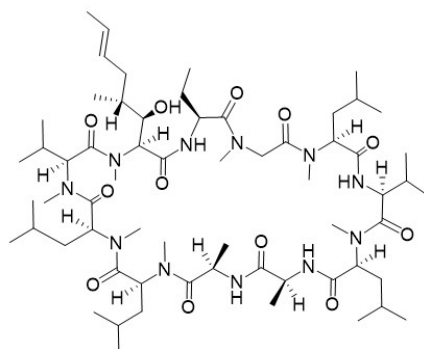


Fig. 1-2 Structure of Cyclosporin A.

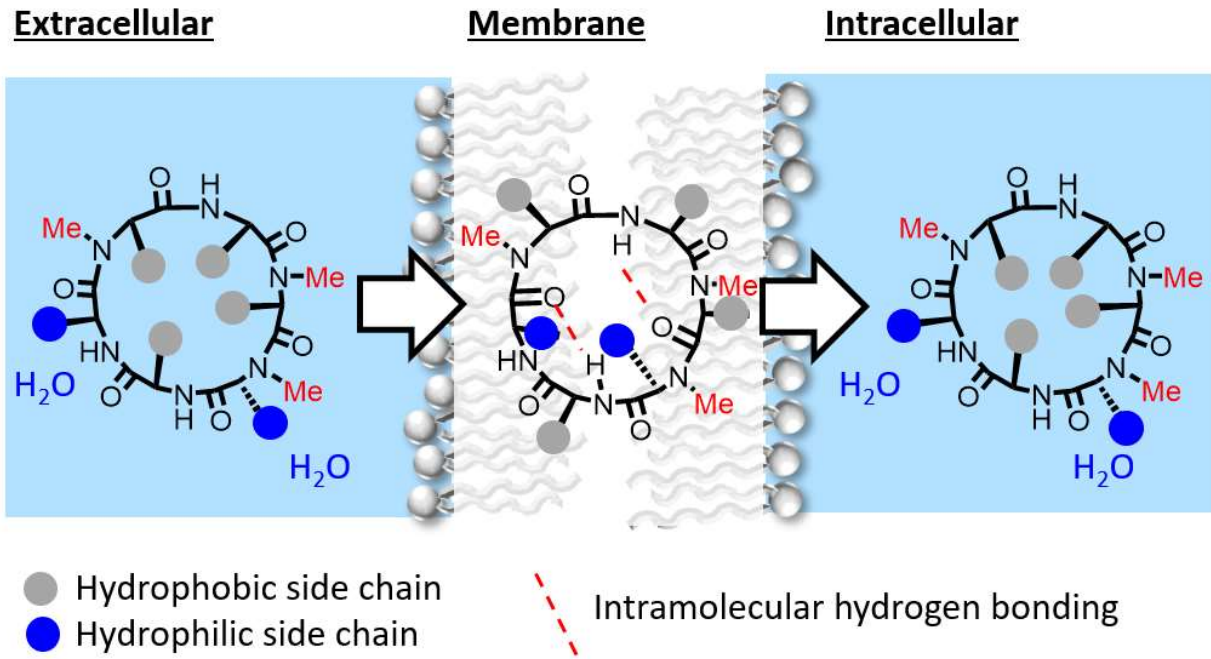


Fig. 1-3 Membrane permeation mechanisms of cyclic peptides by environmental conformational changes.

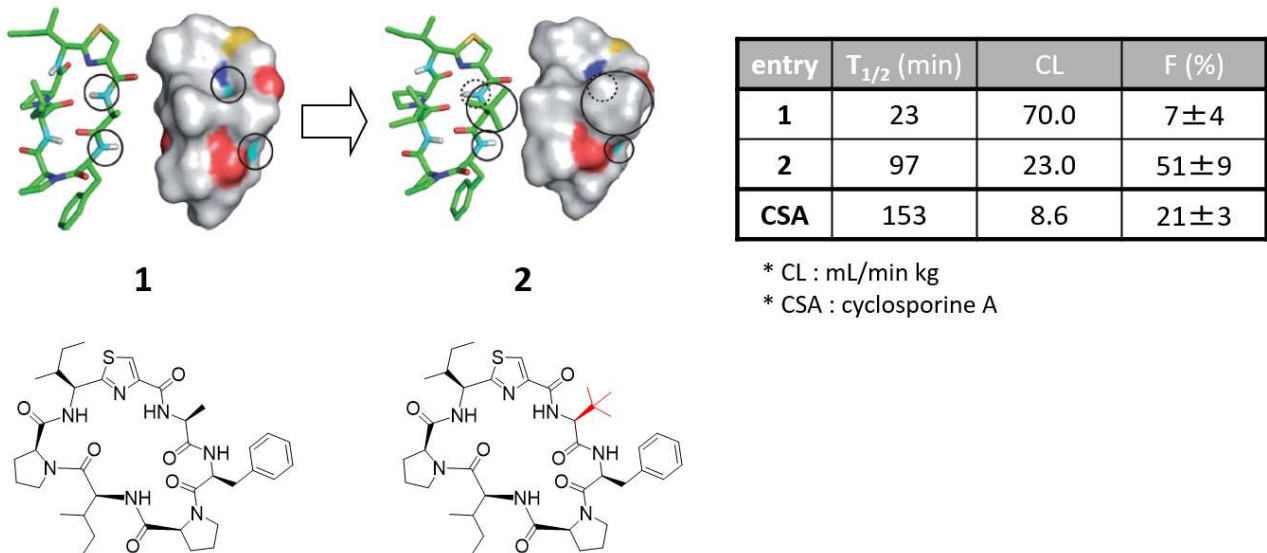
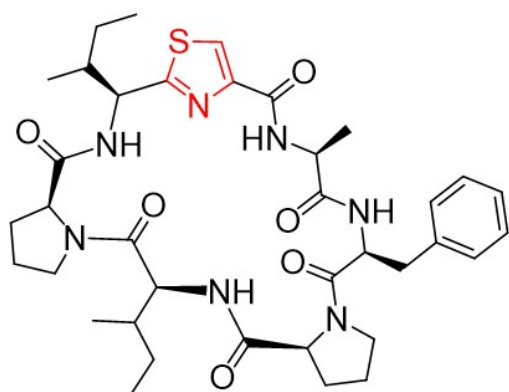


Fig. 1-4 Control of solvation and adjustment of bioavailability by substituents.⁵¹⁾



Sanguinamide A

HBA 13

CLogP 5.4

F 7 ± 4 %

C_{max} 40 nM

T_{max} 60 min

T_{1/2} 23 min

(Wistar rat, 10 mg/kg, oral)

Fig. 1-5 Structure and pharmacokinetic parameters of Sanguinamide A.

1. 6 Peptide screening system

An innovative technology called "in vitro display technology" has been developed for the acquisition of starting materials for peptide drug discovery. In vitro display technology includes the generation of peptide libraries and selection of starting materials in a short period of time using a protein synthesis system of biological origin. There are several types of in vitro display technologies: phage display, mRNA display, cDNA display, and ribosome display.

Phage display is a technique for selecting hit peptides by constructing a library of peptides with different sequences on each phage. Random peptide sequences are introduced into the phage, and the host is infected to release the peptide-displaying phage. The peptide-displaying phage will be incubated with the drug target, and the phage bound to the drug target will be collected. The selected phage is then transfected into the host microorganism and amplified to read the peptide sequence. However, phage display has some limitations such as small library size ($\sim 10^8$ species), bias in translatable peptide sequences depending on the host, and usually cannot produce peptides containing non-natural amino acids.

Szostak et al. and Fushimi et al. groups developed mRNA display respectively, utilizing a cell-free biochemical peptide synthesis system⁵⁵⁾ at the same time. Since no cells are used, hit peptides can be selected from a huge peptide library of $\sim 10^{13}$ species. The main steps of mRNA display are shown below⁵⁶⁾ (Fig. 1-6).

- Preparation of mRNA from DNA encoding random peptide sequence.
- Conjugation of mRNA with puromycin linker and translation in cell-free translation system.
- Puromycin-mediated ligation of the peptide to the mRNA to form a peptide-mRNA complex.
- Selection of the complex on immobilized drug target to obtain the complex that can bind to the target.
- Reverse transcription of mRNA encoding the selected peptide and amplification of cDNA.
- Repeat a) through e) to select for peptides that bind more strongly.
- Sequencing of the cDNA to confirm the sequence of the hit peptide.

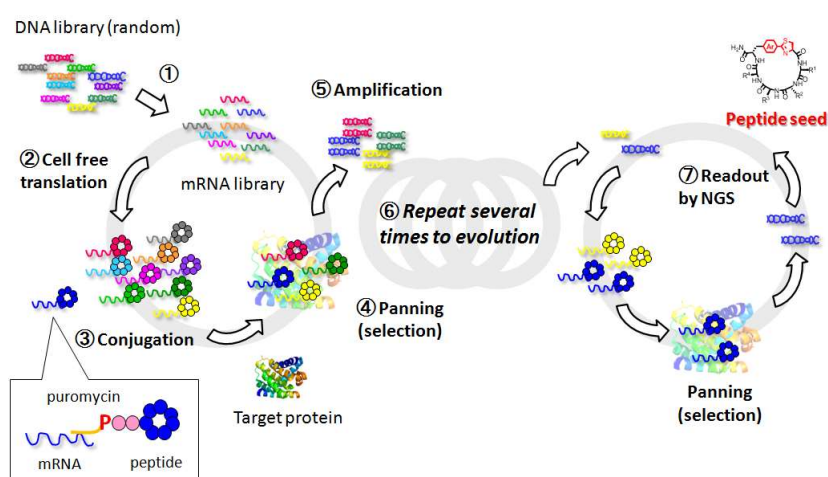


Fig. 1-6 Process of mRNA display.

1.7 Cell-free translation using non-natural amino acids

Cell-free translation system that can introduce a wide variety of non-natural amino acids in addition to the 20 natural amino acids used for protein synthesis could be applied to mRNA display. The incorporation of non-natural amino acids can expand the chemical space of the peptide library and the possibility of obtaining hit peptides for various disease targets.

There are many studies that have reported successful incorporation of non-natural amino acids in cell-free translation. Schultz et al. chemically acylated amber suppressor tRNA corresponding to amber stop codon UAG with non-natural amino acids, and used them to regioselectively introduce non-natural amino acids into proteins⁵⁷. Chamberlin et al. synthesized non-natural amino acid-containing peptides based on a similar concept at the same time⁵⁸. Foster et al. used a reconstituted cell-free translation system without aminoacyl-tRNA synthetase to translate a peptide consisting of two natural amino acids and three non-natural amino acids using multiple sense codons⁵⁹. Suga et al. used an enzymatic RNA catalyst, Flexizyme, for aminoacylation of artificial tRNAs, and constructed a peptide synthesis system that efficiently introduces non-natural amino acids in response to sense codons vacated by excluding some of the 20 natural amino acids⁶⁰. Szostak et al. constructed a peptide synthesis system simultaneously encoding 10 non-natural amino acids that can be recognized by aminoacyl-tRNA synthetases⁶¹. On the other hand, Hohsaka et al. constructed a system that translates four-base codons into non-natural amino acids while natural amino acids are encoded by triplet codons, and synthesized proteins containing one or two non-natural amino acids⁶². Bain et al. succeeded in synthesizing polypeptides containing non-natural amino acids by additional codon-anticodon pairs having non-natural nucleobases with different styles of hydrogen bonding pairs⁶³. Hirao et al. reported the synthetic nucleobases of pyridine-2-one and 2-amino-6-(thienyl) purine pair, and they have successfully synthesized proteins using codon-anticodon pairs containing these artificial nucleic acids⁶⁴.

Roberts et al. reported the first example of mRNA display including non-natural amino acids⁶⁵. A peptide library was constructed by mRNA display from 20 natural amino acids and biocytin, a lysine derivative with biotin on a side chain, as a non-natural amino acid. The introduction of the non-natural amino acid was performed at the position of UAG in the mRNA (Fig. 1-7). Currently, diverse peptide libraries including non-natural amino acids have been constructed by mRNA display and applied to peptide drug discoveries.

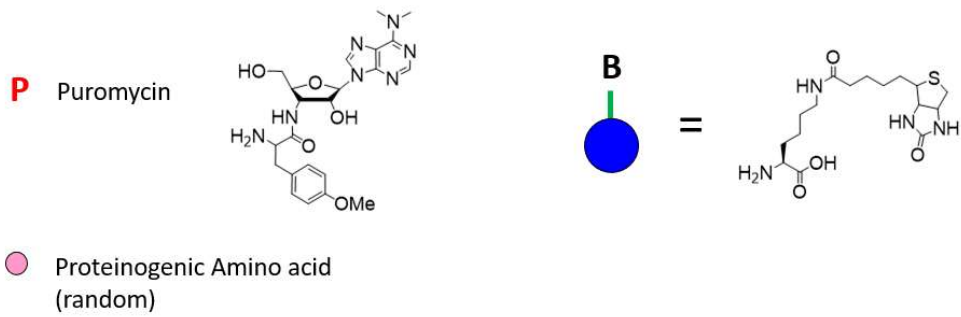
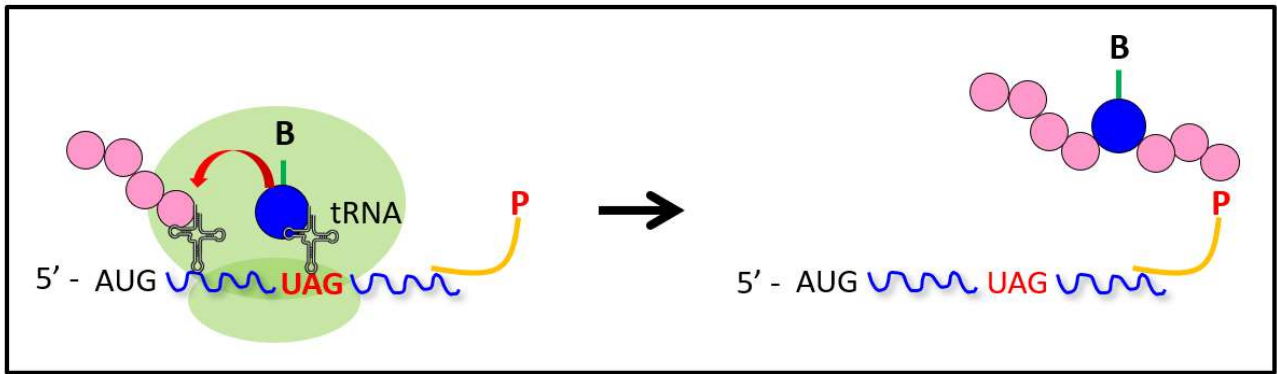


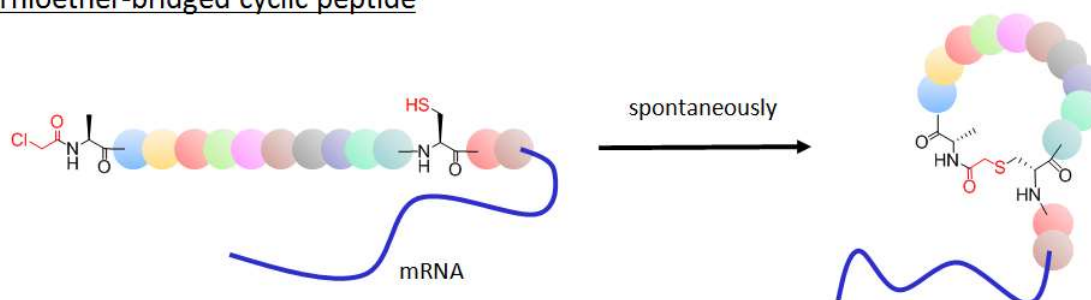
Fig. 1-7 First example of mRNA display including non-natural amino acids.

1-8. mRNA display of cyclic peptide library

As described in 1-4, cyclic peptides are regarded as a promising modality for peptide drugs because of their ability to enhance metabolic stability, membrane permeability, and target affinity. In order to screen for cyclic peptide-type hit compounds that can bind to desired drug targets, peptide cyclization reactions have been incorporated into mRNA display⁶⁶. mRNA display of cyclic peptides can be divided into two types based on the form of the cyclization reaction: one is cyclization using the introduced non-natural amino acids (Fig. 1-8), and the other is cyclization by the addition of polycyclic cross-linkers (Fig. 1-9).

As an example of the former, Suga et al. developed cell-free translation in which a non-natural amino acid with a chloroacetyl group is placed at the N-terminus and undergoes intramolecular nucleophilic substitution reaction with the thiol group of Cys in the peptide chain to generate cyclic peptides (Fig. 1-8a)⁶⁷. Using this cyclization reaction, hit peptides against drug targets such as E6AP⁶⁸, SIRT2⁶⁹, VEGFR2⁷⁰ and MATE⁷¹ were obtained. In addition, intramolecular peptide cyclization was applied to mRNA display using the native chemical ligation between N-terminal Cys and non-natural amino acids carrying thioesters (Fig. 1-8b)⁷².

a) Thioether-bridged cyclic peptide



b) Amide-bridged cyclic peptide

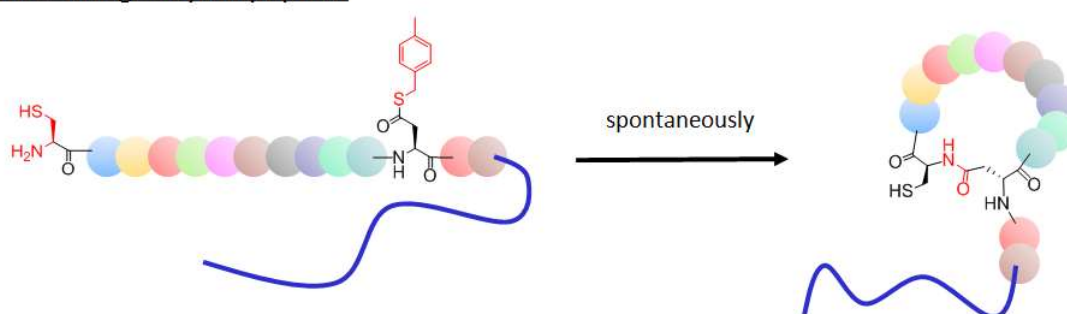


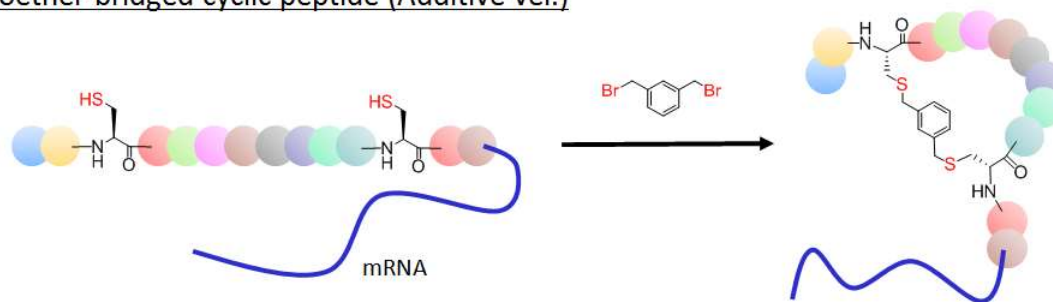
Fig. 1-8 Methods of peptide cyclization by introducing non-natural amino acids into peptides.

As an example of the latter, Szostak et al. synthesized a linear peptide containing two Cys by cell-free translation and adapted the system to mRNA display by adding dibromoxylene for peptide cyclization to screen for cyclic peptides that have affinity to thrombin⁷³). Roberts et al. prepared a cyclic peptide library by cross-linking the N-terminal amino group of a linear peptide generated by cell-free translation with the amino group of the Lys side chain in an elongated chain by adding disuccinimidyl glutarate, and obtained a cyclic peptide that binds to Gαi1⁷⁴).

Although both cyclization methods have been able to obtain hit peptides by mRNA display, in the latter case, there are some risks that highly reactive cross-linker reacts with the materials involved in the display method and generation of peptide dimerization may affect the screening results.

Most of the cyclization methods used for mRNA display are based on the formation of amide bonds or thioethers, and there are no reports of cyclization methods that form ring structures on the main chain. For example, cell-free translation using the Huisgen reaction to form triazole rings has been reported⁷⁵), but there are no reports of its adaptation to mRNA display. Furthermore, there are no reports on the construction of large cyclic peptide libraries with high cell membrane permeability.

Thioether-bridged cyclic peptide (Additive ver.)



Amide-bridged cyclic peptide (Additive ver.)

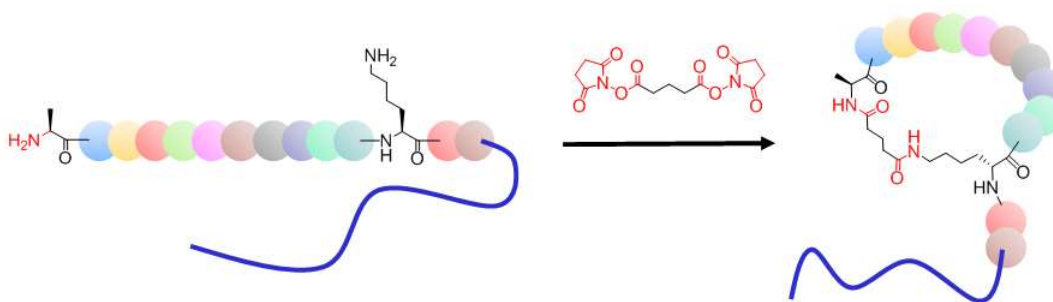


Fig. 1-9 Methods of peptide cyclization by adding multifunctional crosslinking agents.

1.9 Content of this thesis

In this thesis, I described that thiazoline ring-bridged peptide cyclization proceeds in a variety of amino acid sequences, and discuss the cyclization reactivity. In addition, I demonstrated that thiazoline ring-bridged cyclic peptides have membrane permeability and revealed the factors responsible for the membrane permeability. Furthermore, I described the synthesis of thiazoline ring-bridged cyclic peptides with cell-free translation.

In Chapter 2, I described the development of a new peptide cyclization method with a ring structure in the main chain of cyclic peptides. The concept of the cyclization reaction is based on the synthetic method of Luciferin, in which a Cys residue is placed at the N-terminus and a non-natural amino acid with a cyano group on the side chain is placed at the C-terminus, resulting in the spontaneous formation of a thiazoline ring. The control of the cyclization reaction rate and the diversity of amino acid sequences of peptides that can be adapted to the cyclization reaction were also examined.

In Chapter 3, I described the PAMPA model membrane permeability of thiazoline ring-bridged cyclic peptides. The characteristics of thiazoline ring-bridged cyclic peptides were compared with those of thioether- and amide-bridged cyclic peptides. In order to analyze the membrane permeability factors, the effect of changing the amino acid sequence and hydrophobicity on the membrane permeability and the solution structure were analyzed using NMR.

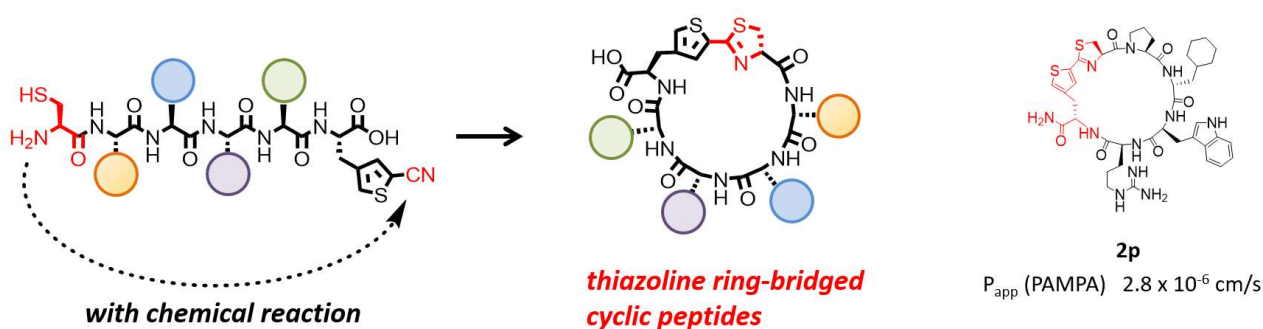


Fig. 1-10 Synthesis and model membrane permeability of thiazoline ring-bridged cyclic peptides.

In Chapter 4, I described adaptation of the thiazoline ring-bridged cyclization to cell-free translation systems based on the fact that the cyclization reaction proceeds in aqueous solution. To confirm that the reaction proceeds in a variety of peptide sequences, I examined the effect of the length of the amino acid sequence and the presence of Cys in the chain other than the N terminus on the cyclization reaction.

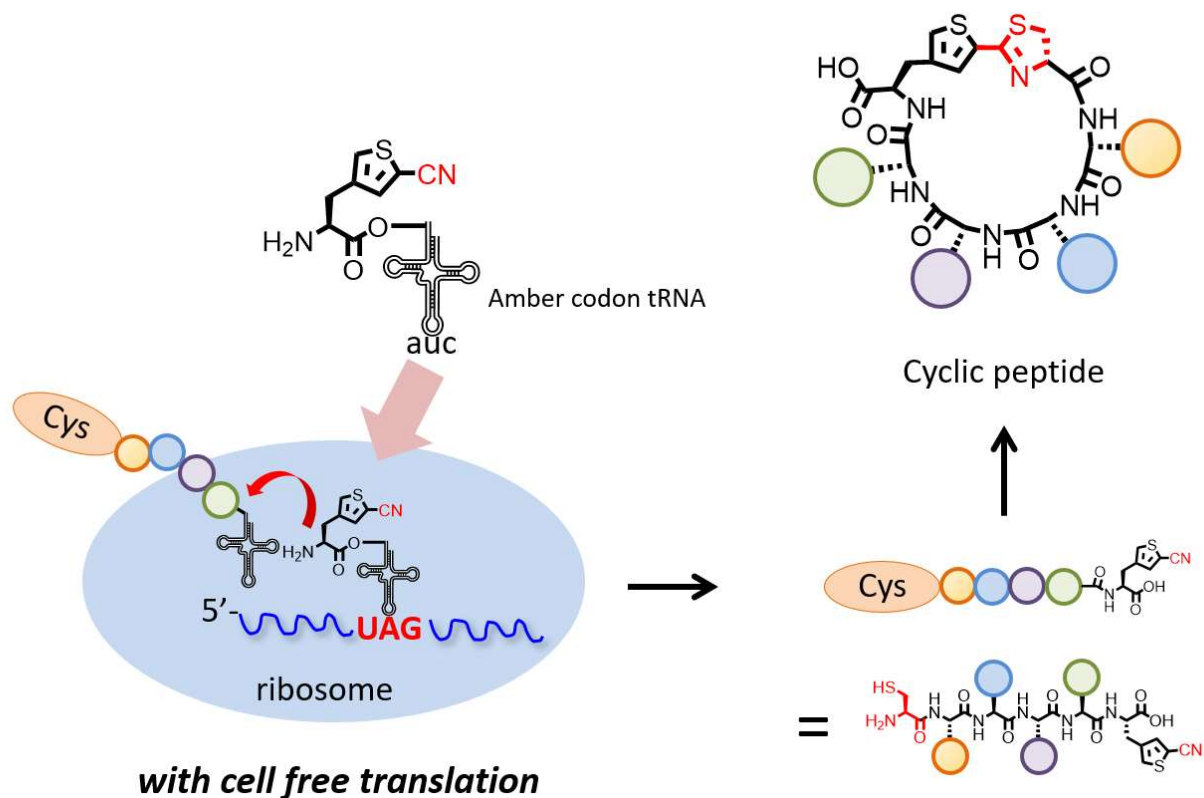


Fig. 1-11 Synthesis of thiazoline-ring bridged cyclic peptides by cell-free translation.

References

- 1) Antoine Henninot, James C. Collins, John M. Nuss The Current State of Peptide Drug Discovery: Back to the Future? *J. Med. Chem.* **2018**, *61*, 1382-1414
- 2) Anna Malovannaya, Rainer B. Lanz, Sung Yun Jung, Yaroslava Bulynko, Nguyen T. Le, Doug W. Chan, Chen Ding, Yi Shi, Nur Yucer, Giedre Krenciute, Beom-Jun Kim, Chunshu Li, Rui Chen, Wei Li, Yi Wang, Bert W. O'Malley, Jun Qin Analysis of the human endogenous coregulator complexome *Cell* **2011**, *145*, 787-799
- 3) Duncan E. Scott, Andrew R. Bayly, Chris Abell, John Skidmore Small molecules, big targets: drug discovery faces the protein-protein interaction challenge *Nat. Rev. Drug Discovery* **2016**, *15*, 533-550
- 4) Gustavo P. Amarante-Mendes, Anne J. McGahon, Walter K Nishioka, Daniel E. H. Afar, Owen N. Witte, Douglas R Green Bcl-2-independent Bcr–Abl-mediated resistance to apoptosis: protection is correlated with up regulation of Bcl-x_L *Oncogene* **1998**, *16*, 1383-1390
- 5) a) Elisa J. Cabré, Alicia Sánchez-Gorostiaga, Paolo Carrara, Noelia Roper, Mercedes Casanova, Pilar Palacios, Pasquale Stano, Mercedes Jiménez, Germán Rivas, Miguel Vicente Bacterial Division Proteins FtsZ and ZipA Induce Vesicle Shrinkage and Cell Membrane Invagination *J. Biol. Chem.* **2013**, *288*, 26625-26634, b) Lidia Mosyak, Yan Zhang, Elizabeth Glasfeld, Steve Haney, Mark Stahl, Jasbir Seehra, William S. Somers The bacterial cell-division protein ZipA and its interaction with an FtsZ fragment revealed by X-ray crystallography *EMBO J.* **2000**, *19*, 3179-3191
- 6) Chihoko Yoshimura, Takamitsu Miyafusa, Kouhei Tsumoto Identification of small-molecule inhibitors of the human S100B–p53 interaction and evaluation of their activity in human melanoma cells *Bioorg. Med. Chem.* **2013**, *21*, 1109-1115
- 7) Kenzui Taniue, Akiko Kurimoto, Yasuko Takeda, Takeshi Nagashima, Mariko Okada-Hatakeyama, Yuki Katou, Katsuhiko Shirahige, Tetsu Akiyama ASBEL–TCF3 complex is required for the tumorigenicity of colorectal cancer cells *Proc. Natl. Acad. Sci. USA* **2016**, *113*, 12739-12744
- 8) Stefan P. Glaser, Erinna F. Lee, Evelyn Trounson, Philippe Bouillet, Andrew Wei, W. Douglas Fairlie, David J. Izon, Johannes Zuber, Amy R. Rappaport, Marco J. Herold, Warren S. Alexander, Scott W. Lowe, Lorraine Robb, Andreas Strasser, Anti-apoptotic Mcl-1 is essential for the development and sustained growth of acute myeloid leukemia *Genes Dev.* **2012**, *26*, 120-125
- 9) Shinichi Asada, Yongmun Choi, Masaki Yamada, Shao-Chun Wang, Mien-Chie Hung, Jun Qin, and Motonari Uesugi External control of Her2 expression and cancer cell growth by targeting a Ras-linked coactivator *Proc. Natl. Acad. Sci. USA* **2002**, *99*, 12747-12752
- 10) Eric M. Poeschla Integrase, LEDGF/p75 and HIV Replication *Cell Mol Life Sci.* **2008**, *65*, 1403-1423
- 11) Klaus Ley, Jesus Rivera-Nieves, William J. Sandborn, Sanford Shattil Integrin-based therapeutics: biological basis, clinical use and new drugs *Nat. Rev. Drug Discov.* **2016**, *15*, 173-183
- 12) Taha Shahid, Joanna Soroka, Eric Kong, Laurent Malivert, Michael J McIlwraith, Tillman Pape, Stephen C West, Xiaodong Zhang Structure and mechanism of action of the BRCA2 breast cancer tumor suppressor *Nat. Struct Mol Biol.* **2014**, *21*, 962-968
- 13) Nick X. Wang 1, Ho-Jin Lee, Jie J. Zheng Therapeutic use of PDZ protein-protein interaction antagonism *Drug*

News Perspect. **2008**, *21*, 137-141

14) Benjamin Beck, Gregory Driessens, Steven Goossens, Khalil Kass Youssef, Anna Kuchnio, Amélie Caauwe, Panagiota A. Sotiropoulou, Sonja Loges, Gaelle Lapouge, Aurélie Candi, Guilhem Mascre, Benjamin Drogat, Sophie Dekoninck, Jody J. Haigh, Peter Carmeliet, Cédric Blanpain A. vascular niche and a VEGF-Nrp1 loop regulate the initiation and stemness of skin tumours *Nature* **2011**, *478*, 399-403

15) Bin Xu, Shan-Hua Li, Rong Zheng, Shu-Bin Gao, Li-Hong Ding, Zhen-Yu Yin, Xiao Lin, Zi-Jie Feng, Sheng Zhang, Xiao-Min Wang, Guang-Hui Jin Menin promotes hepatocellular carcinogenesis and epigenetically up-regulates Yap1 transcription *Proc. Natl. Acad. Sci. USA* **2013**, *110*, 17480-17485

16) a) Zhisen Zhang, Zhaohu Lin, Zheng Zhou, Hong C. Shen, S. Frank Yan, Alexander V. Mayweg, Zhiheng Xu, Ning Qin, Jason C. Wong, Zhenshan Zhang, Yiping Rong, David C. Fry, Taishan Hu Structure-Based Design and Synthesis of Potent Cyclic Peptides Inhibiting the YAP–TEAD Protein–Protein Interaction *ACS Med. Chem. Lett.* **2014**, *5*, 993-998, b) Gavitt A. Woodard, Yi-Lin Yang, Liang You, David M. Jablons Drug development against the hippo pathway in mesothelioma *Transl. Lung Cancer Res.* **2017**, *6*, 335-342

17) Chenere P. Ramsey, Charles A. Glass, Marshall B. Montgomery, Kathryn A. Lindl, Gillian P. Ritson, Luis A. Chia, Ronald L. Hamilton, Charleen T. Chu, Kelly L. Jordan-Sciutto Expression of Nrf2 in neurodegenerative diseases *J. Neuropathol Exp. Neurol.* **2007**, *66*, 75-85

18) a) Akihiko Yokoyama, Zhong Wang, Joanna Wysocka, Mrinmoy Sanyal, Deborah J. Aufiero, Issay Kitabayashi, Winship Herr, Michael L. Cleary Leukemia proto-oncoprotein MLL forms a SET1-like histone methyltransferase complex with menin to regulate Hox gene expression *Mol. Cell Biol.* **2004**, *24*, 5639-5649, b) Ji-Joon Song, Robert E Kingston WDR5 interacts with mixed lineage leukemia (MLL) protein via the histone H3-binding pocket *J. Biol. Chem.* **2008**, *283*, 35258-35264

19) Susanne Muller, Panagis Filippakopoulos, Stefan Knapp Bromodomains as therapeutic targets *Expert Rev. Mol. Med.* **2011**, *13*, e29

20) a) Gunther Zimmermann, Björn Papke, Shehab Ismail, Nachiket Vartak, Anchal Chandra, Maike Hoffmann, Stephan A. Hahn, Gemma Triola, Alfred Wittinghofer, Philippe I. H. Bastiaens, Herbert Waldmann Small molecule inhibition of the KRAS–PDEδ interaction impairs oncogenic KRAS signaling *Nature* **2013**, *497*, 638-642, b) Björn Papke, Sandip Murarka, Holger A. Vogel, Pablo Martín-Gago, Marija Kovacevic, Dina C. Truxius, Eyad K. Fansa, Shehab Ismail, Gunther Zimmermann, Kaatje Heinelt, Carsten Schultz-Fademrecht, Alaa Al Saabi, Matthias Baumann, Peter Nussbaumer, Alfred Wittinghofer, Herbert Waldmann, Philippe I.H. Bastiaens Identification of pyrazolopyridazinones as PDEδ inhibitors *Nat. Commun.* **2016**, *7*, 11360

21) a) Christopher J. Danpure, Gill Rumsby Molecular aetiology of primary hyperoxaluria and its implications for clinical management *Expert Rev. Mol. Med.* **2004**, *6*, 1-16, b) Pietro Morlacchi, Fredika M. Robertson, Jim Klostergaard, John S. McMurray Targeting SH2 domains in breast cancer *Future Med. Chem.* **2014**, *6*, 1909-1926

22) a) Melanie Janning, Walter Fiedler Volasertib for the treatment of acute myeloid leukemia: a review of preclinical and clinical development *Future Oncology* **2014**, *10*, 1157-1165, b) Hartmut Döhner, Michael Lübbert, Walter Fiedler, Loic Fouillard, Alf Haaland, Joseph M. Brandwein, Stephane Lepretre, Oumedaly Reman, Pascal Turlure, Oliver G. Ottmann, Carsten Müller-Tidow, Alwin Krämer, Emmanuel Raffoux, Konstanze Döhner, Richard F. Schlenk, Florian Voss, Tillmann Taube, Holger Fritsch, Johan Maertens Randomized, phase 2 trial of

- low-dose cytarabine with or without volasertib in AML patients not suitable for induction therapy *Blood* **2014**, *124*, 1426-1433, c) B. T. Gjertsen, P Schöffski Discovery and development of the Polo-like kinase inhibitor volasertib in cancer therapy *Cancer* **2014**, *120*, 976-982
- 23) Kyeong Lee, Jung Eun Kang, Song-Kyu Park, Yinglan Jin, Kyung-Sook Chung, Hwan-Mook Kim, Kiho Lee, Moo Rim Kang, Myung Kyu Lee, Kyung Bin Song, Eun-Gyeong Yang, Jung-Jun Lee, Misun Won LW6, a novel HIF-1 inhibitor, promotes proteasomal degradation of HIF-1 α via upregulation of VHL in a colon cancer cell line *Biochem Pharmacol.* **2010**, *80*, 982-989
- 24) Tao Jiang, Caicun Zhou, Shengxiang Ren Role of IL-2 in cancer immunotherapy *Oncoimmunology* **2016**, *5*, e1163462
- 25) Maida Wong, David Ziring, Yael Korin, Sheetal Desai, Sungjin Kim, Jan Lin, David Gjertson, Jonathan Braun, Elaine Reed, Ram Raj Singh TNF α blockade in human diseases: mechanisms and future directions *Clin Immunol.* **2008**, *126*, 121-136
- 26) J. Sedman, A. Stenlund The initiator protein E1 binds to the bovine papillomavirus origin of replication as a trimeric ring-like structure *EMBO J.* **1996**, *15*, 5085-5092
- 27) a) Catherine M. Shachaf and Dean W. Felsher Tumor Dormancy and MYC Inactivation: Pushing Cancer to the Brink of Normalcy *Cancer Res.* **2005**, *65*, 4471-4474, b) Laura Soucek, Jonathan Whitfield, Carla P. Martins, Andrew J. Finch, Daniel J. Murphy, Nicole M. Sodik, Anthony N. Karnezis, Lamorna Brown Swigart, Sergio Nasi, Gerard I. Evan Modelling Myc inhibition as a cancer therapy *Nature* **2008**, *455*, 679-683
- 28) Sander W. Tas, Margriet J. Vervoordeldonk, Najat Hajji, Michael J. May, Sankar Ghosh, Paul P. Tak Local treatment with the selective I κ B kinase β inhibitor NEMO-binding domain peptide ameliorates synovial inflammation *Arthritis Res. Ther.* **2006**, *8*, R86, b) Shaival H. Davé, Jeremy S. Tilstra, Katsuyoshi Matsuoka, Fengling Li, Thomas Karrasch, Jennifer K. Uno, Antonia R. Sepulveda, Christian Jobin, Albert S. Baldwin, Paul D. Robbins, Scott E. Plevy Amelioration of Chronic Murine Colitis by Peptide-Mediated Transduction of the I κ B Kinase Inhibitor NEMO Binding Domain Peptide *J. Immunol.* **2007**, *179*, 7852-7859
- 29) a) Hongyu Bao, Miao Jiang, Mingqing Zhu, Fei Sheng, Jia Ruan, Changgeng Ruan Overexpression of Annexin II affects the proliferation, apoptosis, invasion and production of proangiogenic factors in multiple myeloma *Int. J. Hematol.* **2009**, *90*, 177-185, b) Mahesh C. Sharma, Meena Sharma, The role of annexin II in angiogenesis and tumor progression: a potential therapeutic target *Curr. Pharm. Des.* **2007**, *13*, 3568-3575, c) Noor A. Lokman, Miranda P. Ween, Martin K. Oehler, Carmela Ricciardelli The role of annexin A2 in tumorigenesis and cancer progression *Cancer Microenviron.* **2011**, *4*, 199-208
- 30) Ziqing Qia, Patrick G Dougherty, Dehua Pei Targeting intracellular protein-protein interactions with cell-permeable cyclic peptides *Curr Opin Chem Biol.* **2017**, *38*, 80-86
- 31) Heriberto Bruzzoni-Giovanelli, Valerie Alezra, Nicolas Wolff, Chang-Zhi Dong, Pierre Tuffery, Angelita Rebollo Interfering peptides targeting protein-protein interactions: the next generation of drugs? *Drug Discovery Today* **2018**, *23*, 272-285
- 32) Joel D A Tyndall, Tessa Nall, David P Fairlie Proteases universally recognize beta strands in their active sites *Chem Rev.* **2005**, *105*, 973-999
- 33) Alessandro Zorzi, Kaycie Deyle, Christian Heinis Cyclic peptide therapeutics: past, present and future *Curr*

Opin Chem Biol. **2017**, *38*, 24-29

- 34) a) Modern Supramolecular Chemistry: Strategies for Macrocyclic Synthesis 2008, 1-28, b) Christian Heinis, Trevor Rutherford, Stephan Freund, Greg Winter Phage-encoded combinatorial chemical libraries based on bicyclic peptides *Nat. Chem. Biol.* **2009**, *5*, 502-507
- 35) Vernon Seow, Junxian Lim, Adam J. Cotterell, Mei-Kwan Yau, Weijun Xu, Rink-Jan Lohman, W. Mei Kok, Martin J. Stoermer, Matthew J. Sweet, Robert C. Reid, Jacky Y. Suen, David P. Fairlie Receptor residence time trumps drug-likeness and oral bioavailability in determining efficacy of complement C5a antagonists *Sci Rep.* **2016**, *6*, 24575.
- 36) a) Yu Heng Lau, Peterson de Andrade, Yuteng Wua, David R. Spring Peptide stapling techniques based on different macrocyclisation chemistries *Chem.Soc.Rev.* **2015**, *44*, 91-102, b) Christopher J. White, Andrei K. Yudin Contemporary strategies for peptide macrocyclization *Nat.Chem.* **2011**, *3*, 509-524, c) John S. Davies The cyclization of peptides and depsipeptides *J. Pept Sci.* **2003**, *9*, 471-501
- 37) Philip E. Dawson, Tom W. Muir, Ian Clark-Lewis, Stephen B. H. Kent Synthesis of Proteins by Native Chemical Ligation *Science* **1994**, *266*, 776-779
- 38) Yangmei Li, Austin Yongye, Marc Giulianotti, Karina Martinez-Mayorga, Yongping Yu, Richard A. Houghten Synthesis of Cyclic Peptides through Direct Aminolysis of Peptide Thioesters Catalyzed by Imidazole in Aqueous Organic Solutions *J. Comb. Chem.* **2009**, *11*, 1066-1072
- 39) Florian Rohrbacher, Gildas Deniau, Anatol Lutherb, Jeffrey W. Bode Spontaneous head-to-tail cyclization of unprotected linear peptides with the KAHA ligation *Chem. Sci.* **2015**, *6*, 4889-4896
- 40) Rolf Kleinewieschede, Christian P. R. Hackenberger Chemoselective Peptide Cyclization by Traceless Staudinger Ligation *Angew. Chem. Int. Ed.* **2008**, *47*, 5984-5988
- 41) Kaname Sasaki, David Crich Cyclic Peptide Synthesis with Thioacids *Org. Lett.* **2010**, *12*, 3254-3257
- 42) Carolyn Hede, T. Johnson, D. Owen, M. Quibell, R.C. Sheppard Some 'difficult sequences' made easy *Int. J. Pept. Protein Res.* **1994**, *43*, 431-440
- 43) David Y. Jackson, David S. King, Jean Chmielewski, Sunil Singh, Peter G. Schultz General approach to the synthesis of short α -helical peptides *J. Am. Chem. Soc.* **1991**, *113*, 9391-9392
- 44) Scott J. Miller, Helen E. Blackwell, Robert H. Grubbs Application of Ring-Closing Metathesis to the Synthesis of Rigidified Amino Acids and Peptides *J. Am. Chem. Soc.* **1996**, *118*, 9606-9614
- 45) Sonia Cantel, Alexandra Le Chevalier Isaad, Mario Scrima, Jay J. Levy, Richard D. DiMarchi, Paolo Rovero, Jose A. Halperi, Anna Maria D' Ursi, Anna Maria Papini, Michael Chorev Synthesis and Conformational Analysis of a Cyclic Peptide Obtained via i to i+4 Intramolecular Side-Chain to Side-Chain Azide-Alkyne 1,3-Dipolar Cycloaddition *J. Org. Chem.* **2008**, *73*, 5663-5674
- 46) a) Alexander M. Spokoyny, Yekui Zou, Jingjing J. Ling, Hongtao Yu, Yu-Shan Lin, and Bradley L. Pentelute A Perfluoroaryl-Cysteine S_NAr Chemistry Approach to Unprotected Peptide Stapling *J. Am. Chem. Soc.* **2013**, *135*, 5946-5949, b) Guillaume Lautrette, Fayçal Touti, Hong Geun Lee, Peng Dai, Bradley L. Pentelute Nitrogen Arylation for Macrocyclization of Unprotected Peptides *J. Am. Chem. Soc.* **2016**, *138*, 8340-8343
- 47) Lorena Mendive-Tapia, Sara Preciado, Jesús García, Rosario Ramón, Nicola Kielland, Fernando Albericio, Rodolfo Lavilla New peptide architectures through C-H activation stapling between

tryptophan-phenylalanine/tyrosine residues *Nat. Commun.* **2015**, *6*, 7160.

48) a) Christopher A. Lipinski, Franco Lombardo, Beryl W. Dominy, Paul J. Feeney Experimental and computational approaches to estimate solubility and permeability in drug discovery and development settings *Adv. Drug Delivery Rev.* **1997**, *23*, 3-25, b) C. A. Lipinski Drug-like properties and the causes of poor solubility and poor permeability *J. Pharmaco. Toxicol Methods.* **2000**, *44*, 235-249

49) a) Taha Rezai, Jonathan E. Bock, Mai V. Zhou, Chakrapani Kalyanaraman, R. Scott Lokey, Matthew P. Jacobson Conformational Flexibility, Internal Hydrogen Bonding, and Passive Membrane Permeability: Successful in Silico Prediction of the Relative Permeabilities of Cyclic Peptides *J. Am. Chem. Soc.* **2006**, *128*, 14073-14080, b) Andrew T. Bockus, Joshua A. Schwochert, Cameron R. Pye, Chad E. Townsend, Vong Sok, Maria A. Bednarek, R. Scott Lokey Going Out on a Limb: Delineating The Effects of β -Branching, N-Methylation, and Side Chain Size on the Passive Permeability, Solubility, and Flexibility of Sanguinamide A Analogues *J. Med. Chem.* **2015**, *58*, 7409-7418

50) a) Jayanta Chatterjee, Chaim Gilon, Amnon Hoffman, Horst Kessler N-Methylation of Peptides: A New Perspective in Medicinal Chemistry *Acc. Chem. Res.* **2008**, *41*, 1331-1342, b) Eric Biron, Jayanta Chatterjee, Oded Ovadia, Daniel Langenegger, Joseph Brueggen, Daniel Hoyer, Herbert A. Schmid, Raz Jelinek, Chaim Gilon, Amnon Hoffman, Horst Kessler Improving Oral Bioavailability of Peptides by Multiple N-Methylation: Somatostatin Analogues *Angew. Chem. Int. Ed.* **2008**, *47*, 2595-2599, c) Tina R. White, Chad M. Renzelman, Arthur C. Rand, Taha Rezai, Cayla M McEwen, Vladimir M. Gelev, Rushia A. Turner, Roger G. Linington, Siegfried S. F. Leung, Amit S. Kalgutkar, Jonathan N. Bauman, Yizhong Zhang, Spiros Liras, David A. Price, Alan M. Mathiowetz, Matthew P. Jacobson, R. Scott Lokey On-resin N-methylation of cyclic peptides for discovery of orally bioavailable scaffolds *Nat. Chemical Biology* **2011**, *7*, 810-817, d) Oded Ovadia, Sarit Greenberg, Jayanta Chatterjee, Burkhardt Laufer, Florian Opperer, Horst Kessler, Chaim Gilon, Amnon Hoffman The effect of multiple N-methylation on intestinal permeability of cyclic hexapeptides *Mol. Pharm.* **2011**, *8*, 479-487, e) Andreas F. B. Räder, Florian Reichart, Michael Weinmüller, Horst Kessler Improving oral bioavailability of cyclic peptides by N-methylation *Bioorg. Med. Chem.* **2018**, *26*, 2766-2773

51) a) William M. Hewitt, Siegfried S. F. Leung, Cameron R. Pye, Alexandra R. Ponkey, Maria Bednarek, Matthew P. Jacobson, R. Scott Lokey Cell-Permeable Cyclic Peptides from Synthetic Libraries Inspired by Natural Products *J. Am. Chem. Soc.* **2015**, *137*, 715-721, b) Daniel S. Nielsen, Dr. Huy N. Hoang, Dr. Rink-Jan Lohman, Dr. Timothy A. Hill, Dr. Andrew J. Lucke, David J. Craik, David J. Edmonds, David A. Griffith, Charles J. Rotter, Roger B. Ruggeri, David A. Price, Spiros Liras, David P. Fairlie Improving on Nature: Making a Cyclic Heptapeptide Orally Bioavailable *Angew. Chem. Int. Ed.* **2014**, *53*, 12059-12063

52) Yong S. Chang, Bradford Graves, Vincent Guerlavais, Christian Tovar, Kathryn Packman, Kwong-Him To, Karen A. Olson, Kamala Kesavan, Pranoti Gangurde, Aditi Mukherjee, Theresa Baker, Krzysztof Darlak, Carl Elkin, Zoran Filipovic, Farooq Z. Qureshi, Hongliang Cai, Pamela Berry, Eric Feyfant, Xiangguo E. Shi, James Horstick, D. Allen Annis, Anthony M. Manning, Nader Fotouhi, Huw Nash, Lyubomir T. Vassilev, Tomi K. Sawyer Stapled α -helical peptide drug development: A potent dual inhibitor of MDM2 and MDMX for p53-dependent cancer therapy *Proc. Natl. Acad. Sci. USA* **2013**, *110*, E3445-E3454

53) a) Daniel S. Nielsen, Huy N. Hoang, Rink-Jan Lohman, Frederik Diness, and David P. Fairlie Total Synthesis,

- Structure, and Oral Absorption of a Thiazole Cyclic Peptide, Sanguinamide A *Org. Lett.* **2012**, *14*, 5720-5723, b) Harjeet S. Soor, Solomon D. Appavoo, Andrei K. Yudin Heterocycles: Versatile control elements in bioactive macrocycles *Bioorg. Med. Chem.* **2018**, *26*, 2774-2779
- 54) Kouhei Matsui, Yasuto Kido, Ryosuke Watari, Yousuke Kashima, Yutaka Yoshida, Satoshi Shuto Highly Conformationally Restricted Cyclopropane Tethers with Three-Dimensional Structural Diversity Drastically Enhance the Cell Permeability of Cyclic Peptides *Chem. Eur. J.* **2017**, *23*, 3034-3041
- 55) Yoshihiro Shimizu, Akio Inoue, Yukihide Tomari, Tsutomu Suzuki, Takashi Yokogawa, Kazuya Nishikawa, Takuya Ueda Cell-free translation reconstituted with purified components *Nat. Biotechnol.* **2001**, *19*, 751-755
- 56) a) N. Nemoto, E. Miyamoto-Sato, Y. Husimi, H. Yanagawa In vitro virus: bonding of mRNA bearing puromycin at the 3'-terminal end to the C-terminal end of its encoded protein on the ribosome in vitro *FEBS Lett.* **1997**, *414*, 405-408, b) Richard W. Roberts, Jack W. Szostak RNA-peptide fusions for the in vitro selection of peptides and proteins *Proc. Natl. Acad. Sci. USA* **1997**, *94*, 12297-12302, c) David S. Wilson, Anthony D. Keefe, Jack W. Szostak The use of mRNA display to select high-affinity protein-binding peptides *Proc. Natl. Acad. Sci. USA* **2001**, *98*, 3750-3755
- 57) Christopher J. Noren, Spencer J. Anthony-Cahill, Michel C. Griffith, Peter G. Schultz A General Method for Site-specific Incorporation of Unnatural Amino Acids into Proteins *Science* **1989**, *244*, 182-188
- 58) J. D. Bain, Edward S. Diala, Charles G. Glabe, Thomas A. Dix, A. Richard Chamberlin Biosynthetic site-specific incorporation of a non-natural amino acid into a polypeptide *J. Am. Chem. Soc.* **1989**, *111*, 8013-8014
- 59) Anthony C. Forster, Zhongping Tan, Madhavi N. L. Nalam, Hening Lin, Hui Qu, Virginia W. Cornish, Stephen C. Blacklow Programming peptidomimetic syntheses by translating genetic codes designed de novo *Proc. Natl. Acad. Sci. USA* **2003**, *100*, 6353-6357
- 60) A. Ohta, Y. Yamagishi, H. Suga Synthesis of biopolymers using genetic code reprogramming *Curr Opin Chem Biol.* **2008**, *12*, 159-167
- 61) Kristopher Josephson, Matthew C. T. Hartman, Jack W. Szostak Ribosomal Synthesis of Unnatural Peptides *J. Am. Chem. Soc.* **2005**, *127*, 11727-11735
- 62) Takahiro Hohsaka, Yuki Ashizuka, Hiroshi Murakami, and Masahiko Sisido Incorporation of Nonnatural Amino Acids into Streptavidin through In Vitro Frame-Shift Suppression *J. Am. Chem. Soc.* **1996**, *118*, 9778-9779
- 63) J. D. Bain, Christopher Switzer, Richard Chamberlin, Steven A. Benner Ribosome-mediated incorporation of a non-standard amino acid into a peptide through expansion of the genetic code *Nature*, **1992**, *356*, 537-539
- 64) a) Ichiro Hirao, Takashi Ohtsuki, Tsuyoshi Fujiwara, Tsuneo Mitsui, Tomoko Yokogawa, Taeko Okuni, Hiroshi Nakayama, Koji Takio, Takashi Yabuki, Takanori Kigawa, Koichiro Kodama, Takashi Yokogawa, Kazuya Nishikawa, Shigeyuki Yokoyama An unnatural base pair for incorporating amino acid analogs into proteins *Nature Biotechnology*, **2002**, *20*, 177-182, b) Tsuyoshi Fujiwara, Michiko Kimoto, Hiroshi Sugiyama, Ichiro Hirao, Shigeyuki Yokoyama Synthesis of 6-(2-thienyl)purine nucleoside derivatives that form unnatural base pairs with pyridin-2-one nucleosides *Bioorg. Med. Chem. Lett.* **2001**, *11*, 2221-2223, c) Michiko Kimoto, Rie Kawai, Tsuneo Mitsui, Shigeyuki Yokoyama, Ichiro Hirao An unnatural base pair system for efficient PCR amplification and functionalization of DNA molecules *Nucleic Acids Res.* **2009**, *37*, e14
- 65) a) Shuwei Li, Steven Millward, Richard Roberts In Vitro Selection of mRNA Display Libraries Containing an

- Unnatural Amino Acid *J. Am. Chem. Soc.* **2002**, *124*, 9972-9973, b) César Fernández, Gerhard Wider TROSY in NMR studies of the structure and function of large biological macromolecules *Curr Opin Struct Biol.* **2003**, *13*, 506-512
- 66) a) Toby Passioura, Takayuki Katoh, Yuki Goto, Hiroaki Suga Selection-based discovery of druglike macrocyclic peptides *Annu. Rev. Biochem.* **2014**, *83*, 727-752, b) Kristopher Josephson, Alonso Ricardo, Jack W Szostak mRNA display: from basic principles to macrocycle drug discovery *Drug Discovery Today* **2014**, *19*, 388-399
- 67) Yuki Goto, Atsushi Ohta, Yusuke Sako, Yusuke Yamagishi, Hiroshi Murakami, Hiroaki Suga Reprogramming the Translation Initiation for the Synthesis of Physiologically Stable Cyclic Peptides *ACS Chem. Biol.* **2008**, *3*, 120-129
- 68) Yusuke Yamagishi 1, Ikuo Shoji, Shoji Miyagawa, Takashi Kawakami, Takayuki Katoh, Yuki Goto, Hiroaki Suga Natural product-like macrocyclic N-methyl-peptide inhibitors against a ubiquitin ligase uncovered from a ribosome-expressed de novo library *Chem Biol.* **2011**, *18*, 1562-1570
- 69) Jumpei Morimoto, Yuuki Hayashi, Hiroaki Suga Discovery of Macrocyclic Peptides Armed with a Mechanism-Based Warhead: Isoform-Selective Inhibition of Human Deacetylase SIRT2 *Angew. Chem. Int. Ed.* **2012**, *51*, 3423-3427
- 70) Takashi Kawakami, Takahiro Ishizawa, Tomoshige Fujino, Patrick C. Reid, Hiroaki Suga, Hiroshi Murakami In Vitro Selection of Multiple Libraries Created by Genetic Code Reprogramming To Discover Macrocyclic Peptides That Antagonize VEGFR2 Activity in Living Cells *ACS Chem. Biol.* **2013**, *8*, 1205-1214
- 71) Yoshiki Tanaka, Christopher J. Hipolito, Andrés D. Maturana, Koichi Ito, Teruo Kuroda, Takashi Higuchi, Takayuki Katoh, Hideaki E. Kato, Motoyuki Hattori, Kaoru Kumazaki, Tomoya Tsukazaki, Ryuichiro Ishitani, Hiroaki Suga, Osamu Nureki Structural basis for the drug extrusion mechanism by a MATE multidrug transporter *Nature* **2013**, *496*, 247-251
- 72) a) Shiori Kariyuki, Takeo Iida, Miki Kojima, Ryuichi Takeyama, Mikimasa Tanada, Tetuo Kijima, Hitoshi Iikura, Atsushi Matsuno, Takuya Shiraishi, Takashi Emura, Kazuhiko Nakano, Koji Takano, Kousuke Asou, Takuya Trizawa, Ryosuke Takano, Nozomi Hisada, Nakaoki Murao, Atsushi Ohta, Kaori Kimura, Yusuke Yamagishi, Tatsuya Kato Peptide-Compound Cyclization Method WO2013100132, b) Kazuhiko Nakano, Atsushi Ohta, Takeo Iida, Hitoshi Iikura Production Method for Noncyclic Peptide-Nucleic Acid Complex Having, at N-Terminal, Amino Acid with Thiol Group near Amino Group, Library Thereof, and Cyclic Peptide-Nucleic Acid Complex Library Derived from Same WO2017150732
- 73) Yollete V. Guillen Schlippe, Matthew C. T. Hartman, Kristopher Josephson, Jack W. Szostak In Vitro Selection of Highly Modified Cyclic Peptides That Act as Tight Binding Inhibitors *J. Am. Chem. Soc.* **2012**, *134*, 10469-10477
- 74) a) Steven W. Millward, Terry T. Takahashi, Richard W. Roberts A General Route for Post-Translational Cyclization of mRNA Display Libraries *J. Am. Chem. Soc.* **2005**, *127*, 14142-14143, b) Steven W. Millward, Stephen Fiacco, Ryan J. Austin, Richard W. Roberts Design of Cyclic Peptides That Bind Protein Surfaces with Antibody-Like Affinity *ACS Chem. Biol.* **2007**, *2*, 625-634
- 75) Yusuke Sako, Jumpei Morimoto, Hiroshi Murakami, Hiroaki Suga Ribosomal Synthesis of Bicyclic Peptides

via Two Orthogonal Inter-Side-Chain Reactions *J. Am. Chem. Soc.* **2008**, *130*, 7232-7234

Chapter 2

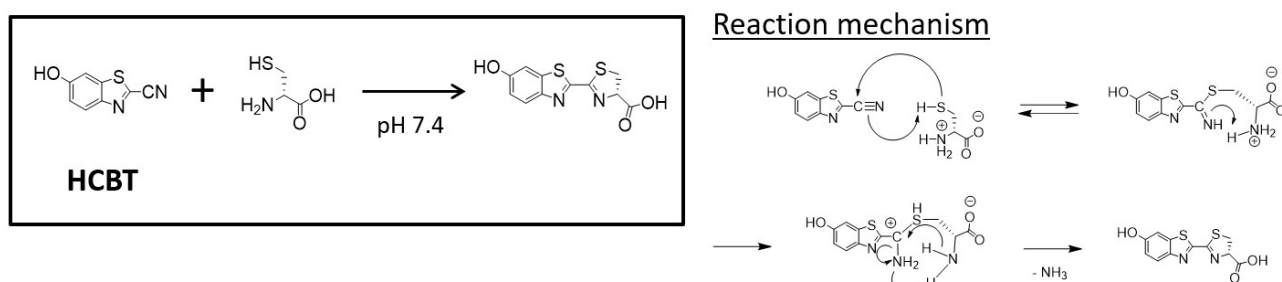
Reaction Characteristics and Versatility of Thiazoline Ring-Bridged Peptide Cyclization

2. 1 Introduction

Peptides have target binding properties and selectivity comparable to that of biopharmaceuticals such as antibodies. Peptides are easy to synthesize chemically and versatile enough to be used in drug discovery for a variety of target proteins by changing the amino acid residues. Due to their relatively small molecular weight, peptides can also permeate cell membranes and bind to intracellular target proteins. While linear peptides generally have low metabolic stability and cell membrane permeability, cyclic peptides have high metabolic stability and cell membrane permeability. For example, natural cyclic peptides such as cyclosporine A (CSA) and griselimycin, as well as some synthetic peptides, are known to penetrate the cell membrane ¹⁾.

As a way to design cell membrane-permeable peptides with intramolecular hydrogen bond formation between amide groups constituting cyclic peptides, new cyclization methods of peptides have been studied. For example, cyclic peptides composed of 1,3,4-oxadiazole in the main chain have been synthesized from cyclization reactions through three-component system of linear peptides, aldehydes, and (N-isocyanimino)triphenylphosphorane. It has been reported that this cyclic peptide has higher model membrane permeability than the structurally homologous peptide without 1,3,4-oxadiazole structure ²⁾. This is expected to be due to the formation of β -turn intramolecular hydrogen bonds in the cyclic peptide at the amino group adjacent to oxadiazole and oxadiazole, resulting in a reduction of the polar surface area (PSA). Considering these previous works, the development of synthetic methods for cyclic peptides with heterocycles in the main chain would be useful because they could provide a variety of unique structures for drug discovery against a large number of intracellular target proteins.

In this chapter, I describe the development of a new synthetic method for cyclic peptides with heterocycles in the main chain. D-Luciferin, a substrate of luciferase, is produced by the reaction between 2-cyano-6-hydroxybenzothiazole (HCBT) and D-Cys ³⁾. Since this reaction proceeds in neutral aqueous condition without catalysis, it has been used for chemical modification of N-terminal Cys-containing proteins with functional molecules ⁴⁾ (Fig. 2-1). The resulting linkage formed between thiazoline and (hetero)aryl groups is a drug-like structure that can be found in bioactive substances derived from natural products ⁵⁾ (Fig. 2-2). Recently, the utilization of this reaction for intramolecular cyclization of peptides had been reported ⁶⁾. In this study, I focused on the potential of the thiazoline ring-bridged cyclization and examined its substrate versatility and cyclization reactivity using chemically synthesized peptides.



Application for bioconjugation

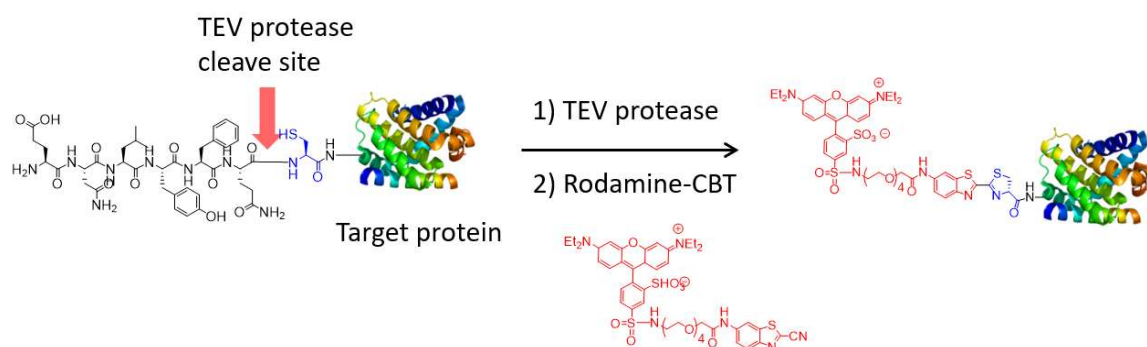


Fig. 2-1 Example of protein labeling using the Luciferin synthesis reaction.

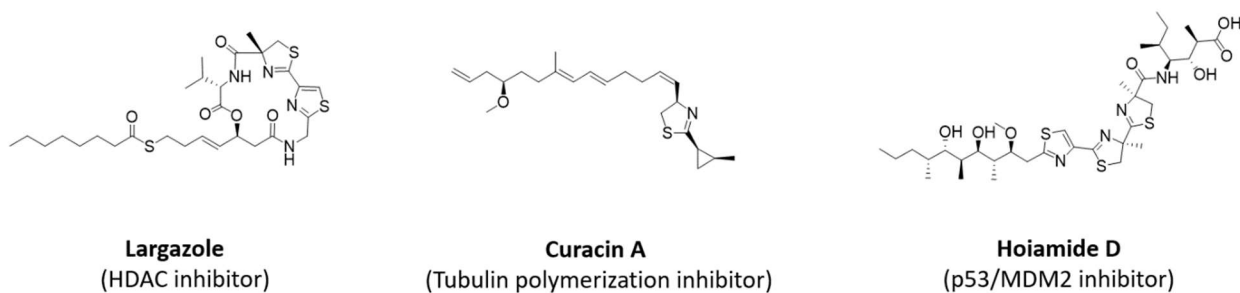


Fig. 2-2 Examples of bioactive natural products with thiazoline rings.

2. 2 Materials and methods

2. 2. 1 Synthesis of Fmoc-protected amino acid 1 (Fig. 2-3)

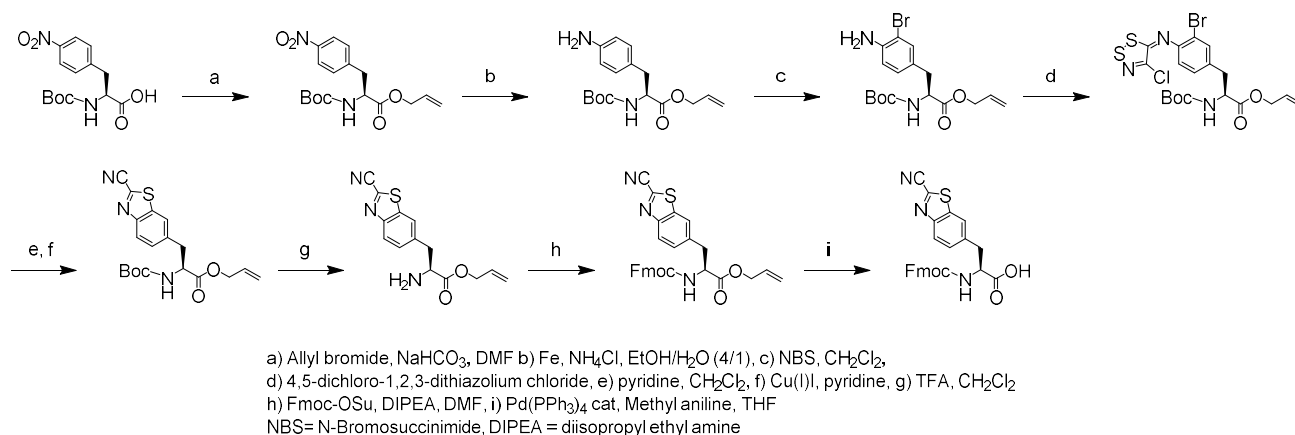


Fig. 2-3 Synthetic route of Fmoc-protected non-natural amino acid 1 with CBT moiety as a side chain

(1) Synthesis of allyl (S)-2-((tert-butoxycarbonyl)amino)-3-(4-nitrophenyl)propanoate

Boc-Phe(*p*-NO₂)-OH (2.0g, 6.45 mmol) was dissolved in 25 mL of N,N-dimethylformamide (DMF). To the solution, sodium bicarbonate (2.27g, 27.0 mmol) was added. Then, after dropping allyl bromide (1.19 mL, 13.8 mmol), the mixture was stirred at room temperature for 20 hours. After the disappearance of the raw material was confirmed by LC-MS, distilled water and ethyl acetate were added to the reaction solution, and extraction was carried out with ethyl acetate. The organic layer was washed with distilled water and saturated brine and dried with magnesium sulfate. The solvent was removed under reduced pressure and used directly in the next step without further purification. The products were analyzed for mass (ESI-MS) and retention time (RT) using ACQUITY UPLC system (Waters) as described below. MS (ESI *m/z*): 351.2 [M+H]⁺. RT (min): 1.63.

(2) Synthesis of allyl (S)-3-(4-aminophenyl)-2-((tert-butoxycarbonyl)amino)propanoate

Reduced iron (1.81 g, 32.4 mmol) and ammonium chloride (3.1 g, 58.0 mmol) were dissolved in 40 mL of EtOH and 20 mL of distilled water, and the mixture was heated at 80°C for 20 minutes. To the solution, 20 mL of ethanol solution of allyl (S)-2-((tert-butoxycarbonyl) amino)-3-(4-nitrophenyl) propanoate (crude) was added and the mixture was stirred at 80°C for 3 hours. Insoluble matter was removed by Celite filtration, and the filtrate was distilled off under reduced pressure. Distilled water and ethyl acetate were added to the residue obtained, and extraction was carried out with ethyl acetate. The organic layer was washed with saturated brine, dried over magnesium sulfate, and the solvent was removed under reduced pressure to give 2.15 g of the yellow oily title compound. MS (ESI *m/z*): 321.2 [M+H]⁺. RT (min): 1.02.

(3) Synthesis of allyl (S)-3-(4-amino-3-bromophenyl)-2-((tert-butoxycarbonyl) amino)propanoate

Allyl (S)-3-(4-aminophenyl)-2-((tert-butoxycarbonyl)amino)propanoate (2.15 g, 6.71 mmol) was added to 20 mL of dichloromethane (CH₂Cl₂) solution of N-bromosuccinimide (NBS) (1.31 g, 7.36 mmol) on an ice bath, followed by stirring for 1 hour at room temperature. The reaction solution was distilled off under reduced pressure and purified by column chromatography (silica gel, ethyl acetate/hexane = 0/100 to 20/80) to obtain 1.91 g of the title compound in yellow liquid. MS (ESI *m/z*): 400.1 [M+H]⁺. RT (min): 1.56.

(4) Synthesis of allyl (S,E)-3-(3-bromo-4-((4-chloro-5H-1,2,3-dithiazol-5-ylidene) amino)phenyl)-2-((tert-butoxycarbonyl) amino) propanoate

To a solution of allyl (S)-3-(4-amino-3-bromophenyl)-2-((tert-butoxycarbonyl)amino)propanoate (1.91 g, 4.78 mmol) in 30 mL of CH₂Cl₂ solution, Appel's salt (1.21 g, 5.80 mmol) was added and stirred for 1.5 hours at room temperature. To the solution, pyridine (0.80 mL, 9.95 mmol) was added, and the mixture was further stirred for 1 hour at room temperature. The solvent was removed under reduced pressure, and the product was purified by column chromatography (silica gel, ethyl acetate/hexane = 0/100 to 20/80) to obtain 1.63 g of the brown oily title compound. MS (ESI *m/z*): 535.0 [M+H]⁺. RT (min): 1.97.

(5) Synthesis of allyl (S)-2-((tert-butoxycarbonyl)amino)-3-(2-cyanobenzo[d]thiazol-6-yl)propanoate

CuI (I) (640 mg, 3.36 mmol) was added to the solution of allyl(S,E)-3-(3-bromo-4-((4-chloro-5H-1,2,3-dithiazol-5-ylidene)amino)phenyl)-2-((tert-butoxycarbonyl)amino)propanoate (3-chloro-5H-1,2,3-dithiazol-5-ylidene)amino)phenyl)-2-((tert-butoxycarbonyl)amino)propanoate (1.63 g, 3.05 mmol) in 15 mL of pyridine and irradiated with microwaves (InitiatorTM, 110 °C, 30 min, 2.45 GHz, 0-240 W). Distilled water and ethyl acetate were added to the reaction solution, and extraction was carried out with ethyl acetate. The organic layer was washed with distilled water and saturated brine and dried with magnesium sulfate. The solvent was removed under reduced pressure, and the product was purified by column chromatography (silica gel, ethyl acetate/hexane = 0/100 to 15/85) to afford 872 mg of the title compound as a yellow solid. MS (ESI *m/z*): 388.2 [M+H]⁺. RT (min): 1.69.

(6) Synthesis of allyl (S)-2-(((9H-fluoren-9-yl)methoxy)carbonyl)amino)-3-cyanobenzo[d]thiazol-6-yl)propanoate

Allyl (S)-2-((tert-butoxycarbonyl)amino)-3-(2-cyanobenzo[d]thiazole-6-yl)propanoate (751 mg, 1.94 mmol) in 25 mL of ethyl acetate was added 25 mL of ethyl acetate solution of hydrochloric acid (4 M) and the mixture was stirred at room temperature for 1.5 hours. To the reaction solution, 200 mL of hexane was added, the precipitated solid was filtered off, and the resulting solid was washed with hexane. The individual was dissolved in 50 mL of DMF and 5.0 ml of N, N-diisopropylethylamine (DIPEA) and Fmoc-OSu (785 mg, 2.33 mmol) were added, and the mixture was stirred for 2 hours at room temperature. The reaction solution was distilled off under reduced pressure and purified by column chromatography (silica gel, ethyl acetate/hexane = 0/100 to 20/80) to give 335 mg of the yellow oily title compound. MS (ESI *m/z*): 510.2 [M+H]⁺. RT (min): 1.92.

(7) Synthesis of (S)-2-(((9H-fluoren-9-yl)methoxy)carbonyl)amino)-3-cyanobenzo[d]thiazol-6-yl)propionic acid (Fmoc-protected amino acid **1**)

To a solution of allyl(S)-2-(((9H-fluoren-9-yl)methoxy)carbonyl)amino)-3-cyanobenzo[d]thiazol-6-yl)propanoate (335 mg, 0.657 mmol) in 10 mL of THF, N-methylaniline (80 μL, 0.74 mmol) and tetrakis(triphenyl)phosphine palladium (0

(Pd(PPh₃)₄) (77 mg, 0.0667 mmol) were added and the mixture was stirred at room temperature for 1 hour. Distilled water and ethyl acetate were added to the reaction solution, and the organic layer was washed with distilled water, hydrochloric acid solution (0.1 M), saturated brine, and dried with magnesium sulfate. The solvent was removed under reduced pressure, and the product was purified by column chromatography (silica gel, methanol/ethyl acetate/hexane = 0/40/60 to 20/80/0) to give 237 mg of Fmoc-protected amino acid **1** as a yellow solid. MS (ESI *m/z*): 470.2 [M+H]⁺. RT (min): 1.64. ¹H-NMR (MeOD) δ: 8.09 (1H, d, J = 8.6 Hz), 7.98 (1H, s), 7.77 (2H, d, J = 7.9 Hz), 7.62-7.48 (3H, m), 7.36 (2H, t, J = 10.2 Hz), 7.28-7.17 (2H, m), 4.58-4.48 (1H, m), 4.34-4.17 (2H, m), 4.08 (1H, t, J = 6.9 Hz) -7.17 (2H, m), 4.58-4.48 (1H, m), 4.34-4.17 (2H, m), 4.08 (1H, t, J = 6.9 Hz), 3.44 (1H, dd, J = 13.9, 4.6 Hz), 3.20 -3.08 (1H, m).

2. 2. 2 Synthesis of Fmoc-protected amino acids 2, 3, and 5 (Fig. 2-4)

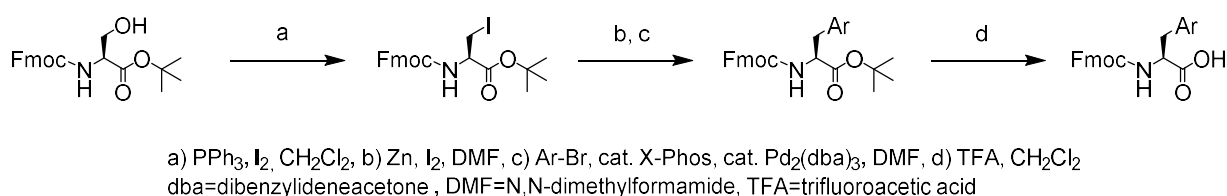


Fig. 2-4 Synthetic route for Fmoc-protected non-natural amino acids 2, 3, and 5

(1) Synthesis of tert-butyl (R)-2-(((9H-fluoren-9-yl)methoxy)carbonyl)amino-3-iodopropanoate (Fmoc-iodo Ala)

Fmoc-Ser-OtBu (30 g, 78.2 mmol) was dissolved in 300 mL of CH₂Cl₂ solution and triphenylphosphine (PPh₃) (24.7 g, 94.2 mmol) and iodine (21.8 g, 85.9 mmol) were added. The reaction vessel was then immersed in a water bath and imidazole (5.83 g, 85.6 mmol) was slowly added, followed by stirring for 2 hours. After filtration of the insoluble material, the solvent was removed under reduced pressure, and the residue was purified by column chromatography (silica gel, ethyl acetate/hexane = 0/100 to 10/90) to obtain 34 g of the title compound as a white solid. MS (ESI *m/z*): 494.3 [M+H]⁺. RT (min): 2.03.

(2) Synthesis of Fmoc-protected amino acid 2

To a solution of zinc powder (2.4 g, 36.7 mmol) in 2.6 mL of DMF, iodine (46 mg, 0.181 mmol) was added and the mixture was stirred for 5 minutes at room temperature under nitrogen atmosphere. tert-Butyl (R)-2-(((9H-fluoren-9-yl)methoxy)carbonyl)amino (R)-3-iodopropanoate (600 mg, 1.22 mmol) in 1.4 mL of DMF was added to the reaction mixture, then iodine (46 mg, 0.181 mmol) was added under room temperature, and the mixture was stirred for 160 minutes. 4-Bromo-2-cyanothiophene (298 mg, 1.58 mmol), 2-dicyclohexylphosphino-2',4',6'-triisopropyl-1,1'-biphenyl (29 mg, 0.061 mmol), and tris(dibenzylideneacetone)dipalladium (28 mg, 0.031 mmol) were added to the reaction mixture under a nitrogen atmosphere, followed by stirring for 3 hours at room temperature. After filtration of the insoluble material, ethyl acetate was added to the filtrate, and the mixture was washed with sodium thiosulfate solution. The organic layer

was dried over magnesium sulfate and then the solvent was removed under reduced pressure. The residue obtained was purified by silica gel chromatography (n-hexane: ethyl acetate = 90:10 to 30:70), and tert-butyl (S)-2-(((9H-fluoren-9-yl)methoxy)carbonyl)amino)-3-(5-cyanothiophen-3(-yl)propanoate (127 mg) was obtained. MS (ESI m/z): 475.1 [M+H]⁺. RT (min): 1.95.

tert-Butyl (S)-2-(((9H-fluoren-9-yl)methoxy)carbonyl)amino)-3-(5-cyanothiophen-3(-yl)propanoate (127 mg) was dissolved in 1 mL of trifluoroacetic acid (TFA) and stirred at room temperature for 30 minutes, then the solvent was removed under reduced pressure. The resulting residue was purified by silica gel chromatography (n-hexane: ethyl acetate = 70:30 to 0:100) to afford Fmoc-protected amino acid **2** (63 mg) as a white solid. MS (ESI m/z): 419.0 [M+H]⁺. RT (min): 1.55. ¹H-NMR (MeOD) δ : 7.78 (2H, d, J = 7.3 Hz), 7.59 (2H, d, J = 7.3 Hz), 7.53-7.24 (6H, m), 4.53-4.43 (1H, m), 4.36-4.11 (3H, m), 3.25-2.93 (2H, m).

(3) Synthesis of Fmoc-protected amino acid **3**

To a solution of zinc powder (780 mg, 11.9 mmol) in 9 mL of DMF, iodine (150 mg, 0.59 mmol) was added and the mixture was stirred at room temperature under nitrogen atmosphere for 5 minutes. To the reaction mixture was added tert-butyl (R)-2-(((9H-fluoren-9-yl)methoxy)carbonyl)amino (R)-3-iodopropanoate (2.0 g, 4.05 mmol) in 5 mL of DMF, then iodine (150 mg, 0.59 mmol) was added under room temperature, and the mixture was stirred for 2 hours. 5-Bromo-3-cyanothiophene (1.0 g, 5.32 mmol), 2-dicyclohexylphosphino-2',4',6'-triisopropyl-1,1'-biphenyl (111 mg, 0.233 mmol), and tris(dibenzylideneacetone)dipalladium (114 mg, 0.124 mmol) were added to the reaction mixture at room temperature. After filtration of the insoluble material, ethyl acetate was added to the filtrate, and the mixture was washed with sodium thiosulfate solution. The organic layer was dried over magnesium sulfate and then the solvent was removed under reduced pressure. The residue obtained was purified by silica gel chromatography (n-hexane: ethyl acetate = 90:10 to 30:70), and (S)-2-(((9H-fluoren-9-yl)methoxy)carbonyl)amino)-3-(4-cyanothiophen-2-yl)propanoic acid tert-butyl (121 mg) was obtained as a yellow oil. MS (ESI m/z): 475.0 [M+H]⁺. RT (min): 1.90.

(S)-2-(((9H-fluoren-9-yl)methoxy)carbonyl)amino)-3-(4-cyanothiophen-2-yl)propanoic acid tert-butyl (121 mg) was dissolved in 1 mL of TFA and stirred at room temperature for 30 min, then the solvent was removed under reduced pressure. The resulting residue was purified by silica gel chromatography (n-hexane: ethyl acetate = 70:30 to 0:100) to give Fmoc-protected amino acid **3** (90 mg). MS (ESI m/z): 418.1 [M+H]⁺. RT (min): 1.47. ¹H-NMR (CDCl₃) δ : 7.84-7.27 (9H, m), 6.93 (1H, s), 5.51-5.38 (1H, m), 4.78-4.50 (2H, m), 4.47-4.35 (1H, m), 4.27-4.17 (1H, m), 3.49-3.27 (2H, m).

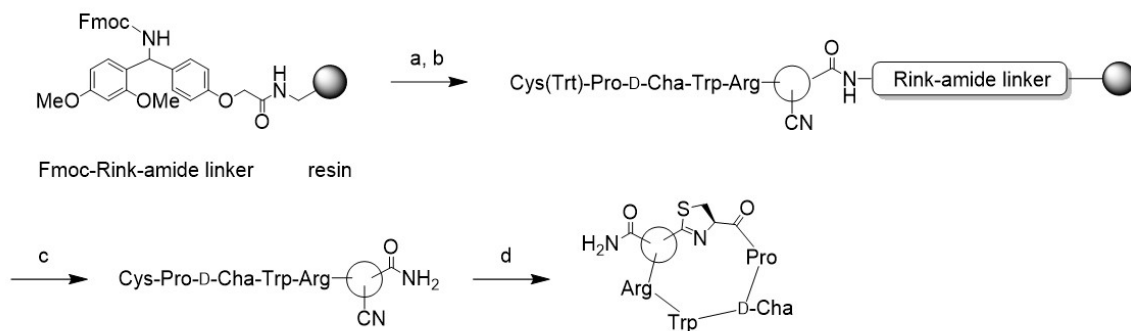
(4) Synthesis of Fmoc-protected amino acid **5**

To a solution of zinc powder (400 mg, 6.12 mmol) in 3 mL of DMF, iodine (66 mg, 0.26 mmol) was added and the mixture was stirred at room temperature under nitrogen atmosphere for 5 minutes. To the reaction mixture was added tert-butyl (R)-2-(((9H-fluoren-9-yl)methoxy)carbonyl)amino (R)-3-iodopropanoate (1.0 g, 2.03 mmol) in 5 mL of DMF, then iodine (25 mg, 0.099 mmol) was added under room temperature, and the mixture was stirred for 2 hours. 5-Bromopyridine-2-carbonitrile (440 mg, 2.40 mmol), 2-dicyclohexylphosphino-2',4',6'-triisopropyl-1,1'-biphenyl (97 mg, 0.203 mmol), and tris(dibenzylideneacetone)dipalladium (Pd₂(dba)₃) (92 mg, 0.100 mmol) were added to the reaction mixture at room temperature. After filtration of the insoluble material, ethyl acetate was added to the filtrate, and the mixture was

washed with sodium thiosulfate solution. The organic layer was dried over magnesium sulfate and then the solvent was removed under reduced pressure. The residue obtained was purified by silica gel chromatography (n-hexane:ethyl acetate = 100:0 to 85/15), and tert-butyl (S)-2-((((9H-fluoren-9-yl)methoxy)carbonyl)amino)-3-(5-cyanopyridin-3-yl)propanoate (310 mg) was obtained as a yellow oil. MS (ESI m/z): 470.3 $[M+H]^+$. RT (min): 1.83.

tert-Butyl (S)-2-((((9H-fluoren-9-yl)methoxy)carbonyl)amino)-3-(5-cyanopyridin-3-yl)propanoate (310 mg) was dissolved in 1 mL of TFA and stirred at room temperature for 30 min, then the solvent was removed under reduced pressure. The resulting residue was purified by silica gel chromatography (MeOH:n-hexane:ethyl acetate = 0:40:60 to 20: 0:80) to give Fmoc-protected amino acid **5** (210 mg). MS (ESI m/z): 414.4 $[M+H]^+$. RT (min): 1.39. $^1\text{H-NMR}$ (CDCl_3) δ : 8.69 (1H, s), 8.51 (1H, s), 7.87-7.79 (2H, m), 7.68 (1H, s), 7.63-7.58(2H, m), 7.45-7.30 (4H, m), 5.48 (1H, d, $J = 3$ Hz), 4.72-4.63 (2H, m), 4.50-4.20 (1H, m), 4.24 (1H, t, $J = 6.9$ Hz), 3.32-3.12 (2H, m)

2. 2. 3 Synthesis of cyclic peptides (general method) (Fig. 2-5)



a) 20% piperidine in NMP (v/v), rt, 20 min,

b) iterative Fmoc SPPS (Fmoc-amino acid (4 equiv), DIC (xx equiv), Oxyma (xx eq), DIPEA (x equiv), NMP, rt, 1 h (deprotection) 20% piperidine in NMP (v/v), rt, 20 min

c) TFA/ H_2O (95:5), rt, 1 h

d) phosphate buffer (pH 7.4), TCEP

DIC=N,N'-diisopropylcarbodiimide, Oxyma=Ethyl (hydroxyimino)cynoacetate, DIPEA=diisopropylethylamine, NMP=N-methylpyrrolidone, TFA=trifluoroacetic acid, Trt=trityl group, D-Cha=D-cyclohexylalanine

Fig. 2-5 Synthetic route to thiazoline ring-bridged cyclic peptides by Fmoc solid phase peptide synthesis.

Peptide solid phase synthesis was performed using an automated peptide synthesizer (Syro I, Biotage). The synthesis apparatus included a Rink Amide-ChemMatrix™ (Biotage), N-methyl-2-pyrrolidone (NMP) solution of Fmoc protected amino acids (0.5 M), NMP solutions of cyanohydroxyiminoacetic acid ethyl ester (1 M) and NMP solution of DIPEA (0.1 M), NMP solution of diisopropylcarbodiimide (DIC) (1 M), and NMP solution of piperidine (20 % v/v) were set up. The peptide chain was elongated by repeating one cycle of Fmoc deprotection (20 min) with NMP solution of piperidine (20 % v/v), washing with NMP, condensation (1 hour) of Fmoc protected amino acids (4 eq.) with NMP solution of diisopropylcarbodiimide (1 M) (4 eq.), and washing with NMP. The resin was

immersed in TFA:TIPS:DODT:H₂O = 92.5:2.5:2.5:2.5 and shaken for 30 minutes, followed by filtration, and the filtrate was distilled off under reduced pressure to obtain linear peptides.

For the thiazoline ring-bridged cyclization reaction, the linear peptide was dissolved in MeOH and the same amount of phosphate buffer (pH 7.0) was added. TCEP (1 eq.) was added and the mixture was stirred. After completion of the reaction, the product was extracted with ethyl acetate and washed with water. The ethyl acetate solution was distilled off under reduced pressure.

For the amide-bridged cyclization reaction, the linear peptide was dissolved in COMU (AR/THF=1/1) (0.5 M) solution and stirred after the addition of diisopropylethylamine (1 M) acetonitrile solution. Four equivalents of COMU and DIPEA were used. After completion of the reaction, the product was extracted with ethyl acetate and washed with water. The ethyl acetate solution was distilled off under reduced pressure.

For the thioether bridged cyclization reaction, the linear peptide was dissolved in triethylammonium bicarbonate buffer solution (pH 8.5), and one equivalent of tris(2-carboxyethyl)phosphine (TCEP) was added and stirred. After completion of the reaction, the product was extracted with ethyl acetate and washed with water. The ethyl acetate solution was distilled off under reduced pressure. Peptides were purified by LCMS system (Waters). Column: X Select CSH130 C18 (19 x 250 mm) from Waters, column temperature: 40 °C, flow rate: 20 mL/min, detection wavelengths: 220 nm and 254 nm.

2. 2. 4 UPLC measurement

The measurement sample was prepared by dissolving 1 µL of the reaction solution in 150 µL of acetonitrile containing 0.1 % formic acid. Retention time and UV area measurements as well as mass spectrometry were performed using ACQUITY UPLC (Waters). Column: Waters BEH C18 1.7 µm, 2.1 x 30 mm, Solvent: Solution A: Aqueous solution containing 0.1 % formic acid, Solution B: Acetonitrile containing 0.1 % formic acid, Gradient cycle: 0.00 min (solution A/B = 95/5), 2.00 min (solution A/B = 5/95), 3.00 min (solution A/B = 95/5), flow rate: 0.5 mL/min, column temperature: room temperature, detection wavelength: 254 nm.

2. 2. 5 MALDI TOF-MS measurement

Saturated α -cyano-4-hydroxycinnamic acid (α -CHCA) dissolved in 50 % aqueous acetonitrile solution (0.1 % TFA) was prepared as the matrix solution. 0.75 µL of the purified peptide solution and 0.75 µL of the matrix solution were mixed and subjected to MALDI TOF-MS (ultrafleXtreme, Bruker Daltonics) using the peptide calibration standard (Bruker Daltonics) as an external standard.

2. 2. 6 Calculation for LUMO orbital energy

This section explains the computational details for the quantum chemical calculations. The geometries of molecules were optimized at the B3LYP level in the density functional theory (DFT) from the initial structures. Then, the LUMO and its energy of the optimized structures were obtained from the single point calculations at the

same level. The basis sets were 6-31G*. All the calculations were performed using the Gaussian09 program⁷⁾.

2. 3 Results and Discussion

2. 3. 1 Synthesis of thiazoline ring-bridged cyclic peptides

Six types of non-natural amino acids having cyano group on their side chain were used for the thiazoline ring-bridged peptide cyclization (Fig. 2-6). As a model cyclic peptide, CP-D-cha-WRX was designed, in which cyanated non-natural amino acids were introduced at position X to react with the N-terminal Cys. The five non-natural amino acids contained cyanated aryl groups, 2-cyanobenzothiazole (**1**), 2-cyanothiophene (**2**), 3-cyanothiophene (**3**), 3-cyanobenzene (**4**), and 3-cyanopyridine (**5**), respectively. Cyanoalanine (**6**) contained cyano group directly on the side chain of alanine.

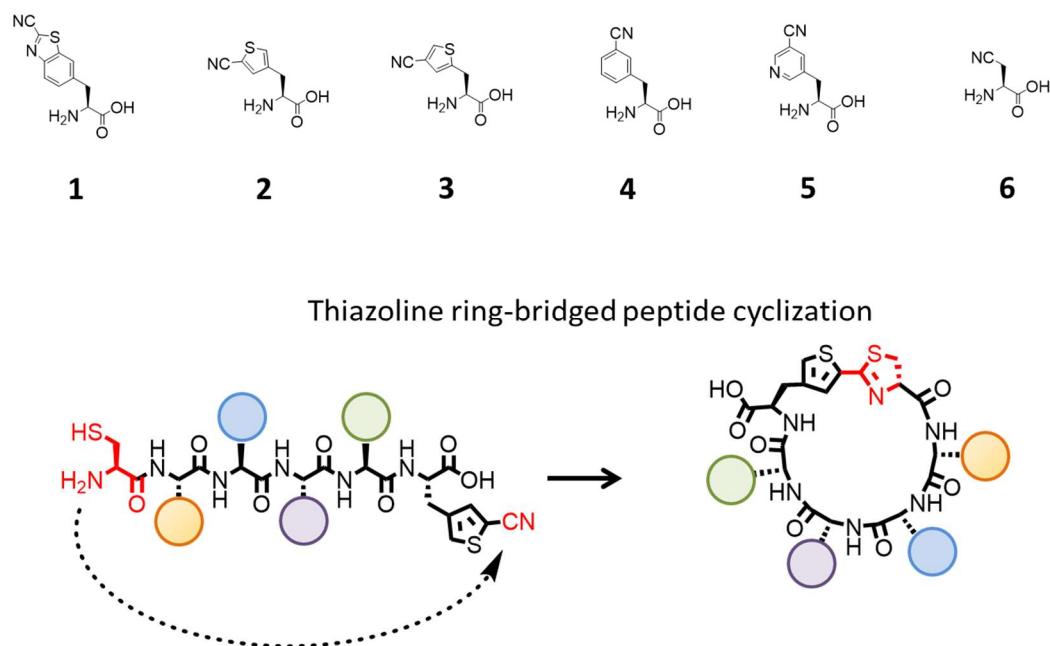
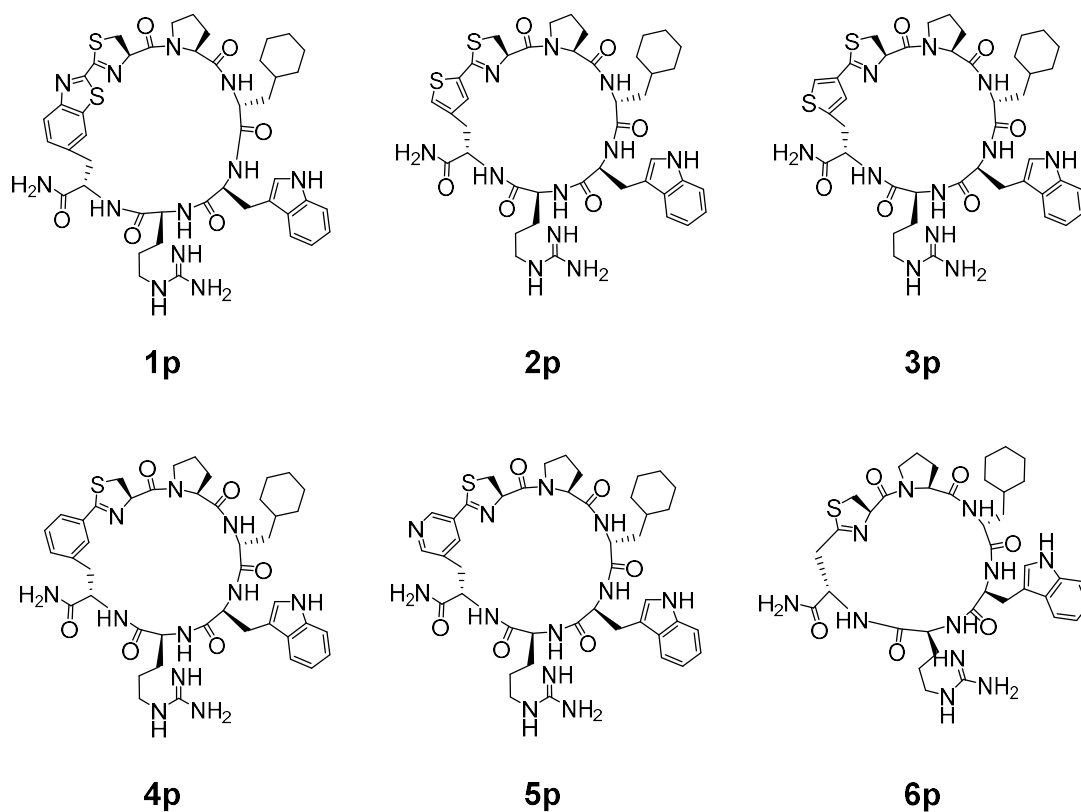


Fig. 2-6 Chemical structures of cyanated non-natural amino acids, and schematic illustration of thiazoline ring-bridged peptide cyclization.

Fmoc-protected non-natural amino acid **1** was synthesized by synthetic route shown in Fig. 2-3. Fmoc-protected forms of **2**, **3**, and **5** were synthesized by Appel reaction of Fmoc-Ser-OtBu to produce the iodinated form, followed by Negishi coupling and deprotection of tBu ester with TFA (Fig. 2-4). Fmoc-protected cyanophenylalanine **4** and cyanoalanine **6** were obtained as commercially products.

Cyclized peptides **1p-6p** (Fig. 2-7) were synthesized as follows (Fig. 2-5). First, linear peptides were synthesized by Fmoc solid-phase synthesis, followed by cyclization by dissolution in a phosphate buffer solution at pH 7. For non-natural amino acid **1**, the cyclized form could not be obtained because the cyano group was rapidly hydrolyzed during the release of the linear peptide from the resin by aqueous TFA mixture solution (TFA/TIPS/DODT/H₂O). After completion of the cyclization reaction, the thiazoline ring-bridged cyclic peptides were purified through a preparative HPLC. MALDI TOF-MS spectra showed that the thiazoline ring-bridged peptides were successfully generated for cyanated non-natural amino acids **2-6** (Fig. 2-8).



Peptide No.	Exact MS	Total yield (%)
1p	924.4	Decomposition
2p	873.4	11.3
3p	873.4	11.1
4p	867.4	12.3
5p	868.4	13.9
6p	791.4	4.0

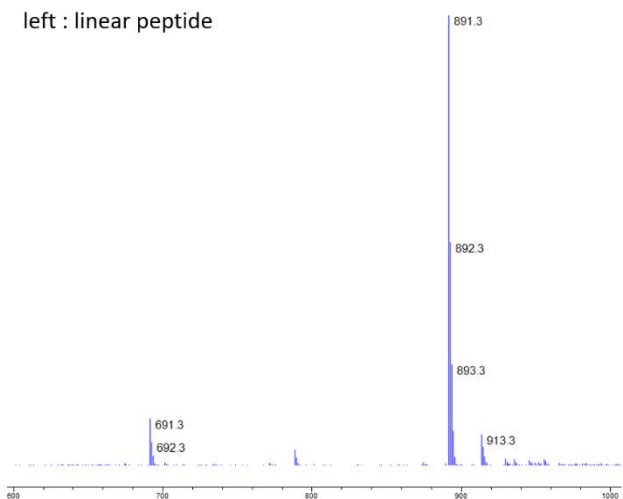
Fig. 2-7 Structure and total yield of cyclic peptides **1p-6p**.

linear peptide	$[M+H]^+$; m/z (calculated)	$[M+H]^+$; m/z (analyzed)
2p	891.4	891.3
3p	891.4	891.3
4p	885.5	885.3
5p	886.4	886.3
6p	809.4	809.3

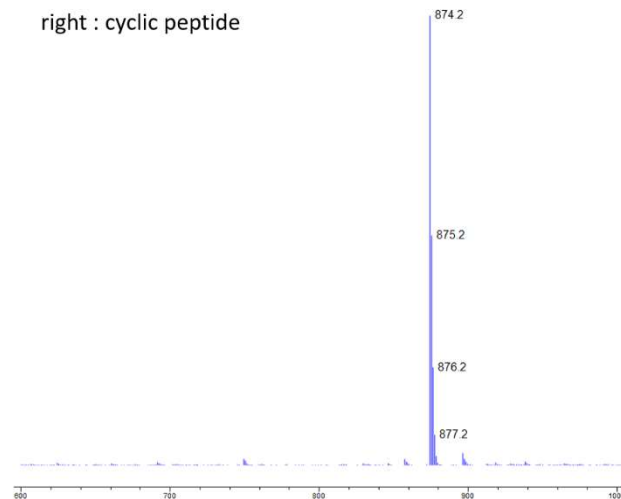
cyclic peptide	$[M+H]^+$; m/z (calculated)	$[M+H]^+$; m/z (analyzed)
2p	874.4	874.2
3p	874.4	874.2
4p	868.4	868.3
5p	869.4	869.3
6p	792.4	792.3

a) 2p

left : linear peptide

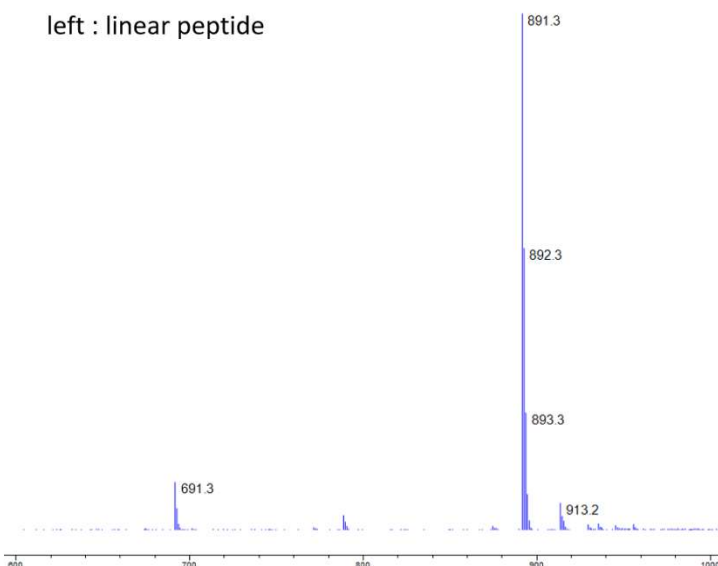


right : cyclic peptide

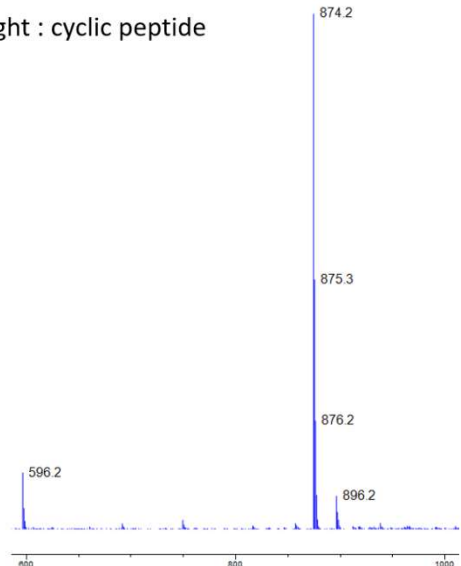


b) 3p

left : linear peptide

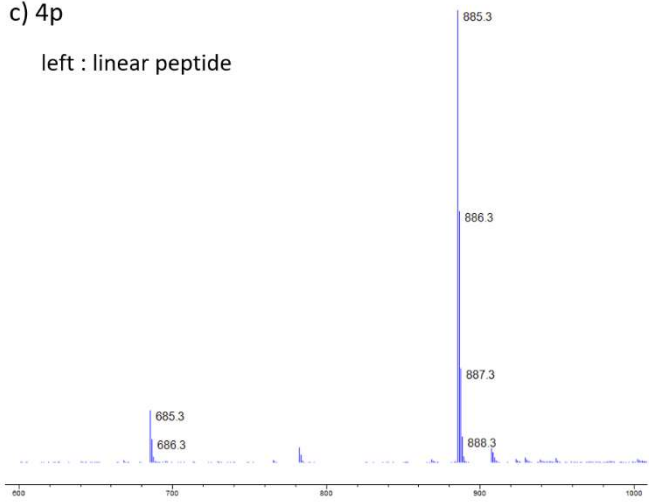


right : cyclic peptide

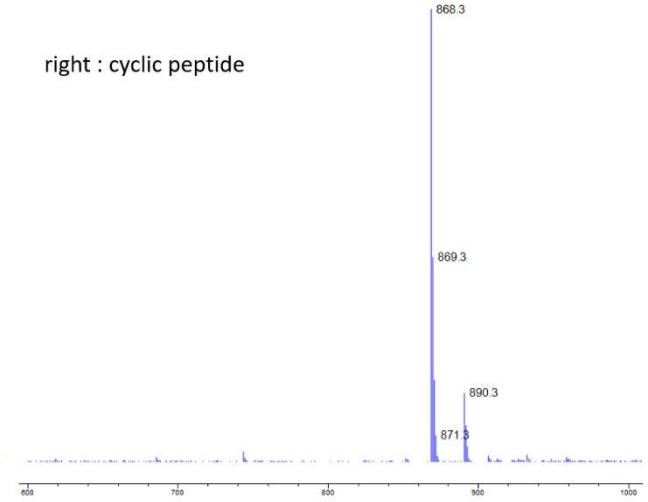


c) 4p

left : linear peptide

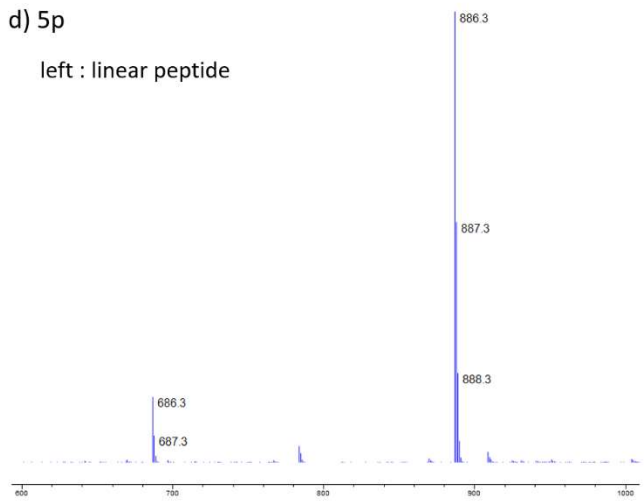


right : cyclic peptide

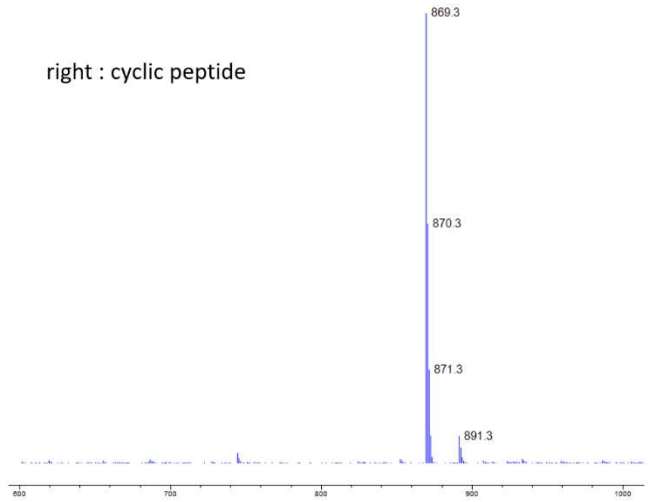


d) 5p

left : linear peptide

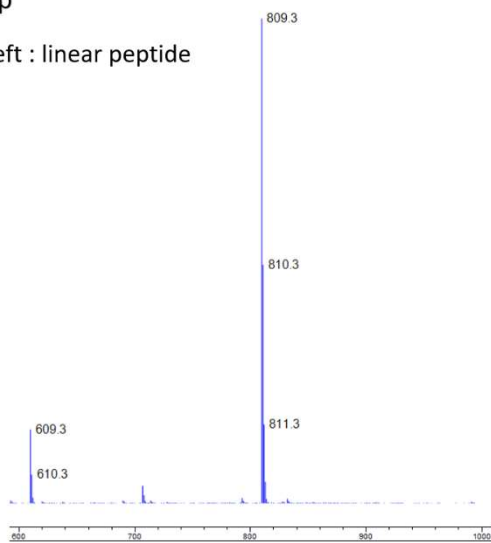


right : cyclic peptide



e) 6p

left : linear peptide



right : cyclic peptide

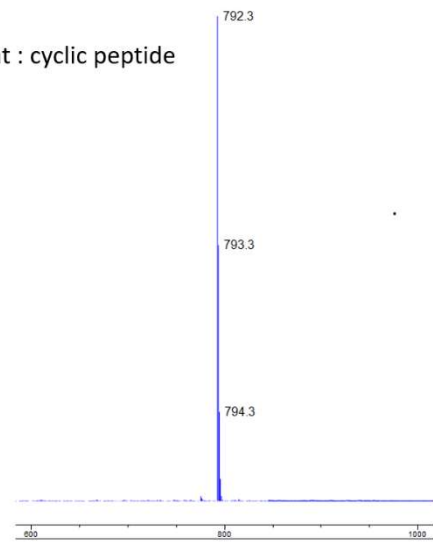
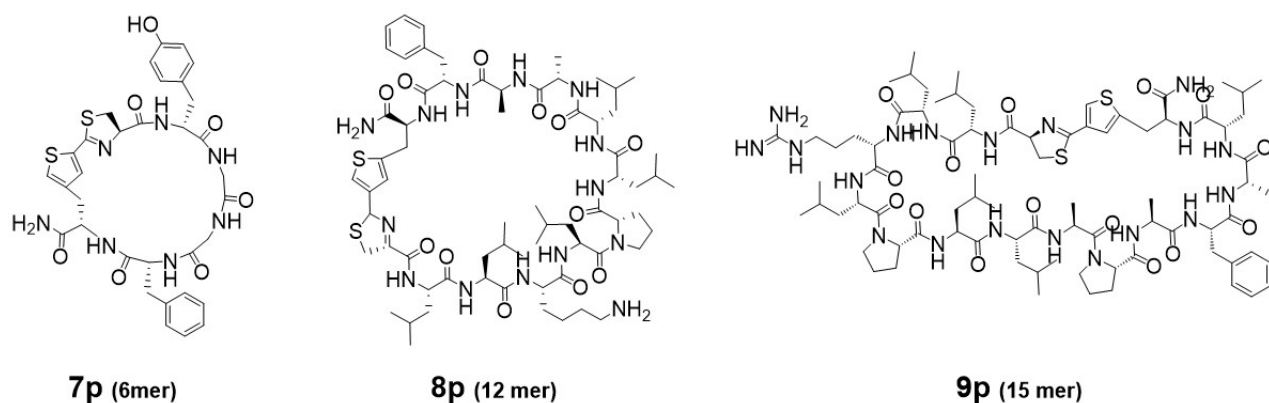


Fig. 2-8 MALDI TOF-MS analysis of peptides **2p-6p** before (left panels) and after cyclization (right panels).

2. 3. 2 Confirmation of Sequence Adaptability of Peptide Cyclization Reactions

In order to confirm that the thiazoline ring-bridged peptide cyclization can be adapted for different amino acid sequences, the formation of cyclic peptides **7p** (CYGGFX), **8p** (CLLKLPLLAAFX), and **9p** (CLLRLPLLAPAFALX) (Fig. 2-9), in which X indicates the position of cyanated amino acid, were examined. Cyanated non-natural amino acid **2** was used because it exhibited high cyclization yield. The cyclic peptides were observed as H⁺ or Na⁺ form by MALDI TOF-MS measurements (Fig. 2-10), demonstrating that cyclic peptides can be obtained even when the sequence and chain length are altered.



cyclic peptide	Sequence	Exact MS
7p	CYGGFX	705.20
8p	CLLKLPLLAAFX	1360.74
9p	CLLRLPLLAPAFALX	1669.92

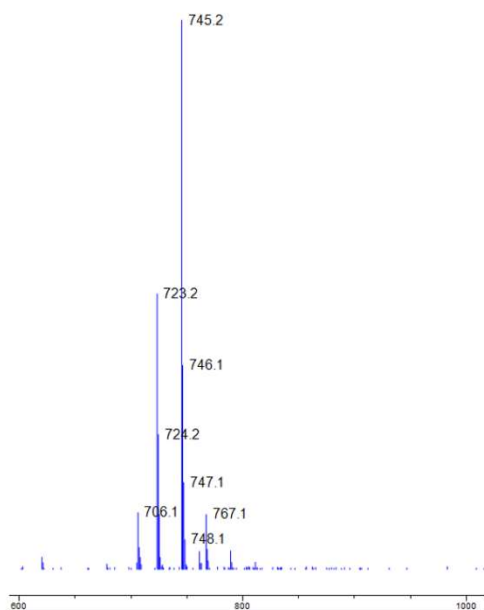
Fig. 2-9 Structure of thiazoline ring-bridged cyclic peptides with different amino acid sequences. X denotes non-natural amino acid **2**.

linear peptide	[M+H] ⁺ ; m/z (calculated)	[M+Na] ⁺ ; m/z (calculated)	[M+H] ⁺ ; m/z (analyzed)	[M+Na] ⁺ ; m/z (analyzed)
7p	723.2	746.2	723.2	746.1
8p	1378.8	1401.8	1378.6	1400.5
9p	1688.0	1710.0	1687.7	1709.7

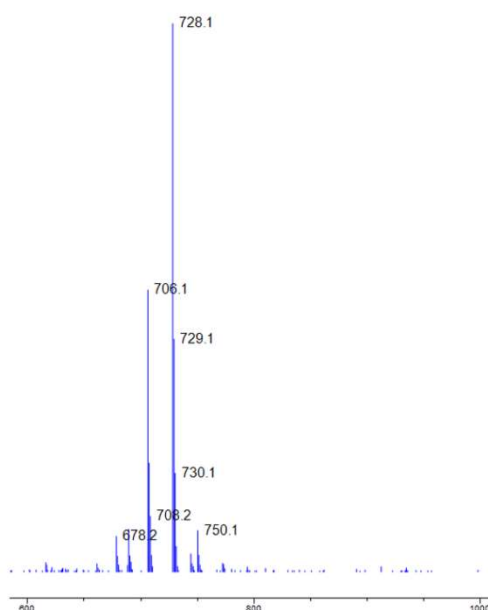
cyclic peptide	[M+H] ⁺ ; m/z (calculated)	[M+Na] ⁺ ; m/z (calculated)	[M+H] ⁺ ; m/z (analyzed)	[M+Na] ⁺ ; m/z (analyzed)
7p	706.2	729.2	706.1	729.1
8p	1361.7	1384.7	1361.5	1384.5
9p	1670.9	1693.9	1670.7	1693.7

a) 7p

left : linear peptide

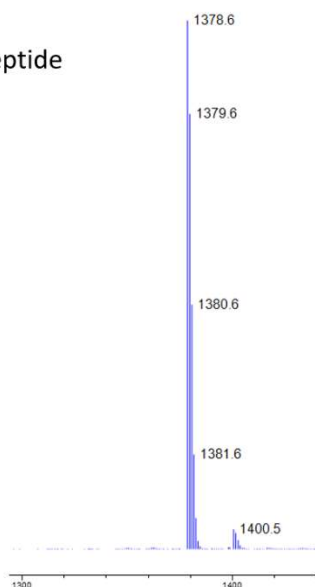


right : cyclic peptide

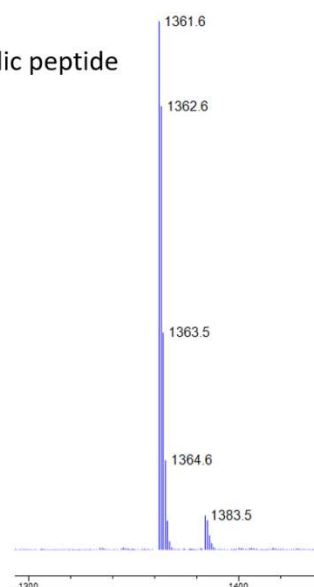


b) 8p

left : linear peptide

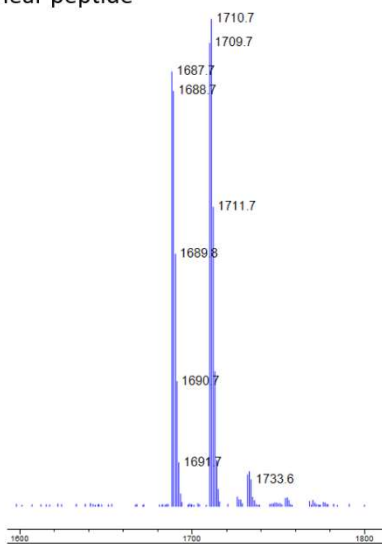


right : cyclic peptide



c) 9p

left : linear peptide



right : cyclic peptide

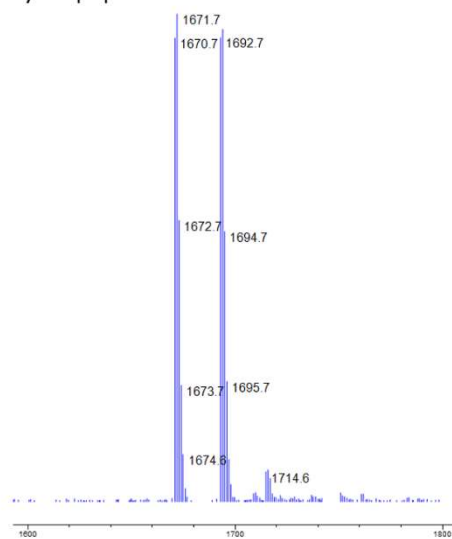


Fig. 2-10 MALDI TOF-MS analysis of thiazoline ring-bridged cyclic peptides **7p-9p** before (left panels) and after cyclization (right panels). Both H^+ and Na^+ adducts were observed.

2. 3. 3 Kinetics of thiazoline ring-bridged peptide cyclization

In order to analyze the cyclization kinetics, linear peptides were synthesized on Barlos resin and released from the resin as protected linear forms having C-terminal COOH. The protecting groups were removed by TFA, and the resulting linear peptides were confirmed not to be cyclized in the TFA salt form. After distilling off TFA under reduced pressure, the cyclization reaction was initiated by dissolving the linear peptides in MeOH/phosphate buffer (pH 7) and monitored by UPLC (Fig. 2-11). Because almost no components other than linear and cyclic peptides were identified on UPLC, the yield of cyclization was determined from the disappearance of linear peptides (Fig. 2-12). Cyclic peptides containing **2** and **5** were very rapidly produced and yields reached more than 80% in 2 hours. Cyclic peptides containing **3** and **4** were formed more slowly, and required 24 hours for 80% yield. On the other hand, the cyclization was very slow for peptide containing **6**.

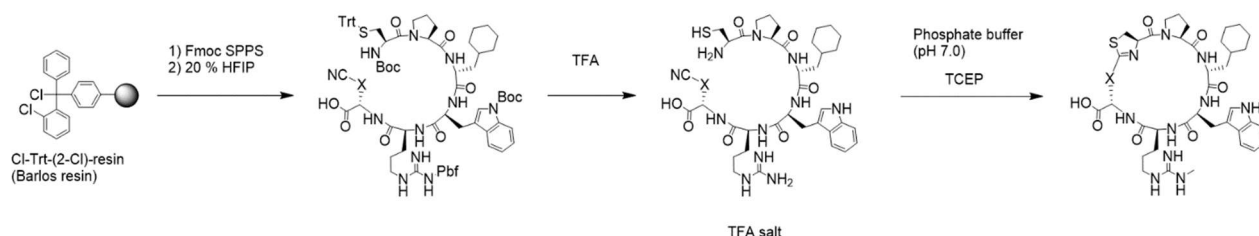


Fig. 2-11 Synthetic routes of cyclic peptides used to validate cyclization reaction kinetics.

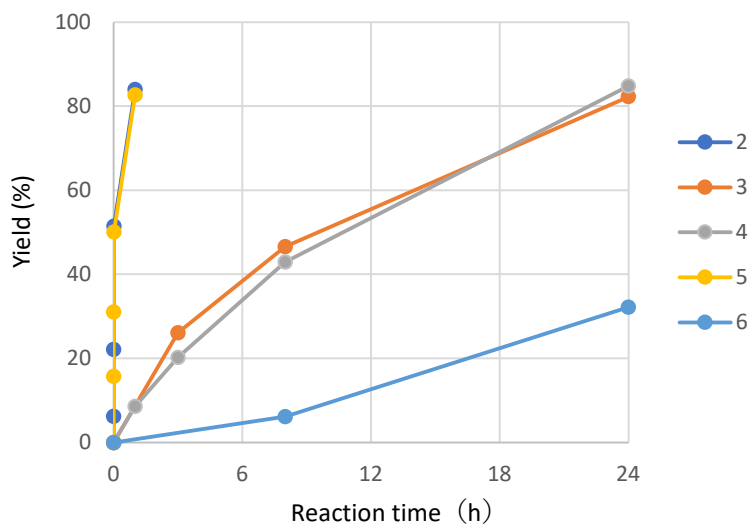
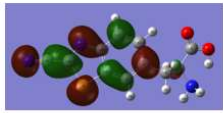
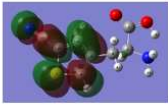
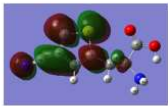
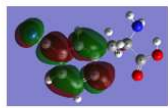
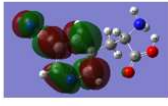



Fig. 2-12 Yield of the formation of the cyclic peptides containing cyanated non-natural amino acids **2-6** from the corresponding linear peptides.

I hypothesized the rate-limiting step is the addition of the thiol group of the N-terminal Cys residue to the carbon atom of the cyano group, and calculated the energy levels of the LUMO orbital on the carbon atom of the cyano group. B3LYP/6-31G* was used for the LUMO orbit calculation⁷⁾. All cyanated non-natural amino acids have LUMO orbital densities on the carbon of cyano group, and amino acids **2** and **5** show lower orbital energy levels than **3** and **4** (Table 2-1). On the other hand, cyanated amino acid **6** has the highest energy level. The order of the energy levels is consistent with that of the cyclization kinetics. These results suggest that the cyclization reaction can be controlled by adjusting the energy level of the LUMO orbital on the carbon atom of the cyano group. It should be noted that cyanated amino acid **1** shows the lowest energy level, suggesting that the hydrolysis of the cyano group by TFA treatment of linear peptide may be due to the high reactivity of the cyano group.

Table 2-1 Energy level of LUMO orbital for cyanated nonnatural amino acids.

Uncognated amino acid	Energy level of LUMO orbital (ev)	LUMO orbital distribution
1	-2.3	
2	-1.6	
3	-1.2	
4	-1.4	
5	-1.7	
6	-0.27	

2. 4 Conclusion

I examined the reaction characteristics and versatility of thiazoline ring-bridged peptide cyclization of linear peptides containing N-terminal Cys and non-natural amino acids having cyano groups. This is a simple method for converting linear peptides into cyclic peptides in neutral aqueous solution at room temperature with addition of a reducing reagent. The cyclization reaction starts with a reversible reaction of thiol and cyano group and is completed irreversibly by nucleophilic attack of the adjacent α -amino group and ammonia elimination. The kinetics of the thiazoline ring formation varied depending on the reactivity of the cyano group, but the reaction proceeded unless the cyano group is hydrolyzed. Furthermore, this cyclization reaction was demonstrated to be used for various peptides with 6 to 15 amino acids, suggesting that the present method can be applied to peptide libraries with different lengths for drug discovery.

References

- 1) a) Angela Kling, Peer Lukat, Deepak V Almeida, Armin Bauer, Evelyne Fontaine, Sylvie Sordello, Nestor Zaburannyi, Jennifer Herrmann, Silke C Wenzel, Claudia König, Nicole C Ammerman, María Belén Barrio, Kai Borchers, Florence Bordon-Pallie, Mark Brönstrup, Gilles Courtemanche, Martin Gerlitz, Michel Geslin, Peter Hammann, Dirk W Heinz, Holger Hoffmann, Sylvie Klieber, Markus Kohlmann, Michael Kurz, Christine Lair, Hans Matter, Eric Nuermberger, Sandeep Tyagi, Laurent Fraisse, Jacques H Grosset, Sophie Lagrange, Rolf Müller Antibiotics. Targeting DnaN for tuberculosis therapy using novel griselimycins *Science* **2015**, *348*, 1106-1112, b) Daniel S. Nielsen, Nicholas E. Shepherd, Weijun Xu, Andrew J. Lucke, Martin J. Stoermer, David P. Fairlie Orally Absorbed Cyclic Peptides *Chem. Rev.* **2017**, *117*, 8094-8128, c) Conan K. Wang, Susan E. Northfield, Barbara Colless, Stephanie Chaousis, Ingrid Haernig, Rink-Jan Lohman, Daniel S. Nielsen, Christina I. Schroeder, Spiros Liras, David A. Price, David P. Fairlie, David J. Craik Rational design and synthesis of an orally bioavailable peptide guided by NMR amide temperature coefficients *Proc. Natl. Acad. Sci. USA* **2014**, *111*, 17504-17509, d) Conan K. Wang, Susan E. Northfield, Joakim E. Swedberg, Barbara Colless, Stephanie Chaousis, David A. Price, Spiros Liras, David J. Craik Exploring experimental and computational markers of cyclic peptides: Charting islands of permeability *Eur. J. Med. Chem.* **2015**, *97*, 202-213, e) Marianne Fouché, Michael Schäfer, Jörg Berghausen, Sandrine Desrayaud, Markus Blatter, Philippe Piéchon, Ina Dix, Aimar Martin Garcia, Hans-Jörg Roth Design and Development of a Cyclic Decapeptide Scaffold with Suitable Properties for Bioavailability and Oral Exposure *ChemMedChem* **2016**, *11*, 1048-1059, f) Marianne Fouché, Michael Schäfer, Markus Blatter, Jörg Berghausen, Sandrine Desrayaud, Hans-Jörg Roth Pharmacokinetic Studies around the Mono- and Difunctionalization of a Bioavailable Cyclic Decapeptide Scaffold *ChemMedChem* **2016**, *11*, 1060-1068
- 2) John R. Frost, Conor C. G. Scully, Andrei K. Yudin Oxadiazole grafts in peptide macrocycles *Nat. Chem.* **2016**, *8*, 1105-1111
- 3) Emil H. White, Frank McCapra, George F. Field, William D. McElroy The Structure and Synthesis of Firefly Luciferin *J. Am. Chem. Soc.* **1961**, *83*, 2402-2403
- 4) a) Hongjun Ren, Fei Xiao, Ke Zhan, Young-Pil Kim, Hexin Xie, Zuyong Xia, Jianghong Rao A Biocompatible Condensation Reaction for the Labeling of Terminal Cysteine Residues on Proteins *Angew. Chem. Int. Ed.* **2009**, *48*, 9658-9662, b) Yue Yuana, Gaolin Liang A biocompatible, highly efficient click reaction and its applications, *Org. Biomol. Chem.* **2014**, *12*, 865-871
- 5) a) Peter L. Toogood, Jessica J. Hollenbeck, Huong M. Lam, Li Li A formal synthesis of althiomycin *Bioorg. Med. Chem. Lett.* **1996**, *6*, 1543-1546, b) Niña Socorro Cortina, Ole Revermann, Daniel Krug, Rolf Müller Identification and Characterization of the Althiomycin Biosynthetic Gene Cluster in *Myxococcus xanthus* DK897 *ChemBioChem* **2011**, *12*, 1411-1416, c) Jiyong Hong, Hendrik Luesch Largazole: from discovery to broad-spectrum therapy *Nat. Prod. Rep.* **2012**, *29*, 449-456, d) Karla L. Malloy, Hyukjae Choi, Catherine Fiorilla, Fred A. Valeriote, Teatulohi Matainaho, William H. Gerwick Hoiamide D, a marine cyanobacteria-derived inhibitor of p53/MDM2 interaction *Bioorg. Med. Chem. Lett.* **2012**, *22*, 683-688, e) William H. Gerwick, Philip J. Proteau, Dale G. Nagle, Ernest Hamel, Andrei Blokhin, and Doris L. Slate, Structure of Curacin A, a Novel Antimitotic, Antiproliferative and Brine Shrimp Toxic Natural Product from the Marine Cyanobacterium *Lyngbya majuscula* *J. Org. Chem.* **1994**, *59*,

6, 1243–1245

6) a) Masaaki Inoue, Takashi Tamura, Yuji Yoshimitsu, Takahiro Hoshaka, Takayoshi Watanabe Peptide Compound and Method for Producing Same, Composition for Screening use, and Method for Selecting Peptide Compound WO2018174078, b) Christoph Nitsche, Hideki Onagi, Jun-Ping Quek, Gottfried Otting, Dahai Luo, Thomas Huber Biocompatible Macrocyclization between Cysteine and 2-Cyanopyridine Generates Stable Peptide Inhibitors *Org. Lett.* **2019**, *21*, 4709-4712

7) Gaussian: <https://gaussian.com/citation/>

Gaussian 16, Revision C.01, M. J. Frisch, G. W. Trucks, H. B. Schlegel, G. E. Scuseria, M. A. Robb, J. R. Cheeseman, G. Scalmani, V. Barone, G. A. Petersson, H. Nakatsuji, X. Li, M. Caricato, A. V. Marenich, J. Bloino, B. G. Janesko, R. Gomperts, B. Mennucci, H. P. Hratchian, J. V. Ortiz, A. F. Izmaylov, J. L. Sonnenberg, D. Williams-Young, F. Ding, F. Lipparini, F. Egidi, J. Goings, B. Peng, A. Petrone, T. Henderson, D. Ranasinghe, V. G. Zakrzewski, J. Gao, N. Rega, G. Zheng, W. Liang, M. Hada, M. Ehara, K. Toyota, R. Fukuda, J. Hasegawa, M. Ishida, T. Nakajima, Y. Honda, O. Kitao, H. Nakai, T. Vreven, K. Throssell, J. A. Montgomery, Jr., J. E. Peralta, F. Ogliaro, M. J. Bearpark, J. J. Heyd, E. N. Brothers, K. N. Kudin, V. N. Staroverov, T. A. Keith, R. Kobayashi, J. Normand, K. Raghavachari, A. P. Rendell, J. C. Burant, S. S. Iyengar, J. Tomasi, M. Cossi, J. M. Millam, M. Klene, C. Adamo, R. Cammi, J. W. Ochterski, R. L. Martin, K. Morokuma, O. Farkas, J. B. Foresman, and D. J. Fox, Gaussian, Inc., Wallingford CT, 2016, b) Frontier Orbitals and Reaction Paths, K. Fukui, H. Fujimoto, Eds., World Scientific, Singapore, 1997, c) Kenichi Fukui, Tejiro Yonezawa, Chikayoshi Nagata, Haruo Shingu Molecular Orbital Theory of Orientation in Aromatic, Heteroaromatic, and Other Conjugated Molecules *J. Chem. Phys.* **1954**, *22*, 1433

Chapter 3

Membrane Permeability of Thiazoline Ring-Bridged Cyclic Peptides

3. 1 Introduction

Cyclic peptides are attracting attention as a new modality for inhibiting intracellular protein-protein interactions (PPIs) and other therapeutic targets which have not previously been targeted for drug discovery¹⁾. However, there are only a few examples of cyclic peptides with high cell membrane permeability that have been used in medicine, such as the natural product cyclosporine A (CSA), and elucidating the factors that improve the membrane permeability of cyclic peptides is an important technological goal²⁾.

Many efforts have been made to improve the cell membrane permeability of cyclic peptides with reference to the mechanism of membrane permeability of CSA³⁾. Hydrophobicity (LogP, LogD, etc.) and polar surface area (tPSA, SASA, EPSA, 3D-PSA, etc.) are potent indicators to design permeable peptides, based on the fact that CSA is composed of highly hydrophobic amino acids. For example, selective methylation of the amides that make up the cyclic peptides and the formation of intramolecular hydrogen bonds between the amide groups of the cyclic peptides to reduce the polarity of the molecule are thought to enhance membrane permeability by shielding water molecules from solvation and facilitating their transfer into the hydrophobic cell membrane⁴⁾. Second, CSA can form different conformations in the cell membrane and in water, and cyclic peptides with so-called "chameleonic" properties are thought to be advantageous for cell membrane permeability⁵⁾. In the case of cyclic peptides with a large molecular size, such as CSA, "chameleonic" properties is considered to be an essential factor for high cell membrane permeability.

On the other hand, as described in Chapter 1, it has been reported that rigid cyclopropane-ring-incorporated peptide molecules are anchored in a conformation favorable for passive diffusion and exhibit high cell membrane permeability. Further research is needed to elucidate the factors that contribute to the membrane permeability of cyclic peptides, and it will be important to obtain the factors that contribute to membrane permeability depending on the structure type.

In this chapter, I examined the membrane permeability of thiazoline-bridged cyclic peptides. Membrane permeability and its factors were discussed by comparing thioether-bridged cyclic peptides and amide-bridged cyclic peptides, which are widely used as cyclic peptides. The membrane permeability was evaluated by PAMPA (Parallel Artificial Membrane Permeation Assay) ⁶⁾ using artificial biological membranes prepared by soaking phospholipids in membrane filters. The factors responsible for membrane permeability were analyzed using ClogP and LogD as hydrophobicity indices, and NMR analysis of intramolecular hydrogen bonds and solution structure.

3. 2 Materials and methods

3. 2. 1 PAMPA measurement

Artificial phospholipid membranes were prepared by adding 5 μL of phospholipid organic solvent solution consisting of L- α -phosphatidylcholine (Avanti, Cat. 840051P, 1.67%) and 1,2-dioleoyl-sn-glycero-3-phospho-L-serine and n-dodecane/1-octanol (=10/1) on filter plate (Merck Millipore, Cat. MAIPN4550). Next, 25 μL of dimethylsulfoxide (DMSO) solution containing the peptide compound at a concentration of 20 μM was diluted to a final concentration of 1 μM by adding 475 μL of 50 mM KPB (potassium phosphate buffer, pH 7.4 or pH 6.5). 300 μL of the compound solution was added to the lower side (donor side) across the artificial phospholipid membrane of a PAMPA 96-well plate (Filter Plate (Merck Millipore, Cat. MAIPN4550)). 200 μL of 5% DMSO KPB (pH 7.4) was added to the upper side (acceptor side) across the artificial phospholipid membrane. Permeation test through the artificial phospholipid membrane was performed at 25°C for 4 hours. The concentration of the compound in solution in the donor and acceptor plates was measured by LC/MS/MS, and the membrane permeation rate (Pe) of the compound was calculated from the following equation, where t is the test time, A is the membrane filter area = 0.3 cm^2 , V_D is the donor solution volume = 300 μL , V_A is the acceptor solution volume = 200 μL , $C_D(t)$ is the compound concentration in the donor solution at time t, $C_A(t)$ is the compound concentration in the acceptor solution at time t.

$$C_{\text{equilibrium}} = [C_D(t) * V_D + C_A(t) * V_A] / (V_D + V_A)$$

$$Pe = -\ln[1 - C_A(t) / C_{\text{equilibrium}}] / [A * (1/V_D + 1/V_A) * t]$$

Pe is synonymous with P_{app} .

Permeability (in unit of cm/s)

3. 2. 2 CLogP and LogD calculation

CLogP: The results were quantified using the logP calculation tool in MarvinSkech 5.3.7 (ChemAxon). The calculation conditions were as follows: Method was set to Weighted mode, Method Weighted was set to VG to 1, KLOG to 1, PHYS to 1, Cl- concentration setting to 0.1 mol/cm^3 , Na^+ , K^+ concentration setting to 0.1 mol/cm^3 .

LogD: To 5 μL of 20 mM DMSO solution of cyclic peptide, 300 μL of octanol and 600 μL of PBS were added and shaken for 30 min. 10 μL of the octanol layer was diluted with 990 μL of ethanol to make a 100-fold dilution. The concentrations of the compounds in the PBS and octanol layers, respectively, were measured by LC-MS. The logD of the compound was calculated from the formula:

$$\log D = \log_{10} (\text{octanol layer peak area} / \text{PBS layer peak area} * 100)$$

3. 2. 3 2D-NMR and variable temperature NMR measurements

Cyclic peptides were dissolved in d_6 -DMSO to a concentration of 5 mg/mL . The sample tube was a SIGEMI tube (BMS-005B) with a sample volume of 400 μL . NMR measurements were performed on a Bruker 600 MHz cryosystem. The following three types of 2D-NMR measurements were performed for attribution. COSY (cosygpppgf, 128 times integration), TOCSY (melvphpp, 128 times integration, 80 msec expansion time), NOESY (noesygpphpp, 64 times integration, 150 msec expansion time, 300 msec). Temperature-variable ^1H NMR

measurements (zg, 64 times in total) were performed at 25°C, 30°C, 35°C, 40°C, 45°C, and 50°C, respectively, and $\Delta\delta_{\text{NH}}/\Delta T$ (ppb/K) values were calculated from the change in chemical shift values with temperature.

3. 2. 4 *Computational analysis*

The calculations for the MD method were performed in AmberTools16. The GAFF force field was used for the interaction, and the RESP charge calculated by Gaussian 09 was used for the charge. The NMR constraint option implemented in AmberTools16 was used to impose the NMR data (main chain dihedral angle and distance between HHs) as constraints. In order to obtain the 3D structure of the cyclic peptide with high accuracy and precision, the calculation steps were devised as follows:

- (1) Prepare 1000 initial structures with different conformations for the linear peptide before cyclization.
- (2) Put the cyclization and NMR data constraints in steps, respectively. The order is (i) main chain dihedral angle, (ii) cyclization and short distance HH distance, (iii) medium distance HH distance, (iv) long distance HH distance, and 0.2 ns is calculated for each of these steps.
- (3) Of the 1000 structures obtained, number them in the order in which they satisfy the NMR data. Draw the top 10, check that the structure remains the same, and make the final 3D structure.

The solvent accessible surface area (SASA) calculations were performed by applying the program implemented in AmberTools16 based on the solution structure obtained from the MD and 2D-NMR methods described above.

3. 3 Results and Discussion

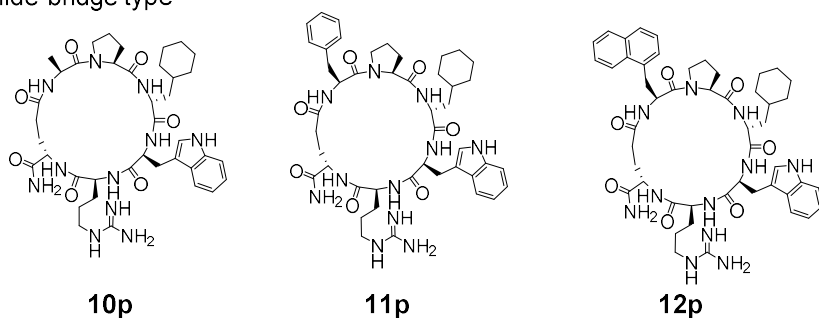
3. 3. 1 Membrane permeability of thiazoline ring-bridged cyclic peptides

For peptide drug discovery, passive diffusional cell membrane permeability of peptides is a key important factor. Therefore, I then examined the model membrane permeability of the thiazoline-bridged cyclic peptides. The hydrophilic parameters (CLogP and LogD) and the formation of intramolecular hydrogen bonds were determined and their correlation to the membrane permeability was examined.

For comparison, homologous amide-bridged and thioether-bridged cyclic peptides were used (Fig. 3-1). The amide-bridged cyclic peptides **10p-12p** contained Z-PF-(D-cha)-WRE-NH₂ sequence, in which Z was Ala, Phe, or 1-naphthylalanine, and the N-terminal amino group and the side chain carboxyl group of the C-terminal Glu were cyclized by amide bond. The thioether-bridged cyclic peptides **13p-15p** contained N-chloroacetate-Z-PF-(D-cha)-WRC-NH₂ sequence, in which Z indicates Ala, Phe, or 1-naphthylalanine, and the N-terminal chloroacetyl group and the C-terminal Cys are cyclized by thioether bond. The thioether-bridged cyclic peptide **16p** had Lys at Arg position in peptide **15p** to further increase the hydrophobicity.

The membrane permeability (P_{app}) of the cyclic peptides was evaluated by using parallel artificial membrane permeability assay (PAMPA). I defined high membrane permeability as $P_{app} > 1.0 \times 10^{-6}$ cm/s according to the literature.⁴ P_{app} and hydrophilic parameters CLogP and LogD were summarized in Table 3-1. Thiazoline ring-bridged cyclic peptides showed clear dependency of P_{app} values upon increase in CLogP (Fig. 3-2). Similar tendency was observed for LogD (Fig. 3-3). Particularly, cyclic peptides **2p-5p** showed P_{app} values above 2×10^{-6} cm/s, suggesting the possibility of high membrane permeability in living cells. On the other hand, P_{app} values were lower than 1.0×10^{-6} cm/s for the amide and thioether-bridged cyclic peptides regardless of CLogP and LogD. These results indicate the superiority of thiazoline ring-bridged cyclic peptides in model membrane permeability.

Amide-bridge type



Thioether-bridge type

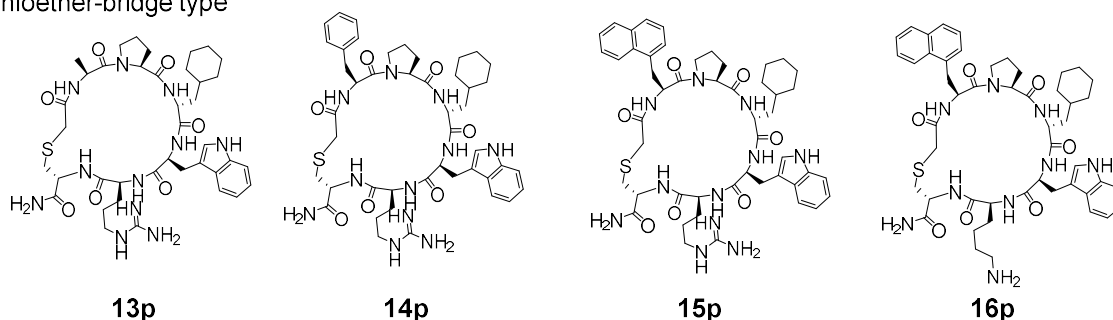


Fig. 3-1 Structure of homologous amide-bridged and thioether-bridged cyclic peptides.

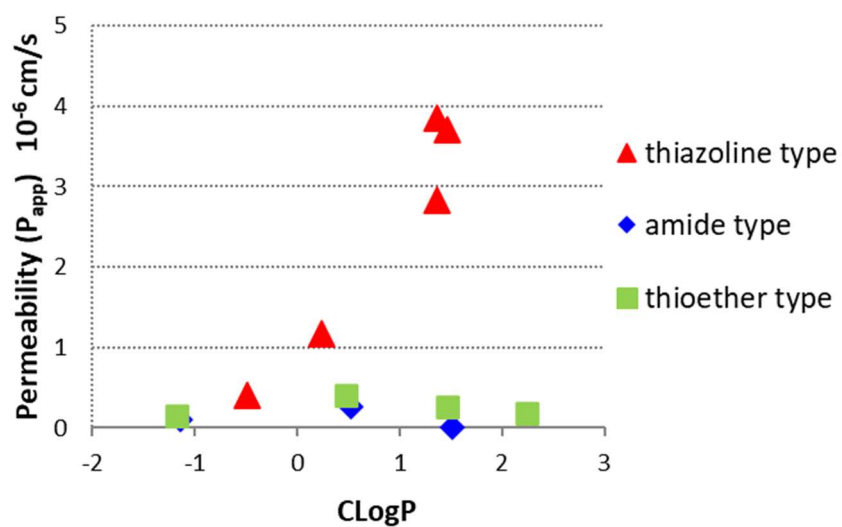


Fig. 3-2 Correlation between CLogP and P_{app} for PAMPA model membranes.

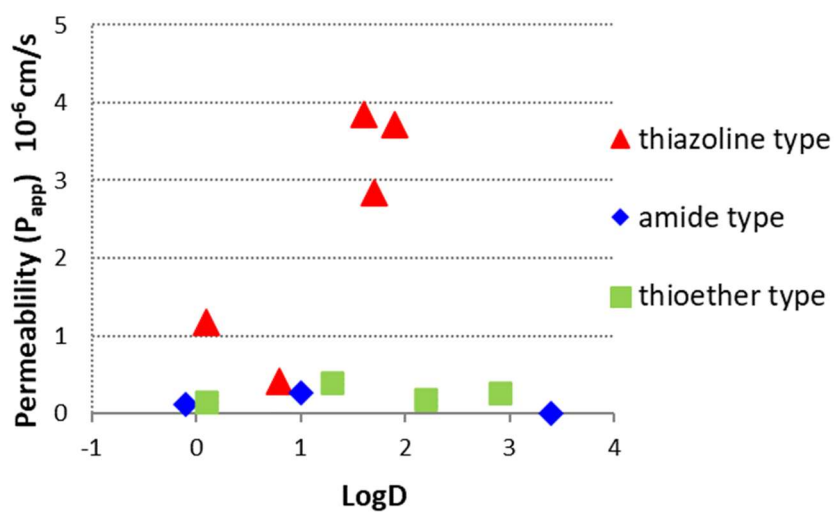


Fig. 3-3 Correlation between LogD and P_{app} for PAMPA model membranes.

Table 3-1 Summary of PAMPA model membrane permeability and hydrophobic parameters of the thiazoline-bridged, amide-bridged, and thioether-bridged cyclic peptides.

Type	Peptide No.	Exact MS	[M+H] ⁺ ; m/z (analyzed)	P _{app} PAMPA (10 ⁻⁶ cm/s)	cLogP	LogD
Thiazoline-linked	2p	873.4	874.2	2.84	1.37	1.7
	3p	873.4	874.2	3.85	1.37	1.6
	4p	867.4	868.3	3.71	1.46	1.9
	5p	868.4	869.3	1.18	0.24	0.1
	6p	791.4	792.3	0.41	-0.49	0.8
Amide-linked	10p	791.4	792.4	0.11	-1.14	-0.1
	11p	867.5	868.5	0.27	0.52	1.0
	12p	917.5	918.5	0	1.51	3.4
Thioether-linked	13p	823.4	824.4	0.15	-1.18	0.1
	14p	899.5	900.5	0.40	0.47	1.3
	15p	949.5	950.5	0.26	1.46	2.9
	16p	921.5	922.5	0	2.24	2.2

3. 3. 2 Evaluation of intramolecular hydrogen bonding

Membrane permeability has been suggested to be enhanced by intramolecular hydrogen bonds in cyclic peptides through decreasing the polarity of the amide group. In order to verify the intramolecular hydrogen bonds of the thiazoline-bridged cyclic peptides, temperature-variable NMR analysis was performed. The peptides **2p** and **3p** with different cyclization substructures and similar CLogP and LogD were used, while amide bridged **10p** and thioether bridged **13p** cyclic peptides were selected for comparison.

The presence or absence of intramolecular hydrogen bond of the amide bond in the main chain is determined based on the magnitude of the chemical shift change ($\Delta\delta_{\text{NH}}$) in response to temperature change (ΔT) in d₆-DMSO. We interpreted $\Delta\delta_{\text{NH}}/\Delta T < -4.6$ ppb/K as no hydrogen bond formation, $-3 > \Delta\delta_{\text{NH}}/\Delta T > -4.6$ ppb/K as weak intramolecular hydrogen bonds, and $\Delta\delta_{\text{NH}}/\Delta T > -3$ ppb/K as forming strong intramolecular hydrogen bonds ⁷.

Figure 3-4a summarizes the $\Delta\delta_{\text{NH}}/\Delta T$ values for each amino acid and the number of strong intramolecular hydrogen bonds in the peptide, along with the P_{app} value of PAMPA. When two chemical shifts of amide bond originating from two different conformers were observed, they were listed separately. For peptides **2p** and **3p**, the strong hydrogen bond was formed in the amide derived from non-natural amino acid **2**. For peptide **3p**, additional strong hydrogen bond was formed for a total of one in Trp and Arg of the two conformers. These thiazoline ring-bridged cyclic peptides had higher membrane permeability than 2×10^{-6} cm/s. On the other hand, no strong hydrogen bonding was observed in the amide-bridged **10p** and thioether-bridged **13p**, which had membrane permeability of less than 1×10^{-6} cm/s. Therefore, a rigid bending structure induced by the thiazoline ring-bridged structure is speculated to facilitate the formation of intramolecular hydrogen bonds. The resulting hydrogen bonds could cause the polarity offset of the amide groups and contribute to the improvement of the model membrane permeability. Further optimization of the thiazoline ring-bridged structure and the intramolecular hydrogen bond formation may be effective to improve the membrane permeability.

For increasing the cell membrane permeability, N-methylation and hydrophobization of peptides have been examined as in case of CSA, although their solubility in aqueous condition might be reduced. Our findings suggest that the thiazoline ring-bridged cyclic peptides can enhance the cell membrane permeability through intramolecular hydrogen bond formation, while the water solubility can be ensured in a highly polar environment in aqueous solution due to dissociation of the hydrogen bonds.

a)

	$\Delta\delta_{\text{NH}}/\Delta T$ (ppb/K)								Number of strong intramolecular hydrogen bonding	P_{app} (PAMPA) $\times 10^{-6}$ cm/s
	Cys	Pro	D-Cha	Trp	Arg					
2p	—	—	-4.6	-3.9	-3.3	2		1	2.84	
3p	—	—	-5.1	-0.9	-4.8	-6.9	-1.0	3	2*	
10p	-5.5	-4.0	—	-5.3	-3.2	-6.8	-3.2	-5.2	0	0.11
13p	-4.2	-4.0	—	-4.6	-6.4	-4.3	Cys		0	0.15

b)

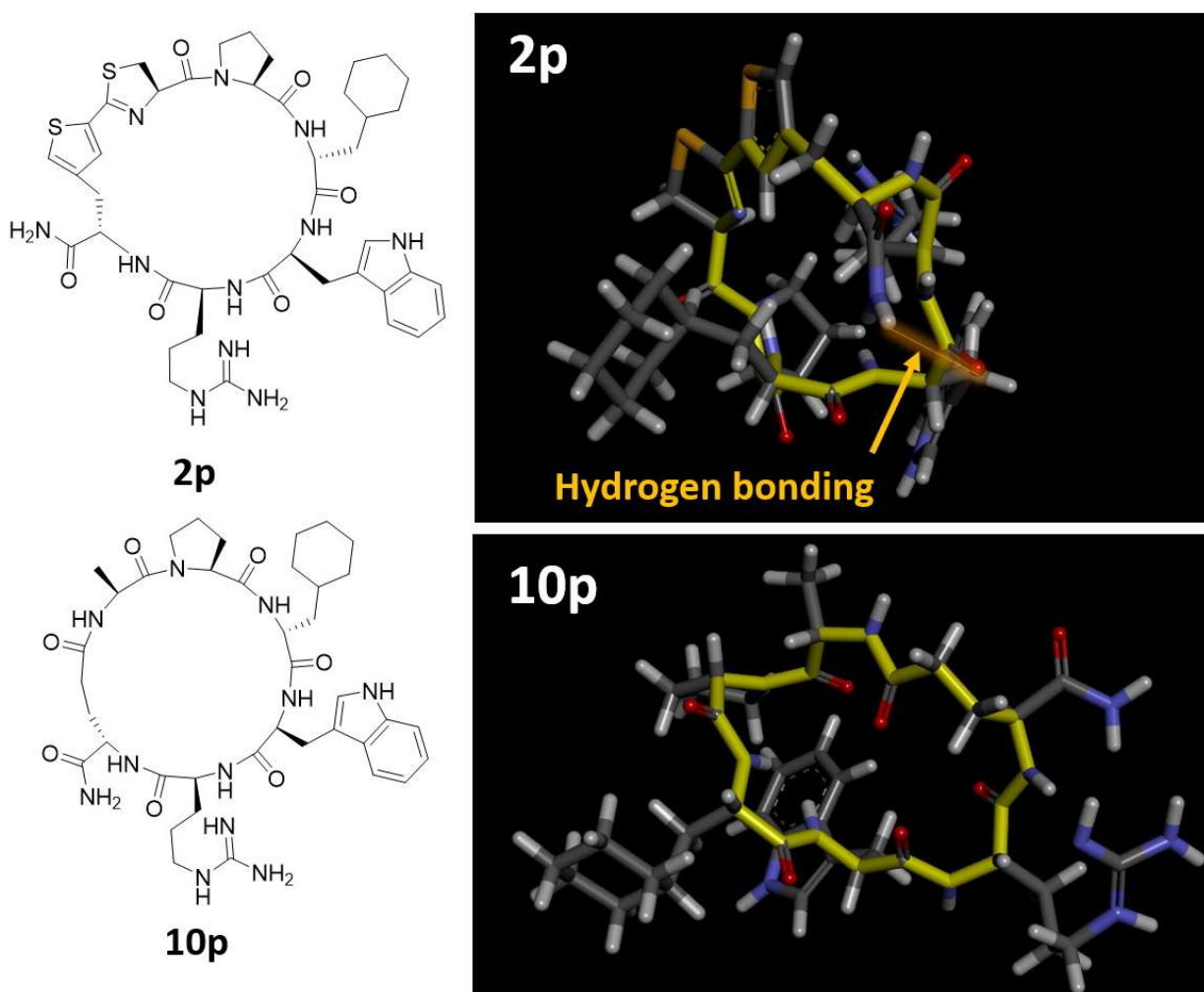


Fig. 3-4 (a) Temperature-variable chemical shift change of the amide bond, the number of strong intramolecular hydrogen bond, and model membrane permeability for the cyclic peptides **2p**, **3p**, **10p**, and **13p**. When two chemical shifts of amide bond originating from two different conformers were observed, they were listed separately. Yellow-colored amide bonds indicate strong intramolecular hydrogen bonds, and green-colored ones indicate weak intramolecular hydrogen bonds. (b) Solution structures of cyclic peptide **2p** and **10p**. The main chains of the cyclic peptides are highlighted in yellow. Polar surface areas were calculated to be 778 \AA^2 and 844 \AA^2 , respectively.

3. 3. 3 *The polar surface area of solution structure*

The effect of hydrophobic groups and intramolecular hydrogen bonding on the shielding of amide groups from polar groups was then evaluated. From the data based on 2D NMR measurements of the thiazoline ring-bridged **2p** and the amide-bridged **10p** peptides in d6-DMSO, each solution structure was determined by quantum dynamics calculations (AmberTools16) and the Solvent Accessible Surface Area (SASA) was calculated (Fig. 3-4b). The results showed that the thiazoline-type peptide **2p** has a lower polar surface area (778 Å²) than the amide type peptide **10p** (844 Å²). The distance between the C-terminal amide nitrogen atom and the carbonyl oxygen of Trp in the peptide **2p** was 3.5 Å. This intramolecular hydrogen bonds could be formed in an aqueous phase near the model membrane, and contribute to reduce the polarity required for the membrane permeability. Furthermore, the polar part of the cyclic peptide was shielded by the hydrophobic surface derived from the thiazoline-bridged structure to suppress the polar surface area. On the other hand, the amide-bridged peptide **10p** gave neither polar offset nor shielding effect. It has been reported that the cell membrane permeability of cyclic peptides correlates with low polar surface area ⁸). The present results that the peptide **2p** with lower surface area had better membrane permeability showed a similar tendency.

3. 4 Conclusion

I revealed that the thiazoline ring-bridged cyclic peptides showed higher membrane permeability on PAMPA model membranes than the amide-bridged and thioether-bridged cyclic peptides. This high permeability can be attributed to the polar offset by intramolecular hydrogen bonding and the introduction of thiazoline ring structures, which reduced the polar surface area of the peptides. In addition, the membrane permeability of the amide-bridged and thioether-bridged types was not improved even though the hydrophobicity parameters increased by the introduction of hydrophobic groups, indicating that the introduction of hydrophobic groups does not always improve the membrane permeability. These results suggest the importance of the control of the steric structure of peptides in the solution state. Previously, it has been reported that polar surface area does not always correlate with the membrane permeability⁹⁾ and various factors including the rate of conformational change in aqueous and membrane environments may affect the membrane permeability. Therefore, further studies should be added to pursue the membrane permeability factors of thiazoline-bridged cyclic peptides.

References

- 1) Ziqing Qian, Patrick G Dougherty, Dehua Pei Targeting intracellular protein-protein interactions with cell-permeable cyclic peptides *Curr Opin Chem Biol.* **2017**, *38*, 80-86
- 2) Pär Matsson, Jan Kihlberg How Big Is Too Big for Cell Permeability? *J. Med. Chem.* **2017**, *60*, 1662–1664
- 3) Karen M. Corbett, Leigh Ford, Dallas B. Warren, Colin W. Pouton, David K. Chalmers Cyclosporin Structure and Permeability: From A to Z and Beyond *J. Med. Chem.* **2021**, *64*, 13131–13151
- 4) a) Alexander Alex, David S. Millan, Manuel Perez, Florian Wakenhuta, Gavin A. Whitlock Intramolecular hydrogen bonding to improve membrane permeability and absorption in beyond rule of five chemical space *Med. Chem. Commun.*, **2011**, *2*, 669-674, b) Tina R. White, Chad M. Renzelman, Arthur C. Rand, Taha Rezai, Cayla M. McEwen, Vladimir M. Gelev, Rushia A. Turner, Roger G. Linington, Siegfried S. F. Leung, Amit S. Kalgutkar, Jonathan N. Bauman, Yizhong Zhang, Spiros Liras, David A. Price, Alan M. Mathiowetz, Matthew P. Jacobson, R. Scott Lokey On-resin N-methylation of cyclic peptides for discovery of orally bioavailable scaffolds *Nat. Chem. Biol.* **2011**, *7*, 810-817, c) Matteo Rossi Sebastiano, Bradley C. Doak, Maria Backlund, Vasanthanathan Poongavanam, Björn Over, Giuseppe Ermondi, Giulia Caron, Pär Matsson, Jan Kihlberg Impact of Dynamically Exposed Polarity on Permeability and Solubility of Chameleonic Drugs Beyond the Rule of 5 *J. Med. Chem.* **2018**, *61*, 4189-4202, d) Matthew R. Naylor, Andrew M. Ly, Mason J. Handford, Daniel P. Ramos, Cameron R. Pye, Akihiro Furukawa, Victoria G. Klein, Ryan P. Noland, Quinn Edmondson, Alexandra C. Turmon, William M. Hewitt, Joshua Schwochert, Chad E. Townsend, Colin N. Kelly, Maria-Jesus Blanco, R. Scott Lokey Lipophilic Permeability Efficiency Reconciles the Opposing Roles of Lipophilicity in Membrane Permeability and Aqueous Solubility *J. Med. Chem.* **2018**, *61*, 11169-11182, e) Kouhei Matsui, Yasuto Kido, Ryosuke Watari, Yousuke Kashima, Yutaka Yoshida, Satoshi Shuto Highly Conformationally Restricted Cyclopropane Tethers with Three-Dimensional Structural Diversity Drastically Enhance the Cell Permeability of Cyclic Peptides *Chem. Eur. J.* **2017**, *23*, 3034-3041, f) Emma Danelius, Vasanthanathan Poongavanam, Stefan Peintner, Lianne H. E. Wieske, Máté Erdélyi, Jan Kihlberg Solution Conformations Explain the Chameleonic Behaviour of Macrocyclic Drugs *Chem. Eur. J.* **2020**, *26*, 5231-5244, g) Gilles H. Goetz, Laurence Philippe, Michael J. Shapiro EPSA: A Novel Supercritical Fluid Chromatography Technique Enabling the Design of Permeable Cyclic Peptides *ACS Med. Chem. Lett.* **2014**, *5*, 1167-1172, h) Akihiro Furukawa, Joshua Schwochert, Cameron R. Pye, Daigo Asano, Quinn D. Edmondson, Alexandra C. Turmon, Victoria G. Klein, Satoshi Ono, Okimasa Okada, R. Scott Lokey Drug-Like Properties in Macrocycles above MW 1000: Backbone Rigidity versus Side-Chain Lipophilicity *Angew. Chem. Int. Ed.* **2020**, *59*, 21571-21577, i) Colin N. Kelly, Chad E. Townsend, Ajay N. Jain, Matthew R. Naylor, Cameron R. Pye, Joshua Schwochert, R. Scott Lokey Geometrically Diverse Lariat Peptide Scaffolds Reveal an Untapped Chemical Space of High Membrane Permeability *J. Am. Chem. Soc.* **2021**, *143*, 705-714, j) Huy N. Hoang, Timothy A. Hill, David P. Fairlie Connecting Hydrophobic Surfaces in Cyclic Peptides Increases Membrane Permeability *Angew. Chem. Int. Ed.* **2021**, *60*, 8385-8390, k) Kyohei Hayashi, Shota Uehara, Shiho Yamamoto, Douglas R. Cary, Junichi Nishikawa, Taichi Ueda, Hiroki Ozasa, Kousuke Mihara, Norito Yoshimura, Taeko Kawai, Takashi Ono, Saki Yamamoto, Masataka Fumoto, Hidenori Mikamiyama Macrocyclic Peptides as a Novel Class of NNMT Inhibitors: A SAR Study Aimed at Inhibitory Activity in the Cell *ACS Med. Chem. Lett.* **2021**, *12*,

- 1093-1101, l) Praew Thansandote, Robert M. Harris, Hannah L. Dexter, Graham L. Simpson, Sandeep Pal, Richard J. Upton, Klara Valko Improving the passive permeability of macrocyclic peptides: Balancing permeability with other physicochemical properties *Bioorg. Med. Chem.* **2015**, *23*, 322-327
- 5) a) Taha Rezai, Bin Yu, Glenn L. Millhauser, Matthew P. Jacobson, R. Scott Lokey Testing the Conformational Hypothesis of Passive Membrane Permeability Using Synthetic Cyclic Peptide Diastereomers *J. Am. Chem. Soc.* **2006**, *128*, 2510-2511, b) Taha Rezai, Jonathan E. Bock, Mai V. Zhou, Chakrapani Kalyanaraman, R. Scott Lokey, Matthew P. Jacobson Conformational Flexibility, Internal Hydrogen Bonding, and Passive Membrane Permeability: Successful in Silico Prediction of the Relative Permeabilities of Cyclic Peptides *J. Am. Chem. Soc.* **2006**, *128*, 14073-14080, c) Jagna Witek, Bettina G. Keller, Markus Blatter, Axel Meissner, Trixie Wagner, Sereina Riniker Kinetic Models of Cyclosporin A in Polar and Apolar Environments Reveal Multiple Congruent Conformational States *J. Chem. Inf. Model.* **2016**, *56*, 1547–1562, d) Adrian Whitty, Mengqi Zhong, Lauren Viarengo, Dmitri Beglov, David R Hall, Sandor Vajda Quantifying the chameleonic properties of macrocycles and other high-molecular-weight drugs *Drugs. Drug Discov. Today* **2016**, *21*, 712–717, e) Conan K. Wang, Joakim E. Swedberg, Peta J. Harvey, Quentin KaasO, David J. Craik Conformational Flexibility Is a Determinant of Permeability for Cyclosporin *J. Phys. Chem. B* **2018**, *122*, 2261-2276, f) Giulia Caron, Jan Kihlberg, Gilles Goetz, Ekaterina Ratkova, Vasanthanathan Poongavanam, Giuseppe Ermondi Steering New Drug Discovery Campaigns: Permeability, Solubility, and Physicochemical Properties in the bRo5 Chemical Space *J. Med. Chem.* **2021**, *64*, 12761–12773
- 6) M Kansy, F Senner, K Gubernator Physicochemical high throughput screening: parallel artificial membrane permeation assay in the description of passive absorption processes *J. Med. Chem.* **1998**, *41*, 1007–1010
- 7) a) Tomasz Cierpicki, Jacek Otlewski Amide proton temperature coefficients as hydrogen bond indicators in proteins *J. Biomol NMR* **2001**, *21*, 249-261, b) Lara R. Malins, Justine N. deGruyter, Kevin J. Robbins, Paul M. Scola, Martin D. Eastgate, M. Reza Ghadiri, Phil S. Baran Peptide Macrocyclization Inspired by Non-Ribosomal Imine Natural Products *J. Am. Chem. Soc.* **2017**, *139*, 5233-5241
- 8) William M. Hewitt, Siegfried S. F. Leung, Cameron R. Pye, Alexandra R. Ponkey, Maria Bednarek, Matthew P. Jacobson, R. Scott Lokey Cell-Permeable Cyclic Peptides from Synthetic Libraries Inspired by Natural Products *J. Am. Chem. Soc.* **2015**, *137*, 715-721
- 9) Flaviu Cipcigan, Paul Smith, Jason Crain, Anders Hogner, Leonardo De Maria, Antonio Llinas, Ekaterina Ratkova Membrane Permeability in Cyclic Peptides is Modulated by Core Conformations *J. Chem. Inf. Model.* **2021**, *61*, 263-269

Chapter 4

Expression of Thiazoline Ring-Bridged Cyclic Peptides in Cell-Free Translation

4.1 Introduction

Cyclic peptides are expected to have higher metabolic stability, cell membrane permeability, and target binding properties, compared to linear peptides, and are attracting attention as a promising modality for peptide drugs ¹⁾. In order to obtain cyclic peptides that can bind to drug targets, the combinatorial use of peptide cyclization reactions and mRNA/cDNA display technology has been investigated ²⁾. There have been two types of peptide cyclization reactions used for mRNA/cDNA display in addition to disulfide- and amide-bridged cyclization. One is cyclization using reactive groups introduced into peptides as non-natural amino acids, and the other is cyclization using cross-linker reagents. As an example of use of non-natural amino acids, N-chloroacetylated amino acid is introduced into the N-terminus of peptides in a cell-free translation system to produce cyclic peptides by intramolecular nucleophilic substitution reaction with the SH group of Cys in the peptide chain ³⁾. Using this cyclization reaction combined with cDNA-display, peptides against drug targets such as E6AP ⁴⁾, SIRT2 ⁵⁾, VEGFR2 ⁶⁾ and MATE ⁷⁾ have been developed. In addition, native chemical ligation between the N-terminal Cys and non-natural amino acids carrying thioester side chains was also applied to mRNA-display ⁸⁾. As an example of use of polycyclic cross-linker, dibromoxylene was used to cyclize peptides with two Cys residues in a cell-free translation, which was applied to mRNA display to obtain cyclic peptides that bind to thrombin ⁹⁾. In addition, disuccinimidyl glutarate was used for cross-linking N-terminal α -amino group with ϵ -amino group of Lys to obtain a cyclic peptide that binds to G α i1 ¹⁰⁾.

On the other hand, there have been a limited number of reports of ring structure-bridged cyclic peptides expressed in cell-free translation systems. The Huisgen reaction was used to form triazole ring-bridged cyclic peptides have been reported, although it has not been adapted to mRNA/cDNA-display.¹¹⁾ Cyclic peptides with a ring structure in the main chain have been reported to improve cell membrane permeability and oral absorption ¹²⁾, and therefore, ring structure-bridged cyclic peptides will be a useful platform for drug discovery. In chapter 2, I have reported on the development of intramolecular cyclization of linear peptides with N-terminal Cys and cyano group-containing nonnatural amino acids to produce thiazoline ring-bridged cyclic peptides. The thiazoline ring-bridged cyclization reaction proceeded in aqueous solution spontaneously and generated a unique heterocyclic structure in the peptide main chain. I also found that the thiazoline ring-bridged cyclic peptides exhibited high model membrane permeability due to the formation of intramolecular hydrogen bonds using chemically synthesized peptides.

In this chapter, I evaluated the applicability of this novel peptide cyclization reaction in a cell-free translation system. The cyanated non-natural amino acids were incorporated into peptides using the amber suppression method

(Fig. 4-1). The effects of the amino acid sequence including internal Cys residues and the chain length of the cyclic peptides on the thiazoline ring-bridged cyclization reaction were examined. The characteristics and versatility of this cyclization reaction will provide basic insights for future applications in peptide drug discovery.

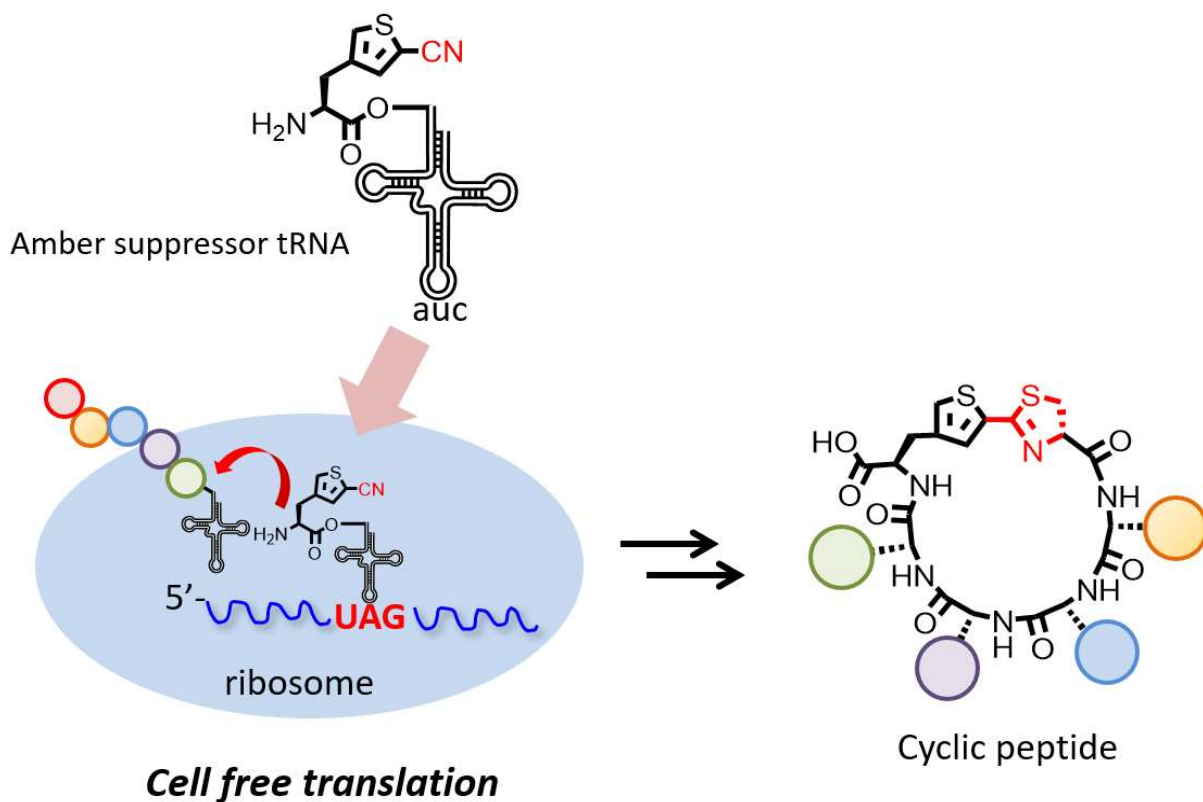


Fig. 4-1 Schematic illustration of expression of cyclic peptides in a cell-free translation system by using non-natural amino acid mutagenesis.

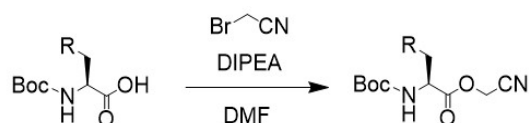
4. 2 Materials and methods

4. 2. 1 Synthetic method for aminoacyl-pdCpAs (general)

Boc-protected amino acids were synthesized using the intermediates in the synthesis of Fmoc-protected amino acids described above. For the synthesis of Boc-protected amino acid cyanomethyl ester, Boc-protected amino acid was dissolved in DMF and DIPEA (1.1 eq) was added, followed by addition of bromoacetonitrile (1.05 eq) and stirring. After completion of the reaction, the reaction solution was distilled off under reduced pressure and purified by silica gel column chromatography (Fig. 4-2).

Next, DMF solution of pdCpA tetrabutylammonium salt (3 eq.) was added to the Boc-protected amino acid cyanomethyl ester, and the mixture was vortexed and shaken for 1 hour. After completion of the reaction, the product was diluted with 0.38 % formic acid solution/acetonitrile (1/1) solution and purified according to the following conditions. High performance liquid chromatography (HPLC) (Agilent 1260 Infinity Binary LC System, column: Agilent ZORBAX SB-C18 (9.4 x 50 mm), column temperature: 40°C, gradient conditions: H₂O (0.1% TFA) / acetonitrile (0.1% TFA) = 90/10 to 0/100, flow rate: 4.0 ml/min, detection wavelength: 254 nm).

The solvent of the eluate was removed under reduced pressure, and TFA was added to the residue obtained. After shaking at room temperature for 1 hour, the solvent was removed under reduced pressure to obtain the aminoacyl-pdCpA (Fig. 4-3).



entry	Structure of Boc-amino acid cyano methyl ester	¹ H-NMR (CHCl ₃)
Boc-1		δ : 8.19 (1H, d, J = 8.6 Hz), 7.81 (1H, d, J = 1.3 Hz), 7.47 (1H, dd, J = 8.6, 1.3 Hz), 5.06-4.92 (1H, m), 4.91-4.60 (3H, m), 3.42-3.20 (2H, m), 1.41 (10H, s)
Boc-2		δ : 7.45 (1H, s), 7.34 (1H, s), 5.05-4.92 (1H, m), 4.91-4.59 (3H, m), 4.42-4.36 (2H, m), 3.26-3.16(1H, m), 3.09 (1H, dd, J = 14.5, 6.6 Hz), 1.44 (9H, s)
Boc-3		δ : 7.83 (1H, s), 7.05 (1H, s), 5.14-5.01 (1H, m), 4.80 (2H, dd, J = 26.8, 15.5 Hz) , 4.71-4.61 (1H, m), 3.50-3.25 (2H, m), 1.45 (9H, s)
Boc-4		δ : 8.81 (1H, d, J = 2.0 Hz), 8.65 (1H, d, J = 2.0 Hz), 7.82 (1H, t, J = 2.0 Hz), 5.11-4.98 (1H, m), 4.90-4.59 (3H, m), 3.36-3.24 (1H, m), 3.14-3.01 (1H, m), 1.42 (9H, s)
Boc-5		δ : 7.59 (1H, d, J = 6.6 Hz), 7.51-7.40 (3H, m), 5.02-4.90 (1H, m), 4.88-4.59 (3H, m), 3.22 (1H, dd, J = 13.9, 5.3 Hz), 3.13-3.01 (1H, m), 1.49 (9H, s)
Boc-6		δ : 5.48-5.35 (1H, m), 4.86 (2H, dd, J = 19.5, 15.5 Hz) , 4.65-4.53 (1H, m), 3.09-2.93 (2H, m), 1.47 (9H, s)

Fig. 4-2 Synthesis and characterization of Boc-protected non-natural amino acid cyanomethyl esters.

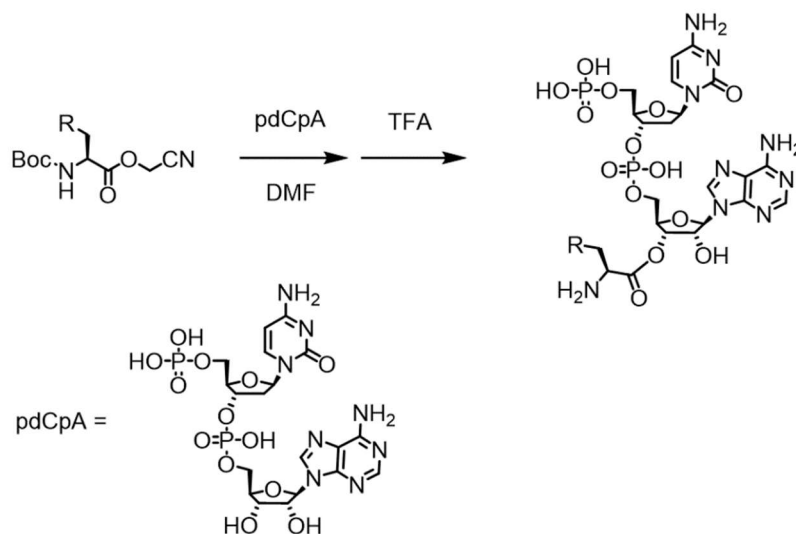


Fig. 4-3 Synthesis of non-natural aminoacyl-pdCpAs.

4. 2. 2 Preparation of aminoacyl-tRNAs

Amber suppressor tRNA(-CA) derived from *Mycoplasma capricolum* Trp tRNA and lacking 3' dinucleotide was prepared as described previously. A reaction mixture containing 55 mM HEPES-Na (pH 7.5), 15 mM MgCl₂, 3.3 mM DTT, 1 mM ATP, 20 µg/mL BSA, 25 µM amber suppressor tRNA(-CA), 1.33 µL of DMSO solution of 0.73 mM aminoacyl-pdCpA, and 16 U of T4 RNA ligase in 13.3 µL was prepared in a 1.5 mL sample tube and incubated at 4°C for 2 hours. Then, 13.3 µL of 0.6 M potassium acetate solution (pH 4.5) and 80 µL of ethanol were added to the reaction solution, and the mixture was allowed to stand at -80°C for 30 min. Then, centrifugation (4°C, 13200 rpm) was performed for 30 minutes to remove the supernatant. Gently add 200 µL of 70% ethanol solution and centrifuge (4°C, 13200 rpm) for 30 minutes. The supernatant was removed again and dried under reduced pressure to obtain aminoacyl-tRNA. The resulting aminoacyl-tRNA was dissolved in 1 mM potassium acetate (pH 4.5) just before adding to the translation mixture.

4. 2. 3 Preparation of mRNAs

The template DNA gene for mRNA was designed to contain T7 promoter and ribosome binding sequence upstream of the open reading frame. The sequence of was:

CGAAATTAATACGACTCACTATAGGGAGACCACAACGGTTTCCTCTAGAAATAATTTTGTTTAACTTTA
 AGAAGGAGATATACATATGTGCAAACAGAAACCGCGGAGCAAAAACTAGAGCGACTACAAAGACGAT
GACGACAAATAAGCTTGAGTATTCTATAGTGT, in which peptide-encoding region was underlined. The DNA was synthesized by primer extension of oligo DNAs, and purified using the QIAquick PCR Purification Kit (QIAGEN).

Next, mRNA was synthesized by transcription reaction. A reaction mixture containing 40 mM Tris-HCl (pH 8.0), 50 mM NaCl, 8 mM MgCl₂, 5 mM DTT, 4 mM each of NTPs, 2 mM spermidine, 20 µg/mL of BSA, 0.5 unit of

inorganic pyrophosphatase , 40 units of RNase inhibitor, 200 units of Thermo T7 RNA polymerase, and 2 µg of template DNA in a 100µL was prepared and incubated at 37°C for 6 hours. To the reaction mixture, 100 µL of 5 M ammonium acetate was added and placed on ice for 20 minutes. The mixture was centrifuged at 13,200 rpm for 20 minutes at 4°C. The supernatant was removed and the precipitate was dissolved in 200 µL of 1xTE buffer (10 mM Tris-HCl (pH 8.0), 1 mM EDTA (pH 8.0)). Equal volume of phenol/chloroform = 1/1 (saturated with 1 x TE) was added, vortexed, and centrifuged. The upper layer was collected and an equal volume of chloroform was added, vortexed, and centrifuged. The upper layer was collected and 20 µL of 3 M potassium acetate pH 4.5 and 600 µL of ethanol were added, mixed gently, and placed at -80°C for 30 minutes. After centrifugation at 13200 rpm for 30 minutes at 4°C, the supernatant was removed and 200 µL of 70 % cold ethanol stored at -30 °C was added, and the mixture was centrifuged at 13200 rpm for 5 seconds at 4°C. The supernatant was removed and the mixture was dried under reduced pressure. The concentration was determined by spectrophotometer and dissolved in water to 16 µM.

4. 2. 4 Cell-free translation

Cell-free translation was carried out using PUREfrex custom ver. 2 (GeneFrontier) manufactured without adding 20 amino acids. The PUREfrex system was mixed with 45 µM amino acid mixture without methionine, 40 pmol of mRNA, and 400 pmol of aminoacylated amber suppressor tRNA solution obtained above, and incubated at 37°C for 30 minutes. The reaction mixture was further incubated at 37°C for 30 minutes in the presence of 1mM tris(2-carboxyethyl)phosphine (TCEP). To the reaction mixture, 31 µL of wash buffer (20 mM phosphate buffer (pH 7.5), 500 mM NaCl, 5 mM imidazole) and 10 µL of magnetic bead solution (MBL Life Sciences, Anti-DDDDK-tag mAb-Magnetic Agarose) were added and shaken using a vortex at room temperature for 30 min. Then, the supernatant was removed by centrifugation, and the washing step for the magnetic beads (addition of 200 µL of wash buffer, shaking with vortex, centrifugation, and removal of supernatant) was repeated three times. To elute the purified products, 10 µL of 2% formic acid solution was added to the resulting magnetic beads and shaken with vortex at room temperature for 1 hour. The magnetic beads were then sedimented by centrifugation, and the supernatant was collected. The purified products were identified by MALDI TOF-MS.

4. 3 Results and Discussion

4. 3. 1 Expression of cyclic peptides in cell-free translation system

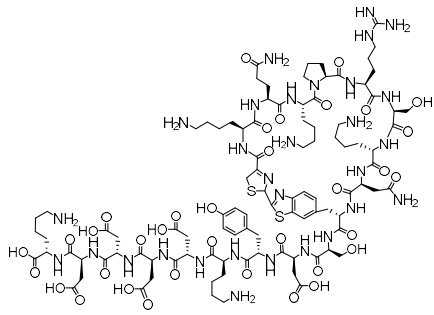
In addition to chemical synthesis of cyclic peptides, peptide expression in a cell-free translation system was investigated to enable rapid synthesis of thiazoline-bridged cyclic peptides in response to the gene code. The cyanated non-natural amino acids were incorporated into peptides using the amber suppressor tRNA (Fig. 4-1).

Aminoacylated tRNAs with non-natural amino acids were synthesized using chemical aminoacylation method¹³. N-Boc-protected non-natural amino acid was esterified with cyanomethyl group (Fig. 4-2), condensed with pdCpA, and deprotected with TFA to obtain non-natural aminoacyl-pdCpAs (Fig. 4-3). Desired aminoacyl-tRNAs were prepared by ligating non-natural aminoacyl-pdCpAs and an amber suppressor tRNA derived from *Mycoplasma capricolum* Trp tRNA lacking two bases of the 3'-terminus¹⁴. As a model peptide, CKQKPRSKNXS-DYKDDDDK sequence was designed, where cyanated non-natural amino acid was designed to be incorporated at X position in response to the amber codon and linked with N-terminal Cys residue to produce cyclic peptides **17p-22p** (Fig. 4-4). The synthetic gene fused with T7 promoter, SD sequence, start codon AUG, and termination codon UAA was constructed by primer extension reaction. The corresponding mRNA was prepared by transcription using T7 RNA polymerase.

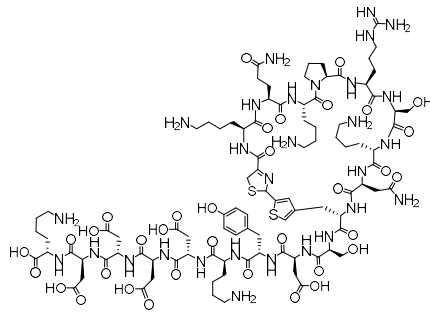
For expression of peptides containing Cys at the N-terminus without the initial Met residue, the cell-free translation was performed without methionine⁸). The non-natural aminoacylated amber suppressor tRNA and the peptide-encoding mRNA were added to the reconstituted cell-free translation system, PURE system (PUREfrex custom ver. 2, GeneFrontier), and incubated at 37 °C for 30 min. After addition of TCEP, the reaction mixture was incubated for another 30 minutes. The expressed peptides were immobilized onto anti-DYKDDDDK antibody-coated magnetic beads, washed with PBS buffer, and eluted by incubation with 2% formic acid for 1 hour. The eluates were analyzed by MALDI TOF-MS.

The results of the MALDI-TOF MS analysis are shown in Fig. 4-5. In case of non-natural amino acid **2**, the cyclic peptide **18p** with expected m/z value of 2331.1 was clearly observed but the linear form was not detected. This indicates that the peptide was expressed in the cell-free translation system and cyclized in a quantitative manner. Non-natural amino acid **1** also gave only the cyclic peptide **17p**.

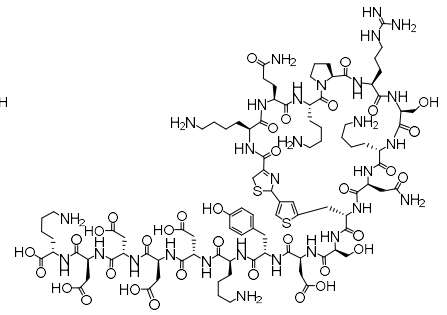
On the other hand, in case of non-natural amino acid **5**, the cyclic peptide **21p** was partly generated but some amount of linear peptides was remained. Moreover, non-natural amino acids **3**, **4**, and **6** gave linear peptides with few amount of cyclized forms. These results indicate that all the non-natural amino acids used in this research were introduced into the peptides through the amber suppression, but the cyclization efficiency depended on the types of cyanated residues. Considering the cyclization efficiency, non-natural amino acids **1** and **2** were preferred for the expression of the thiazoline ring-bridged cyclic peptides. It should be noted that byproducts with m/z 26 larger than that of the linear peptides were detected for non-natural amino acids **3-5**. MS/MS analysis of the byproduct for **19p** gave b fragments with m/z 26 larger than those of the linear peptide, suggesting that the N-terminal Cys was modified to form a cyclic carbamothioic acid derivative (Fig. 4-6).



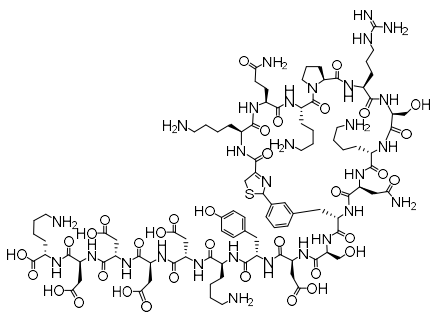
17 p



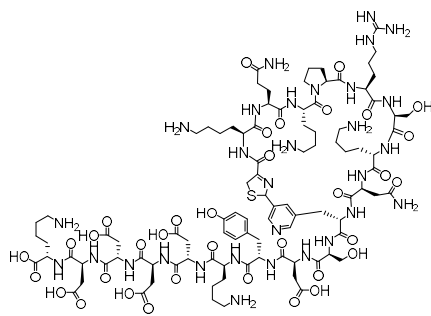
18 p



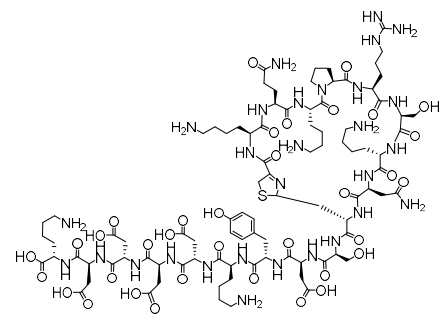
19 p



20 p

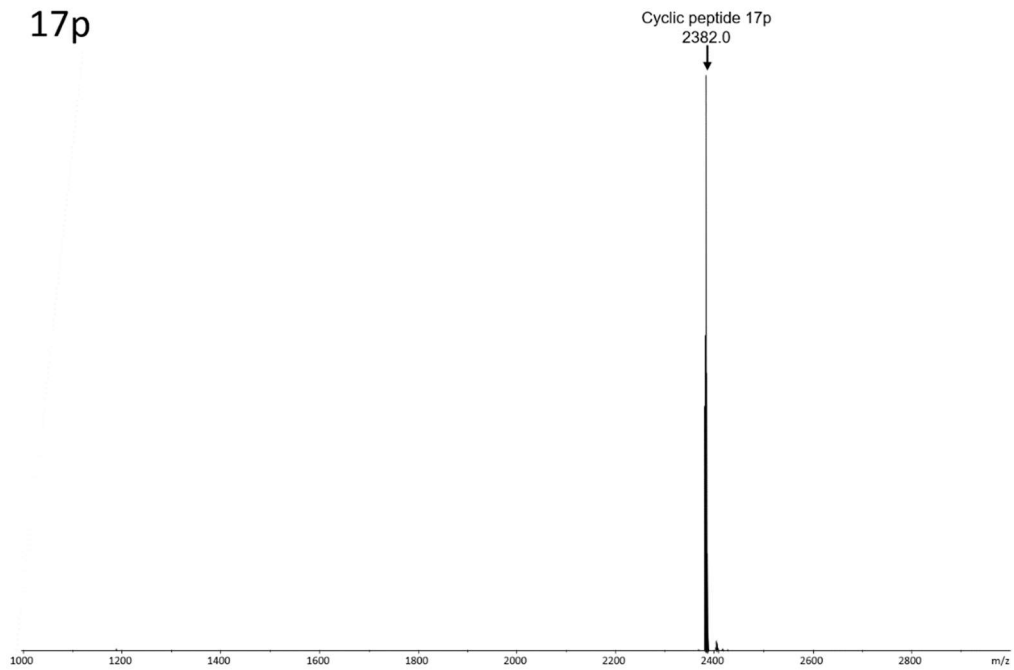


21 p

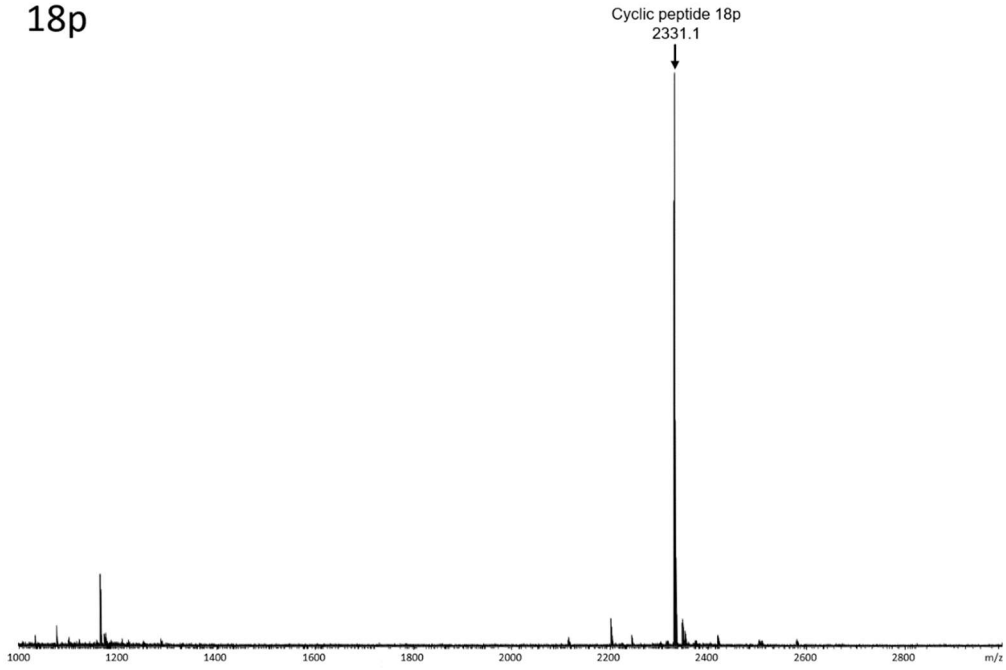


22 p

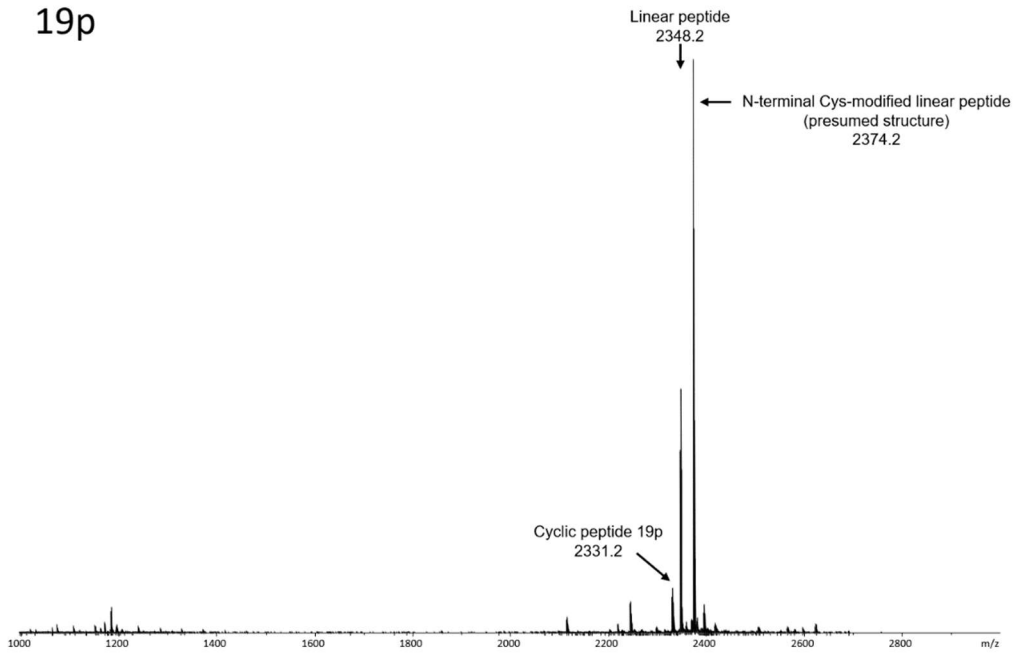
Fig. 4-4 Cyclic peptides expressed in the cell-free translation.



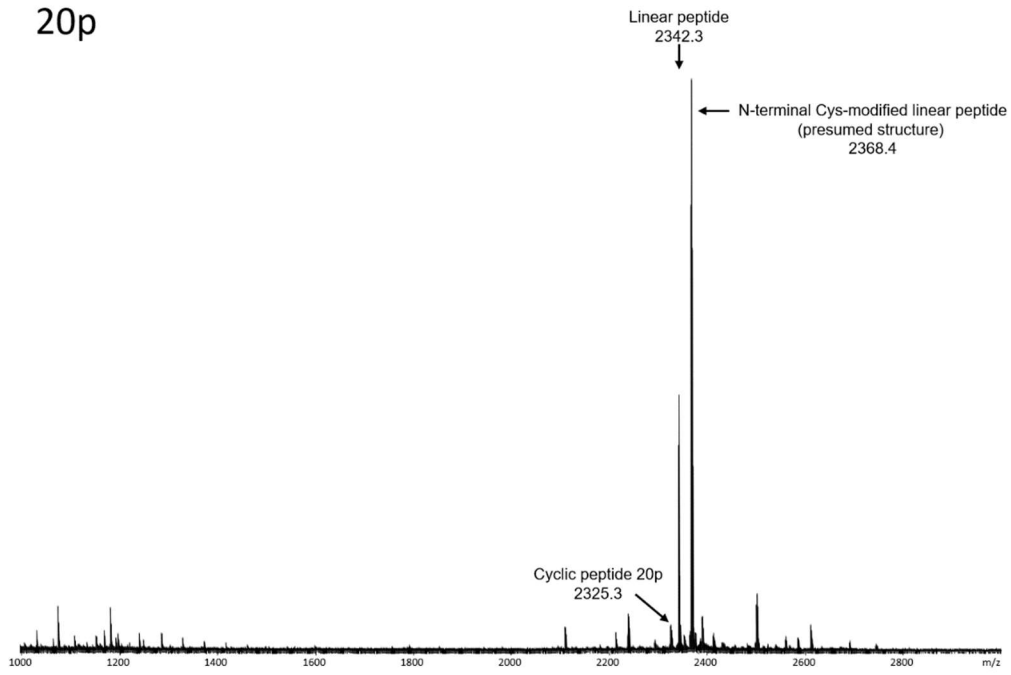
18p



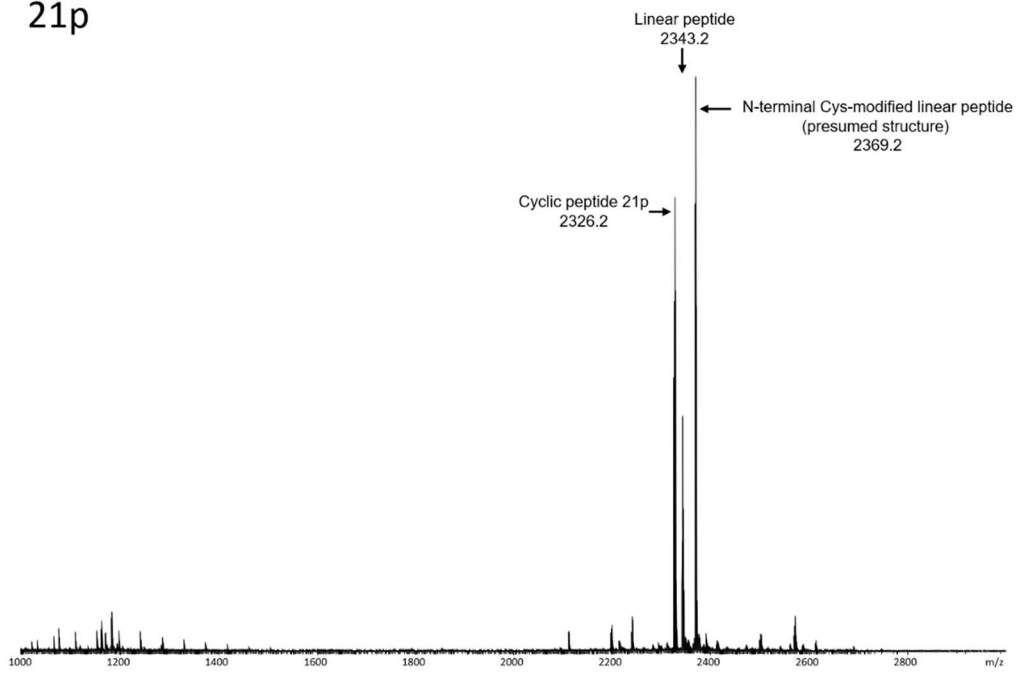
19p



20p



21p



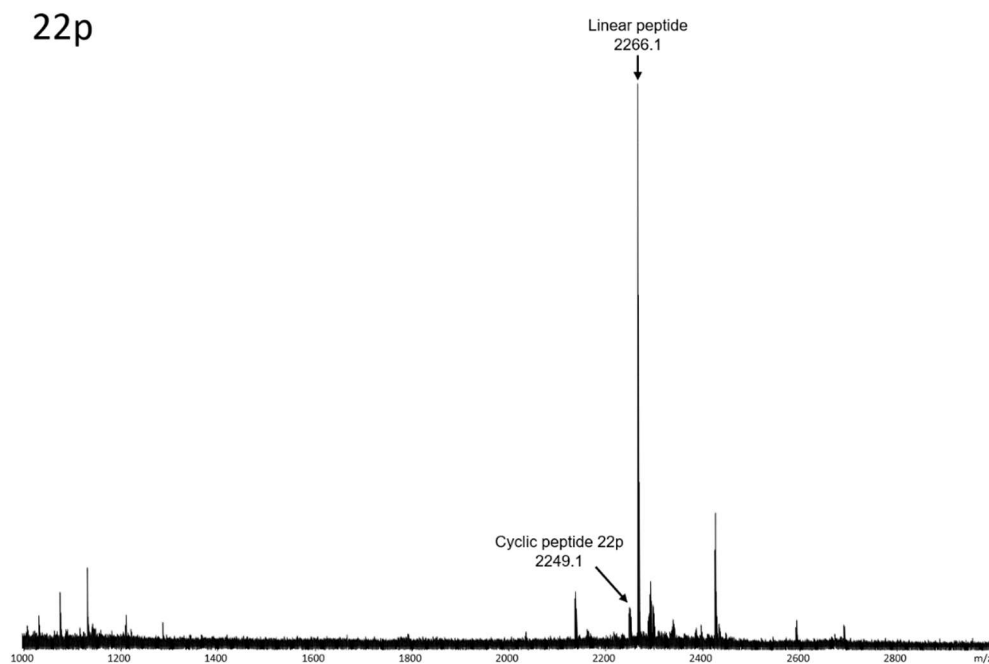


Fig. 4-5 MALDI TOF-MS analysis of thiazoline ring-bridged peptide **17p-22p** containing cyanated non-natural amino acid **1-6** expressed in the cell-free translation system.

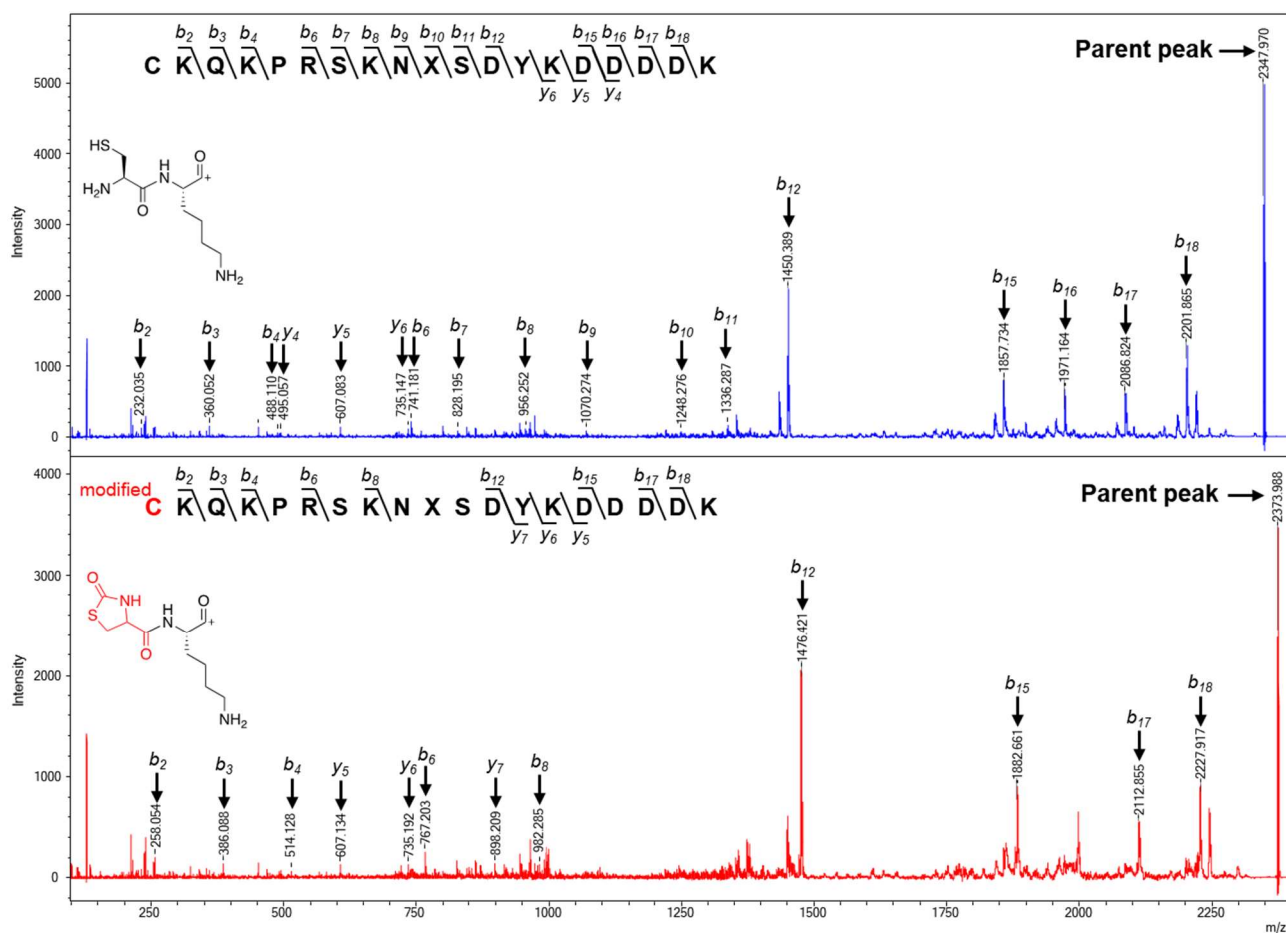


Fig. 4-6 MS/MS analysis of linear peptide (upper panel) and by-product (lower panel) for 19p.

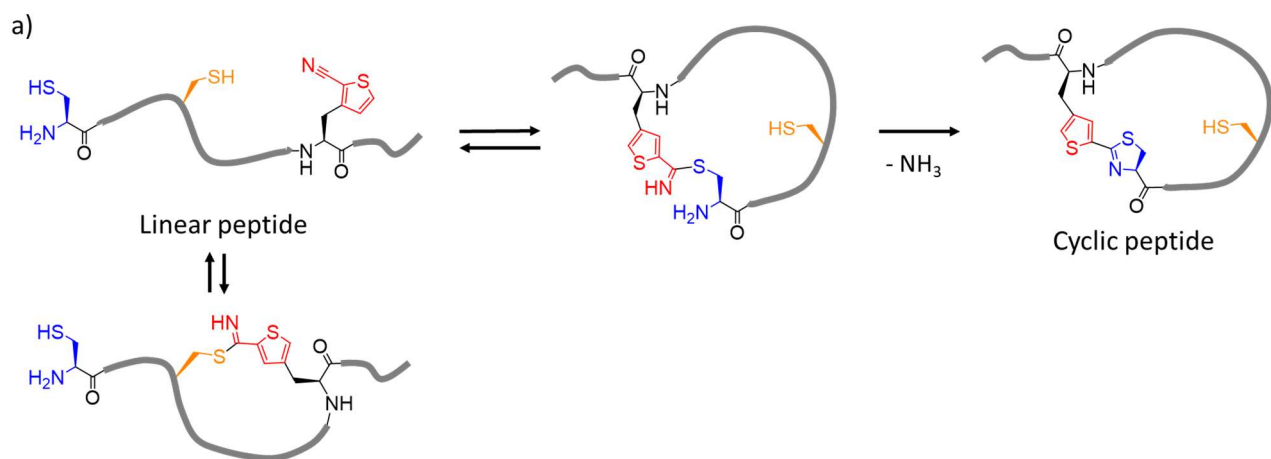
4. 3. 2 Selectivity of thiazoline ring-bridged peptide cyclization for Cys residues

The cyclization reaction starts with reversible nucleophilic attack of the SH group of N-terminal Cys on the cyano group, followed by irreversible nucleophilic attack of the adjacent α -amino group and ammonia elimination (Fig. 4-7a). Therefore, even if peptide contains Cys residues other than at the N-terminus, the internal Cys residue without α -amino group cannot form the thiazoline ring-bridged cyclization, although the internal Cys residues may affect the cyclization reaction.

In order to examine the influence of internal Cys residues on the cyclization reaction, I tested the selectivity of the thiazoline ring-bridged peptide cyclization reaction by using peptide sequences containing N-terminal and internal Cys residues. As a model peptide, CKQKPRSKNXS-DYKDDDDK sequence was also used, and amino acid residues at positions 3 and 7 were replaced by Cys in peptides **23p** and **24p** (Fig. 4-7b). The non-natural amino acid having 2-cyanothiophene residue (**2**, Fig. 4-7c) was introduced at X position, because it achieved the peptide cyclization in a rapid and quantitative manner as describe above. The structures of these target cyclic peptides are shown in Fig. 4-8. These peptides were expressed in the cell-free translation system and analyzed by MALDI TOF-MS.

As shown in Fig. 4-7d, for both peptides **23p** and **24p** containing additional Cys residues, peaks corresponding to the expected m/z values of the cyclized forms were observed. No linear peptide peaks were detected for these peptides. In addition, the conjugates of cyanothiophene and internal Cys residues without the elimination of amino group, whose m/z was expected to be 60 greater than that of the cyclized peptide, were not detected (Fig. 4-7d). These results indicate that the linear peptides containing cyanothiophene residue were synthesized in the ribosomal translation system and spontaneously cyclized in a rapid and quantitative manner. The cyclization reaction proceeded even in the presence of additional Cys residues at varied positions.

The present cyclization method is in contrast to other disulfide-bridged or thioether-bridged cyclization, in which internal Cys residues are involved in the cyclization reaction and produce multiple cyclic peptides with different circular chain lengths. The cyclization at undesired positions in peptide libraries reduces the population of the cyclic peptides with desired circular chain lengths and requires identification of the cyclization position after peptide screening. The thiazoline ring-bridged peptide cyclization will allow to prepare cyclic peptide libraries with defined circular chain lengths.



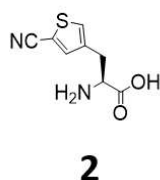
b)

Peptide ID	Sequence	Linear peptide [M+H] ⁺ ; m/z (calculated)	Cyclic peptide [M+H] ⁺ ; m/z (calculated)
18p	NH ₂ - <u>C</u> -K-Q-K-P-R-S-K-N- <u>X</u> -S-(Flag tag)-COOH	2348.03	2331.01
23p	NH ₂ - <u>C</u> -K- <u>C</u> -K-P-R-S-K-N- <u>X</u> -S-(Flag tag)-COOH	2322.98	2305.96
24p	NH ₂ - <u>C</u> -K-Q-K-P-R- <u>C</u> -K-N- <u>X</u> -S-(Flag tag)-COOH	2364.01	2346.98

X is non-natural amino acid **2**

Flag tag : -D-Y-K-D-D-D-D-K-

c)



d)

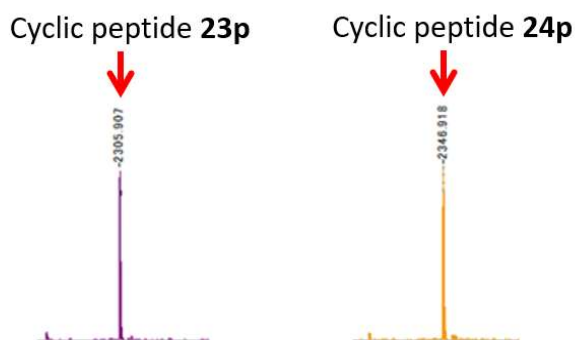


Fig. 4-7 Cyclization of peptides containing Cys at the N-terminus and inside peptide and cyanothiophene residue at the C-terminus. a) Schematic diagram of the cyclization reaction. b) Amino acid sequence and calculated m/z value of the peptides used; X indicates the position of introduction of the non-natural amino acid **2**; c) Chemical structure of the non-natural amino acid **2** with 2-cyanothiophene residue; d) MALDI TOF-MS spectra.

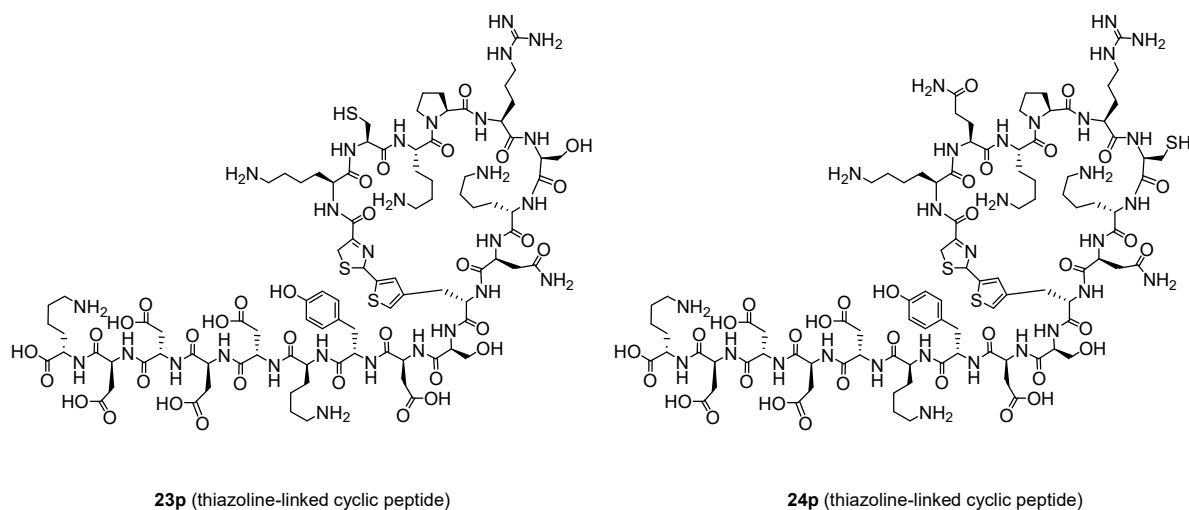


Fig. 4-8 Cyclic peptides structure of peptide **23p** and **24p**

4. 3. 3 Thiazoline ring-bridged cyclization of peptides of different lengths

In the intramolecular cyclization of peptides, the length of the peptide to be cyclized may affect the efficiency of the cyclization reaction. Therefore, I evaluated the efficiency of the cyclization reaction by changing the number of amino acids between the N-terminal Cys and side chain of **2**. For this purpose, I used peptide sequences containing 5-9, 15, and 20 residues in the cyclic portion (**25p-31p**), as shown in Fig. 4-9a. The cell-free expression of the cyclic peptides and MALDI TOF-MS analysis were carried out as described above.

As shown in Fig. 4-9b, peaks corresponding to the cyclic peptides were clearly observed for all peptides **25p-31p**. For peptides **25p**, **26p**, **27p**, **30p** and **31p**, no peaks corresponding to linear peptides were detected, while peptides **25p** and **26p** showed Na^+ adducts of the cyclic form. On the other hand, unreacted linear peptides were observed in peptides **28p** and **29p**, but their peak intensities were much weaker than those of the cyclic peptides.

These results demonstrate that the cyclic peptides can be efficiently produced regardless of the length of the peptides to be cyclized and the surrounding amino acid sequences. Up to at least 20 amino acid residues did not affect the cyclization reaction, suggesting the wide applicability of this reaction.

a)

Peptide ID	Sequence	Linear peptide [M+H] ⁺ ; m/z (calculated)	Cyclic peptide [M+H] ⁺ ; m/z (calculated)
25p	NH ₂ - C - K-Q-K- X -S-(Flag tag)-COOH	1765.71	1748.68
26p	NH ₂ - C* - K-Q-K-P- X -S-(Flag tag)-COOH	1862.76	1845.73
27p	NH ₂ - C - K-Q-K-P-R- X -S-(Flag tag)-COOH	2018.86	2001.84
28p	NH ₂ - C - K-Q-K-P-R-S- X -S-(Flag tag)-COOH	2105.89	2088.87
29p	NH ₂ - C - K-Q-K-P-R-S-K- X -S-(Flag tag)-COOH	2233.99	2216.96
30p	NH ₂ - C -K-Q-K-P-R-S-K-N-P-F-W-C-H- X -S-(Flag tag)-COOH	3018.30	3001.27
31p	NH ₂ - C - K-Q-K-P-R-S-K-N-Q-K-R-N-S-P-F-W-C-H- X -S-(Flag tag)-COOH	3631.63	3614.60

X is non-natural amino acid **2**

Flag tag : -D-Y-K-D-D-D-K-

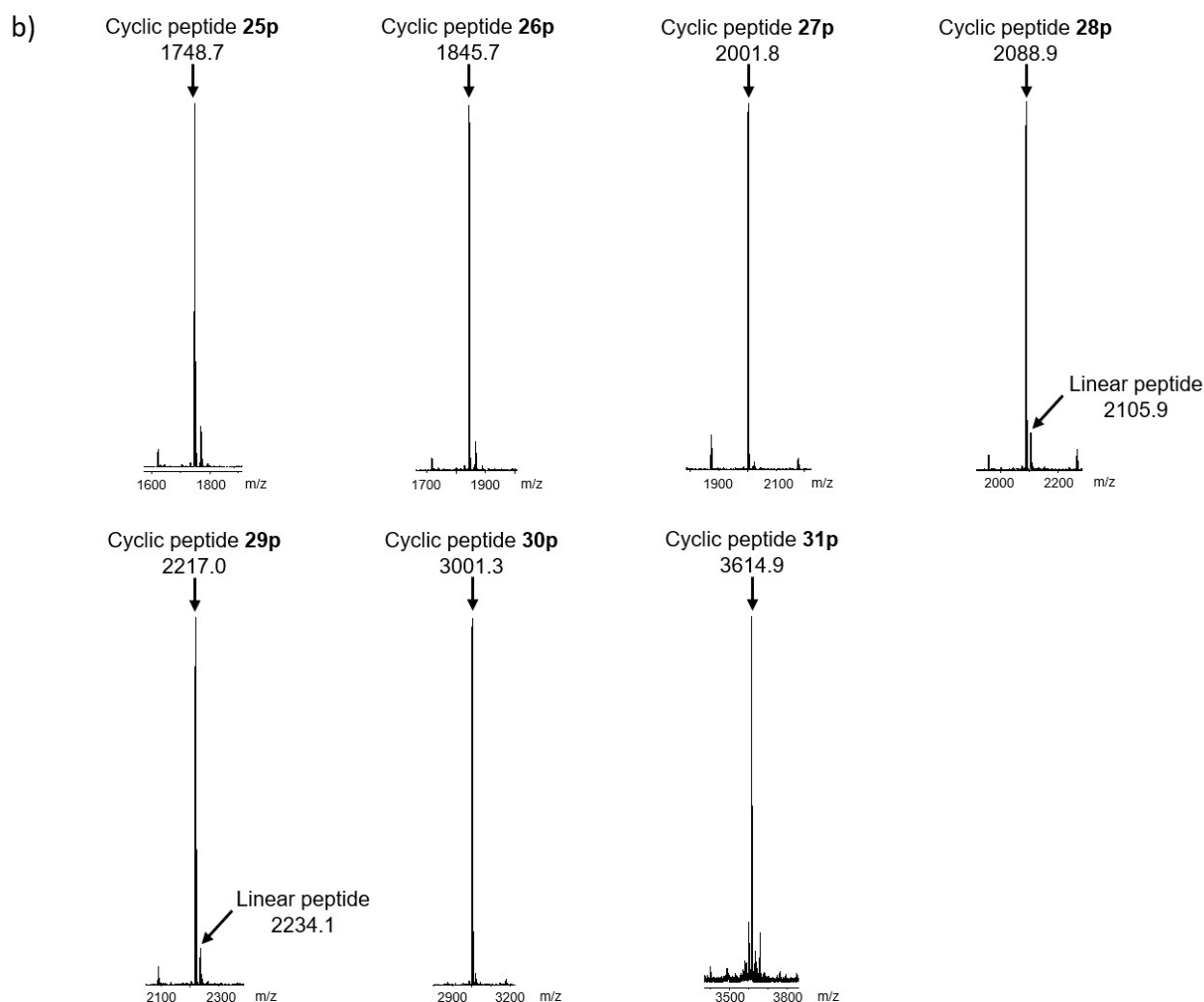


Fig. 4-9 Cyclization of peptides with cyanothiophene residue introduced at different positions. a) Amino acid sequence of the peptides used in this study and calculated m/z values. X indicates the position of the introduced non-natural amino acid **2**. b) MALDI-TOF MS spectra of expressed peptides.

4. 4 Conclusion

I have confirmed that thiazoline ring-bridged peptide cyclization occurs in an N-terminal Cys-selective manner using non-natural amino acids with cyano groups in cell-free translation. All the non-natural amino acids used in this study were introduced into the peptides through the amber suppression, but the cyclization efficiency depended on the types of cyanated residues. Considering the cyclization efficiency, non-natural amino acids **1** and **2** are preferred for the expression of the thiazoline ring-bridged cyclic peptides. I have also confirmed that the N-terminal Cys was selectively cyclized in the thiazoline ring-bridged peptide cyclization even in the presence of Cys in the chain. Furthermore, I confirmed that the cyclization reaction proceeds even for linear peptides with a chain length of 5 to 20 residues. These results obtained in this study demonstrate the usefulness of this cyclization reaction in the construction of cyclic peptide libraries with mRNA display. In other words, this cyclization reaction enable to establish the peptide libraries cyclized at specified positions. This cyclization method is in contrast to disulfide-bridged or thioether-bridged cyclization, where multiple Cys inside peptides are involved in the cyclization reaction and cyclization occurs at multiple positions, requiring identification of the cyclization position after peptide selection. The ability to use Cys without limitation in a random library and the ability to produce cyclic peptides of different lengths are also advantages in increasing the diversity of the library. In addition, the thiazoline ring-bridged cyclization structure is also expected to enhance membrane permeability and is expected to be applied to obtain peptides against intracellular protein-protein interactions.

References

- 1) a) Joel D. A. Tyndall, Tessa Nall, and David P. Fairlie Proteases Universally Recognize Beta Strands In Their Active Sites *Chem. Rev.* **2005**, *105*, 973-1000, b) Alessandro Zorzi, Kaycie Deyle, Christian Heinis Cyclic peptide therapeutics: past, present and future *Curr Opin Chem Biol.* **2017**, *38*, 24-29, c) *Modern Supramolecular Chemistry: Strategies for Macrocyclic Synthesis* **2008**, 1-28, d) Christian Heinis, Trevor Rutherford, Stephan Freund, Greg Winter Phage-encoded combinatorial chemical libraries based on bicyclic peptides *Nat. Chem. Biol.* **2009**, *5*, 502-507
- 2) Toby Passioura, Takayuki Katoh, Yuki Goto, Hiroaki Suga Selection-based discovery of druglike macrocyclic peptides *Annu. Rev. Biochem.* **2014**, *83*, 727-752, b) Kristopher Josephson, Alonso Ricardo, Jack W Szostak mRNA display: from basic principles to macrocycle drug discovery *Drug Discovery Today* **2014**, *19*, 388-399
- 3) Yuki Goto, Atsushi Ohta, Yusuke Sako, Yusuke Yamagishi, Hiroshi Murakami, and Hiroaki Suga Reprogramming the Translation Initiation for the Synthesis of Physiologically Stable Cyclic Peptides *ACS Chem. Biol.* **2008**, *3*, 120-129
- 4) Yusuke Yamagishi, Ikuo Shoji, Shoji Miyagawa, Takashi Kawakami, Takayuki Katoh, Yuki Goto, Hiroaki Suga Natural product-like macrocyclic N-methyl-peptide inhibitors against a ubiquitin ligase uncovered from a ribosome-expressed de novo library *Chem Biol.* **2011**, *18*, 1562-1570
- 5) Jumpei Morimoto, Yuuki Hayashi, Hiroaki Suga Discovery of macrocyclic peptides armed with a mechanism-based warhead: isoform-selective inhibition of human deacetylase SIRT2 *Angew. Chem. Int. Ed.* **2012**, *51*, 3423-3427
- 6) Takashi Kawakami, Takahiro Ishizawa, Tomoshige Fujino, Patrick C. Reid, Hiroaki Suga, Hiroshi Murakami In Vitro Selection of Multiple Libraries Created by Genetic Code Reprogramming To Discover Macrocyclic Peptides That Antagonize VEGFR2 Activity in Living Cells *ACS Chem. Biol.* **2013**, *8*, 1205.
- 7) Yoshiki Tanaka, Christopher J. Hipolito, Andrés D. Maturana, Koichi Ito, Teruo Kuroda, Takashi Higuchi, Takayuki Katoh, Hideaki E. Kato, Motoyuki Hattori, Kaoru Kumazaki, Tomoya Tsukazaki, Ryuichiro Ishitani, Hiroaki Suga, Osamu Nureki Structural basis for the drug extrusion mechanism by a MATE multidrug transporter *Nature* **2013**, *496*, 247.
- 8) a) Shiori Kariyuki, Takeo Iida, Miki Kojima, Ryuichi Takeyama, Mikimasa Tanada, Tetuo Kijima, Hitoshi Iikura, Atsushi Matsuno, Takuya Shiraishi, Takashi Emura, Kazuhiko Nakano, Koji Takano, Kousuke Asou, Takuya Trizawa, Ryosuke Takano, Nozomi Hisada, Nakaoki Murao, Atsushi Ohta, Kaori Kimura, Yusuke Yamagishi, Tatsuya Kato Peptide-Compound Cyclization Method WO2013100132, b) Kazuhiko Nakano, Atsushi Ohta, Takeo Iida, Hitoshi Iikura Production Method for Noncyclic Peptide-Nucleic Acid Complex Having, at N-Terminal, Amino Acid with Thiol Group near Amino Group, Library Thereof, and Cyclic Peptide-Nucleic Acid Complex Library Derived from Same WO2017150732
- 9) Yollete V. Guillen Schlippe, Matthew C. T. Hartman, Kristopher Josephson, Jack W. Szostak In Vitro Selection of Highly Modified Cyclic Peptides That Act as Tight Binding Inhibitors *J. Am. Chem. Soc.* **2012**, *134*, 10469-10477
- 10) a) Steven W. Millward, Terry T. Takahashi, Richard W. Roberts A General Route for Post-Translational

- Cyclization of mRNA Display Libraries *J. Am. Chem. Soc.* **2005**, *127*, 14142-14143, b) Steven W. Millward, Stephen Fiacco, Ryan J. Austin, Richard W. Roberts Design of Cyclic Peptides That Bind Protein Surfaces with Antibody-Like Affinity *ACS Chem. Biol.* **2007**, *2*, 625-634
- 11) Yusuke Sako, Jumpei Morimoto, Hiroshi Murakami, Hiroaki Suga Ribosomal Synthesis of Bicyclic Peptides via Two Orthogonal Inter-Side-Chain Reactions *J. Am. Chem. Soc.* **2008**, *130*, 7232-7234
- 12) a) John R. Frost, Conor C. G. Scully, Andrei K. Yudin Oxadiazole grafts in peptide macrocycles *Nat. Chem.* **2016**, *8*, 1105-1111, b) Solomon D. Appavoo, Takuya Kaji, John R. Frost, Conor C. G. Scully, Andrei K. Yudin Development of Endocyclic Control Elements for Peptide Macrocycles *J. Am. Chem. Soc.* **2018**, *140*, 8763-8770, c) Kouhei Matsui, Yasuto Kido, Ryosuke Watari, Yousuke Kashima, Yutaka Yoshida, Satoshi Shuto Highly Conformationally Restricted Cyclopropane Tethers with Three-Dimensional Structural Diversity Drastically Enhance the Cell Permeability of Cyclic Peptides *Chem. Eur. J.* **2017**, *23*, 3034-3041
- 13) Thomas G. Heckler, Li Ho Chang, Yoshiyuki Zama, Takehiko Naka, Mukund S. Chorghade, Sidney M. Hecht T4 RNA ligase mediated preparation of novel "chemically misacylated" tRNAP^{he}s *Biochemistry* **1984**, *23*, 1468-1473
- 14) Hikaru Taira, Yosuke Matsushita, Kenji Kojima, Kaori Shiraga, Takahiro Hoshika Comprehensive screening of amber suppressor tRNAs suitable for incorporation of non-natural amino acids in a cell-free translation system *Biochem. Biophys. Res. Commun.* **2008**, *374*, 304-308

Chapter 5

Conclusion

In this study, I described the reaction properties and versatility of thiazoline ring-bridged peptide cyclization inspired by Luciferin biosynthesis. This peptide cyclization reaction proceeded in an aqueous solvent spontaneously, and it was possible to construct a characteristic heterocyclic structure in the peptide main chain. The reactivity of cyclization can be tuned by the energy level of the LUMO orbital of the cyano group. Furthermore, we have shown that the present peptide cyclization reaction can be adapted to linear peptides composed of various amino acid sequences. The thiazoline ring-bridged cyclic peptides showed higher membrane permeability than amide- and thioether-bridged ones. To better understand the model membrane permeation phenomenon, I have carried out temperature-variable NMR and computational solution structure analysis and found that the intramolecular hydrogen bonds reduced the polar surface area by the polar offset and solvent molecule shielding effect. In addition, I have applied this thiazoline ring-bridged peptide cyclization reaction to the cell-free translation and revealed that the cyclic peptides were obtained from the cell-free expressed linear peptides in a rapid and quantitative manner.

The advantages of the thiazoline ring-bridged cyclic peptides were summarized as follows: (1) regioselective cyclization of a wide range of amino acid sequences is possible, (2) cyclic peptides with high membrane permeability could be provided, and (3) cyclic peptides also can be expressed in a cell-free translation regioselectively. This type cyclic peptides have a druggable thiazoline ring as a heterocyclic structure in the peptide main chain, thus providing novel peptide libraries that are different from conventional amide and thioether-bridged ones. In addition, the rigidity of the thiazoline ring-bridged structure may also be advantageous to reduce entropy loss upon binding to targets. These characteristics of the thiazoline ring-bridged cyclic peptides are expected to be utilized to develop novel types of peptide drugs in a wide range of areas, from the discovery stage to the development stage.

List of Publications

Chemical synthesis and cell-free expression of thiazoline ring-bridged cyclic peptides and their properties on biomembrane permeability

Takashi Tamura, Masaaki Inoue, Yuji Yoshimitsu, Ichihiko Hashimoto, Noriyuki Ohashi, Kyosuke Tsumura, Koo Suzuki, Takayoshi Watanabe, Takahiro Hohsaka

Bull. Chem. Soc. Jpn. **2022**, *95*, 359-366

Expression of thiazoline ring-bridged cyclic peptides in a cell free translation system

Masaaki Inoue, Takashi Tamura, Takayoshi Watanabe, Takahiro Hohsaka

In preparation.

Acknowledgments

I would like to express my appreciation to Professor Dr. Takahiro Hohsaka and Senior Lecture Dr. Takayoshi Watanabe for their thoughtful guidance and research collaboration. I am grateful to Mr. Masatoshi Yumoto, Dr. Masaaki Inoue, Dr. Yuji Yoshimitsu, Ms. Mai Mizuno, Mr. Shiniji Nakayama, Mr. Shohei Aoyama, Mr. Keishiro Nagoshi, Ms. Hiromi Ishibashi, Ms. Katsuko Sato, Dr. Ichihiko Hashimoto, Dr. Kenta Miyahara, Dr. Kyosuke Tsumura, Mr. Noriyuki Ohashi, and Mr. Koo Suzuki, Mr. Makoto Takahashi, Dr. Motoki Saito, Dr. Shinji Hagiwara for their invaluable contributions to my research. And I wish to thank Dr. Keisuke Fukunaga, Dr. Rumi Shiba and Dr. Dian Novitasari for useful discussion in Hohsaka Laboratory. Fothermore, I would like to thank Dr. Hideyasu Fujiwara for giving me the oppotuniy to earn my degree. Finally, I would like to express my gratitude to my family and my wife for their heartwarming encouragement.